

Enzymatically Crosslinked Poly(Ethylene Glycol) Hydrogels for Tissue Engineering

by

Jeffrey J. Sperinde

B.S., Chemical Engineering
University of California, Berkeley, 1993

Submitted to the Department of Chemical Engineering
in partial fulfillment of the requirements for the degree of

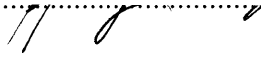
Doctor of Philosophy


at the


Massachusetts Institute of Technology

February, 1999

©1999 Massachusetts Institute of Technology. All rights reserved.

Signature of Author

Department of Chemical Engineering
December 21, 1998

Certified by

Linda G. Griffith
Associate Professor of Chemical Engineering
Thesis Supervisor

Accepted by

Robert E. Cohen
St. Laurent Professor of Chemical Engineering
Chairman, Committee for Graduate Students

Science



Enzymatically-Crosslinked Poly(Ethylene Glycol) Hydrogels for Tissue Engineering

by

Jeffrey J. Sperinde

Submitted to the Department of Chemical Engineering on December 21, 1998
in partial fulfillment of the requirements for the degree of
Doctor of Philosophy in Chemical Engineering

Abstract

This project has addressed the development of a versatile hydrogel for *in vivo* or *in vitro* medical applications such as a scaffold for cells in tissue engineering. In this pursuit I have developed a hydrogel composed of functionalized poly(ethylene glycol) (PEG) that could be injected into the body and induced to gel *in situ* by the addition of a natural crosslinking enzyme, transglutaminase. Enzymatic crosslinking affords the advantages of kinetic control inherent in enzymatically-limited processes as well as specificity, a necessity for engineering controlled chemistry *in vivo*.

This work focused on engineering the gelation process. Through an understanding of transglutaminase specificity a number of substrates, primarily peptides, were designed and implemented as PEG-linked substrates. Models for gelation times were developed and tested based on transglutaminase reaction models as a function of key parameters including substrate kinetics, polymer number functionality and reaction environment.

Enzymatically crosslinked gels were characterized in terms of diffusion and swelling properties as well as cellular compatibility. These tests gave insight into the properties of enzymatically crosslinked PEG gels and most importantly gave every indication that they were suitable for cell encapsulation.

In certain tissue engineering applications it may be important to employ a temporary cell scaffold that will degrade as the cells synthesize and organize molecules specific to their native environment. Enzymatically crosslinked PEG gels were made to be degradable *in vivo* by incorporation of a cleavable peptide sequence into the gel structure. This peptide sequence can be recognized by a native enzyme called collagenase, an enzyme that cells naturally secrete to remodel their own environment. By incorporation of collagenase-sensitive linkages gel degradation is controlled by the cells themselves.

Thesis Supervisor: Linda G. Griffith

Title: Associate Professor of Chemical Engineering and Bioengineering

Acknowledgments

It is fitting that I begin and end these words with an acknowledgment to the constant force in my life that has brought me through these last five years at MIT: my wife, Gizette. In the seven years we have been together she has given me her love, support and understanding -- lots of understanding -- which has enabled me to be everything (only the good stuff, Giz) that I am today. She gets me up in the morning (too early?) and gives me reason to fight through the day. I only hope that I have been at least half as supportive in her life.

During my tenure at MIT family has always been by my side -- unfortunately more in spirit than in physical presence. I am grateful for all the times they were willing to brave the flight out from California to see us. I want to thank my parents, John and Sandy, for raising me the way they did. Whatever you did, you did it right. If I had to put words to it, I would say that you taught by example. I see a lot of you in me, and I am very proud of it. I want to thank my sister, Gina, first for putting up with me. Most importantly, thank you for being a wonderful sister. I really look up to you and admire your accomplishments.

I am also supremely grateful for the continued presence of my 'extended family', the friends I grew up with (still got the righteous goods). Joe (15 years now?) Crazy bread/sauce, Manard ate the bouncy ball, steamroller, cat torture, dial forty cents → attorney: you've got 'em all fooled. Rich, penalty kick - sorry, party people, horse/poison(lost)-ping-pong(lost), golf(lost)-can I buy a handicap?, for all you've been and will be I sometimes envy you. Samir, road-trip: 'too much fun', Patch Adams? - consider it - at least do the clown shoes for me. Ted, don't go a-changin', you're one in a million - Mr. Carpe Diem. Mark, how much we've changed since John Muir, they'll just have to dig deeper (50yrd line)! Monti, can you say, "road trip?!" Andy, thanks for hooking me up in SB, I'm eternally grateful. Along those lines, thank you Clara for telling Gizette to look out for the 'blond kid' - I'm still working on the 'blond part'.

I would like to thank Professor Linda Griffith for her guidance and support. Her leadership was well balance with her willingness to let me explore my own interests and make my own mistakes. I am also grateful for the wisdom of my thesis committee: Professors Daniel Blankschtein, Robert Langer, Peter Lansbury and Edward Merrill. Professor Lauffenburger as well had a profound effect on my development as a scientist; I am better for having known him. I would like to thank past and present members of the DAL and LGG labs for making life in lab enjoyable, and Lily Koo for having the bravery to continue this work (stay tuned for the sequel). I am also thankful for the NIH Biotechnology Training Grant for financial support of this work.

And in the end there is always Gizette (cf Φ). You are there for me from beginning to end. As magnificent as our days have been together I know the best is yet to come. You give me something to look forward to every day. How luck I am to have you in my life.

Table of Contents

1	Introduction and Background	10
1.1	Tissue Engineering	10
1.2	Cell Scaffolds	11
1.3	<i>In Situ</i> Gel Formation	13
1.4	Poly(Ethylene Glycol)	14
1.5	Transglutaminase	15
1.5.1	Overview	15
1.5.2	Enzyme Variants	17
1.5.3	Kinetics	18
1.5.4	Substrates	20
1.5.5	Cofactors	25
1.6	References	35
2	Tresyl-Mediated Synthesis	42
2.1	Background	42
2.2	Experimental Design	43
2.3	Experimental Methods	45
2.4	Results and Discussion	47
2.4.1	Rate Constants for Hydrolytic Processes	47

2.4.2	Development of a Tresyl-Mediated Coupling Model	50
2.4.3	Temperature Effects	54
2.4.4	pH Effects	55
2.4.5	Steric Effects	57
2.4.6	Control of Product Distribution	58
2.5	Conclusions	59
2.6	References	74
3	Kinetics of Transglutaminase	76
3.1	Introduction	76
3.2	Tissue Transglutaminase Self-Crosslinking	76
3.2.1	Experimental Methods	77
3.2.2	Results	80
3.2.2.1	TG Self-Crosslinking Processes	80
3.2.2.2	Kinetic Model	83
3.2.2.3	Temperature, pH and Antioxidant Effects	89
3.2.3	Discussion	91
3.3	Transglutaminase Activity with PEG-Bound Substrates	94
3.4	References	106

4	Enzymatically Crosslinked Poly(Ethylene Glycol)/PolyLysine Gels ..	108
4.1	Introduction	108
4.2	Gel Precursor Design	108
4.3	Materials and Methods	109
4.4	Results and Discussion	117
4.4.1	Equilibrium Swelling Behavior	119
4.4.2	Protein Partitioning and Diffusion	123
4.4.3	Cellular Interactions	129
4.5	References	139
5	Kinetics of Enzymatically Crosslinked Poly(Ethylene Glycol) Gel Formation	141
5.1	Gelation Kinetic Theory	141
5.1.1	Structural Criteria	142
5.1.2	Kinetic Criteria	144
5.2	Materials and Methods	146
5.3	TG Substrate Design	148
5.3.1	Amine Acceptors	148
5.3.2	Amine Donors	151
5.4	Results and Discussion	152
5.4.1	PEG/Poly(KF) Gels	152

5.4.2	PEG/PEG Gels	153
5.5	References	166
6	Enzymatically Degradable Poly(Ethylene Glycol) Gels	167
6.1	Background	167
6.2	Design	167
6.3	Materials and Methods	168
6.4	Results	170
6.5	Cellular Interactions	172
6.6	References	176
7	Alternative Crosslinking Methods	177
7.1	Overview	177
7.2	Ionic Association: Alginate-Poly(Ethylene Glycol) Copolymers	177
7.3	Hydrophobic Association: β -Amyloid-Terminated PEG	178
7.4	Disulfide Bond Formation: Cysteine-Terminated PEG.....	179
7.5	References	185
8	Conclusions	186
8.1	Summary	186
8.2	Future Work	188

8.3	References	191
APPENDICES		192
A	Protocols	192
A1	Poly(Ethylene Glycol) TRESylation	192
	A1.1 Background	192
	A1.1 Materials	192
	A1.2 Procedure	193
A2	Peptide Synthesis	195
	A2.1 Background	195
	A2.2 Procedure	195
A3	Transglutaminase Storage	198
A4	Colorimetric Transglutaminase Activity Assay	200
	A4.1 Materials	200
	A4.2 Procedure	201
A5	SEC PEG/Monodansyl Cadaverine Assay	202
	A5.1 Materials	202
	A5.2 Procedure	203
A6	SEC PEG/Z-Glutaminylglycine Assay	204
	A6.1 Materials	204
	A6.2 Procedure	205

A7	O-Phthaldialdehyde Primary Amine Assay	206
	A7.1 Materials	206
	A7.2 Procedure	206
A8	References	209
B	Poly(Ethylene Glycol)/PolyLysine Gel Structure Predictions	210
	B1 Thermodynamic Predictions	210
	B2 References	220
C	Rate Constant Fitting Algorithm	221
	C1 Background	221
	C2 FORTRAN Code	222
	C3 References	234

1 INTRODUCTION

1.1 Tissue Engineering

Recent decades have witnessed the emergence of therapies designed to replace lost cell and/or tissue function with cell based therapies. This approach has been applied to metabolic and cell-function dependent tissues for treatment of liver^{1, 2}, diabetes³, amyotrophic lateral sclerosis (ALS)⁴, chronic pain⁵ and nerve damage⁶ as well as tissues and organs with more structural roles such as skin⁷, bone⁸, cartilage⁹, cardiovascular¹⁰, and kidney¹¹. The field of tissue engineering is still in its infancy, with only a limited number of applications progressing into clinical trials and fewer still are FDA-approved. Successful products have been concentrated in connective tissues such as skin¹² and cartilage¹³ where the material properties of the construct might be considered more important to the success of the therapy than the cellular component.

A central paradigm in tissue engineering is 'building' tissues *de novo* from cells and polymers. The cells may be human, non-human or isolated directly from the patient to be treated. The latter case may be ideal when sufficient cell numbers are available to eliminate the possibility of immunogenicity and disease transmission associated with transplantation. Whatever the source, it essential to provide the cells with an environment suitable for cell survival. The premise of the work described in this thesis is that the environment should replicate key aspects of the milieu found *in vivo*. Cells in native tissues typically exist in a highly hydrated environment, surrounded by and

adhered to a proteinaceous matrix of natural polymers, including proteins and charged polysaccharides. The properties of these polymers can affect the behavior of cells through specific molecular interactions with cell-surface receptors as well as influences at the length scale of the cell by the polymer chain long-range organization and crosslinking.

1.2 Cell Scaffolds

Construction of a cell scaffold for use in tissue engineering, the polymers to be used may be either natural or synthetic. Natural polymers have the advantage that they are composed of many of the very components that the particular cell type may encounter *in vivo*. Unfortunately, processing steps required to use natural polymers, including solubilizing and re-crosslinking the polymers, can materially alter their properties as perceived by cells. Further, processing can remove a variety of secondary molecules specifically and nonspecifically bound to native extracellular matrix such as cell signaling molecules, enzymes, inhibitors, etc. These missing components can't simply be replaced: the complexity of natural systems precludes complete characterization of the components that comprise native extracellular matrix. Other components in natural polymers may survive the processing steps, but may ultimately prove harmful to an engineered tissue by inciting an immune response. For these reasons a greater degree of control can be exerted over the system by employing chemically defined synthetic polymers.

Yet despite these drawbacks, natural polymers have been successfully used in the a number of the replacement tissues developed to date, most notably skin replacements.

Collagen is one of the most widely used polymers as a natural tissue scaffold. As a natural component of most tissues, collagen scaffolds present encapsulated cells with protein interactions much like the natural cellular environment⁷. Alginate is another widely used natural polymer because of the mild conditions required for gelation¹⁴.

The large diversity of synthetic materials used as cell scaffolds has been summarized in numerous recent reviews¹⁵⁻¹⁷. Materials include polylactides/glycolides, polyurethanes, polyacrolates, polypeptides, poly(ethylene glycol) and others. The suitability of a biomaterial for a particular application is often a trade-off between material/structural properties and aspects at the molecular level such as cellular interactions. Material-cell interactions are critical from the standpoint of preventing or minimizing adverse cellular responses of the immune system as well as promoting desired interactions such as cell adhesion and inciting cell growth that may be necessary for the survival and function of the tissue engineered construct. Most biomaterials suffer from some degree of bio-incompatibility in that they elicit some degree of immune response¹⁸.¹⁹. A notable exception to this is poly(ethylene glycol)²⁰.

In this work we have sought to design a cell scaffold engendered with *only* those specific cellular interactions specified by the user. This confines our universe to synthetic materials, as natural materials are inherently undefined. Therefore the design goal of this work is a cell scaffold built up from a backbone of non-cell interacting polymers, decorated with chemical moieties that interact with cells in a defined and controllable manner.

1.3 *In Situ* Gel Formation

One point of distinction between various potential cell scaffolds is the manner in which cells are introduced into the construct. Scaffolds in which cells are seeded into a pre-formed structure such as polylactide-co-glycolide formulations²¹ are seeded *ex vivo* and then implanted into the target site. A somewhat less invasive procedure might be achieved whereby the cells are injected into the target site along with a scaffold precursor that is designed to form *in situ*.

A number of methods have been proposed as to how to achieve this. Strategies are somewhat restricted by the limitation of cytotoxicity. Any structure formed in contact with living tissues or formed around cells must be relatively mild.

Photopolymerization²² at visible wavelengths of acrylate-functionalized multimeric poly(ethylene glycol) has been used successfully on the surface of tissues and may find use as tissue scaffolds²³. Injectable hydrogels designed for drug delivery²⁴ formed by spontaneous chemical crosslinking may also find use as cell scaffolds. Here we propose inducing gelation by the action of an enzyme which would obviate the need for excessive manipulation required to photopolymerize *in situ* and would eliminate the evolution of chemical leaving groups.

Injectability and specificity are two key advantages to enzyme-mediated gel formation. Injectability is conferred by the kinetic control inherent in an enzymatic system: varying the amount of enzyme added to the pre-gel solution modulates the rate of gel formation (Figure 1-1). Thus the gelation rate can be tuned to the time required to

prepare the pre-gel solution and deliver it to the target site prior to gel formation. Specificity is also achieved by the nature of enzymatic reactions. This could be exceedingly important for directing the specific chemical reactions necessary for crosslinking and gel formation in the undefined chemical environment of the human body. Additionally, chemical moieties incorporated into the polymer backbone to influence cell behavior and function need to remain uncrosslinked to remain active (Figure 1-2).

There are currently two known enzymes found in the human body that are capable of carrying out crosslinking reactions, lysyl oxidase²⁵ which primarily responsible for the stabilization of articular cartilage and other matrix molecules, and transglutaminase, a family of crosslinking enzymes with diverse activities. Because transglutaminase is the most well characterized and readily available, a member of this family of enzymes was chosen for development of enzymatically crosslinked hydrogels.

1.4 Poly(Ethylene Glycol)

Poly(ethylene glycol) (PEG) owes much of its favorable cell interactions from its ability to be almost completely non-adsorbing to proteins. Many of the interactions cells have with their environment are protein- and/or charge-mediated, leaving PEG almost invisible to cells. One of the major contributors to the solution properties of PEG is its high degree of hydrophilicity. This may be explained by comparing the PEG repeat C-O-C with the H-O-H geometry of water²⁶, as well as the hydrogen-bonding available with oxygen. Another significant contributor to PEG's protein repulsive properties is its high

chain mobility²⁷. This results in an entropic expense for any macromolecule to bind to PEG²⁷.

Poly(ethylene glycol) has been used with some success as a surface passivant. Failings in PEG-grafted surfaces to resist protein adsorption can often be attributed to incomplete surface coverage. The same properties that make PEG attractive as a surface passivant make it difficult to pack at high densities on surfaces. When surface coverage is complete, only a small amount of PEG is needed to confer a surface with PEG-like nonbinding properties. When short ethylene oxide oligomers are grafted to a surface as a self-assembled monolayer, it was found that as few as two ethylene oxide units were sufficient to make the surfaces nonadsorbing to proteins²⁸ when the ethylene oxide units were packed to a sufficient density.

Where the goal is to engineer specific cellular interactions into a cell scaffold, poly(ethylene glycol) provides an excellent background of low non-specific cellular interactions while allowing for the introduction of chemical moieties that might mediate desired interactions such as RGD²⁹-type peptides for cell adhesion or covalently linked growth factors³⁰ to accelerated the population of the neo-tissue.

1.5 Transglutaminase

1.5.1 Overview

Transglutaminase (EC 2.3.2.13) is a family of calcium-dependent enzymes which catalyze an amine- γ -glutaminy acyl-transfer reaction shown in Figure 1-3. The active site

in all transglutaminases is a cysteine sulfhydryl. The reaction occurs in two steps. First, the active site sulfhydryl displaces the γ -carboxamide to form a thioester with release of ammonia. This is presumably base-assisted in the active site, as has been shown to be the case for plasma transglutaminase³¹. The protonation of ammonia at physiological pH provides the driving force and virtual irreversibility of this reaction. In the second step, a primary amine displaces the sulfur, regenerating the free enzyme with the formation of an amide bond. In a side reaction, it has been shown that the enzyme-glutamine complex can also be hydrolyzed to glutamic acid and free enzyme³². Once formed, the γ -glutaminy amide bond is thought to be resistant to proteolysis³³.

Transglutaminase activity is found throughout the body, forming crosslinks that stabilize skin, hair and fibrin clots in wound healing. It also is involved in covalently stabilizing structures in the extracellular matrix of variety of tissues. Similar functions have been found in invertebrates, plants, unicellular eukaryotes as well as prokaryotes³³. Aside from the obvious utility of forming crosslinks to stabilize structure, the physiological function of transglutaminases are just beginning to be elucidated. Transglutaminase activity or overexpression has been implicated in programmed cell death³⁴, cell differentiation³⁵, cell adhesion^{36, 37}, initiation and propagation of inflammatory disease³⁸, neurological diseases involving protein aggregation³⁹ and cancer^{40, 41}.

A number of different molecules have been found to have an effect on transglutaminase expression *in vitro*. The most well-studied of these is retinoic acid. A

variety of cell types⁴²⁻⁴⁵ upregulate expression of tissue transglutaminase (TG_{II}) upon exposure to retinoic acid. However, in cultured keratinocytes, retinoic acid can suppress levels of keratinocyte transglutaminase (TG_K)⁴³ Other inducers include cAMP analogs in mouse macrophages⁴², TGF- in normal human epidermal cell⁴⁶ and sodium butyrate in transformed human lung fibroblasts⁴⁷.

1.5.2 Enzyme Variants

At least six transglutaminase variants have been characterized. Historically, they have been identified by a number of different designations. These are tabulated as adapted from a review³³ of the transglutaminase family in Table 1-1. Plasma and Tissue transglutaminase were the first to be identified and are by far the best characterized to date. These two enzymes will be discussed briefly below. Further information on other transglutaminases can be found in excellent reviews^{33, 48}.

Tissue transglutaminase (TG_{II}) was the first of the family to be discovered⁴⁹. TG_{II} is monomeric⁴⁸ and is not glycosylated⁵⁰ and does not contain disulfide bonds despite the presence of multiple cysteine residues⁵¹. Studies on TG_{II} almost exclusively use TG isolated from guinea pig liver, as this is a particularly rich source. In fact, TG_{II} is found in a variety of tissues at different levels: liver ~ spleen > heart, kidney and lung³³. Recently, TG_{II} has been implicated in an array of signaling processes including covalent stabilization of dimers in some cytokines such as IL-2⁵², crosslinking TGF to extracellular matrix⁵³ as well as a possibility of participation⁵³ in calcium-mediated signal transduction in the perinuclear space⁵⁴.

Factor XIII of the blood coagulation cascade is the best physiologically-characterized transglutaminase. It circulates in blood plasma as an inactive $\alpha_2\beta_2$ tetramer. The zymogen is activated by thrombin-mediated cleavage of the α -subunit to form Factor XIIIa. Found in monocytes, macrophages, megakaryocytes, platelets, uterus and placenta⁴⁸, the enzyme exists intracellularly as an α_2 dimer of approximately 83kD⁵⁵. It is free of glycosylation and disulfide bonds⁵⁵ and does not exhibit a typical secretion sequence^{56, 57}, all consistent with an intracellular protein. It is unknown how the α -subunit is excreted to form the extracellular $\alpha_2\beta_2$ tetramer³³ with the 80kD, glycosylated β -subunit⁵⁸.

1.5.3 Kinetics

A number of methods have been devised to measure the activity of transglutaminase-mediated reactions. Most assays involve the incorporation of a labeled amine substrate into a particular glutamine substrate. The label may be radioactive, as in the case of [¹⁴C]-methylamine incorporation into the B chain of oxidized insulin⁵⁹, [1,4-¹⁴C₂]putrescine into N,N'-dimethyl casein⁶⁰, [¹⁴C]-monodansyl cadaverine⁶¹ and others. Because of its excellent substrate properties⁶⁰ unlabelled monodansyl cadaverine is also useful as a fluorophore and a chromophore. These methods can be modified for activity measurements of new substrates by substituting for one of the pair of amine donors and acceptors.

The most versatile method for measurement of the concentration of active enzyme is hydroxylamine incorporation into benzyloxycarbonyl-glutaminy-glycine (ZQG). This

method (Appendix A4) can be scaled to multiple samples in 96-well plates and can be completed in as little as twenty minutes, depending on the number of samples. It should be noted that while ZQG is an excellent substrate for TG_{II}, it is a relatively poor substrate for other transglutaminases including plasma TG⁶².

For measuring the activity of substrates attached to poly(ethylene glycol) (PEG) it has been found useful to take advantage of the size differential between substrate probes and the PEG-bound substrate of interest. For measuring reaction curves on PEG-bound amine acceptor substrates, TG-mediated coupling to monodansyl cadaverine is monitored by size exclusion chromatography (SEC), as described in Appendix A5. For activity measurements on PEG-bound amine donor substrates, coupling to ZQG is measured in a similar manner, as described in Appendix A6.

The kinetics of transglutaminase reactions have been shown to follow a modified double-displacement mechanism^{59, 63, 64}, similar to mechanisms of other enzymes such as glucose-6-phosphatase, sucrose phosphorylase, and glutaminyl transpeptidase as noted in a review of transglutaminase activity⁶⁵. This is different from a standard double-displacement mechanism in that hydrolysis of acyl-enzyme intermediate is possible³². This mechanism accounts for the amine- γ -glutaminyl acyl-transfer function of transglutaminase as well as the observed limited esterase activity⁶³, a representative of the reverse reaction of that shown in Figure 1-3. While the transglutaminase reactions are reversible⁶⁶, under physiological conditions the reaction is driven to completion by the liberation of ammonia. In the presence of amine substrates, a hydrolysis reaction can also

be neglected⁶⁴ wherein the species 'A' in Figure 1-3 would be water, yielding a carboxylic acid as the product. Under the conditions of saturating amine substrate concentrations, the kinetics obey a Michaelis-Menton model:

$$\frac{d[P]}{dt} = \frac{k_{cat}[E]_t[S]}{K_m + [S]} \quad (1-1)$$

where [P], [E] and [S] are concentrations of the γ -glutaminy amide product, enzyme and amine acceptor, respectively. A number of different studies have been published on the substrate kinetics of amine acceptor substrates. Table 1-2 shows a compilation of synthetic glutamine substrates for which values of K_m and k_{cat} values have been published. Details of these substrates are discussed below.

1.5.4 Substrates

Transglutaminases require two substrates and exhibit very different levels of specificity for each. The amine acceptor, sometimes referred to as the acyl donor, is the first substrate to be covalently to the enzyme, and has relatively high specificity requirements. Reactivity of amine acceptors can be a function of primary as well as higher order structures^{50, 67, 68}. In contrast, the amine donor which nucleophilically displaces the enzyme from the amine acceptor does so with relatively lax specificity requirements^{60, 69, 70}. The ϵ -amino group of lysine as well as other polyfunctional amines found *in vivo* are excellent amine donors. A number of studies have been

published that give insight into the activity requirements for these two very different substrates. The details of these requirements, described below, refer to data collected with tissue transglutaminase (TG_{II} from guinea pig liver) except where noted, but are often generalizable to all transglutaminases.

Early studies on glutamine (amine acceptor) substrates focused on common proteins such as fibrinogen, casein and insulin⁷¹⁻⁷³. It was these early studies that suggested that peptide-bound glutamines were reactive whereas asparagines were not, in spite of the small single-methylene difference in structure. It was subsequently discovered that synthetic glutamine-containing peptides, namely benzyloxycarbonyl(Z)-L-glutaminyl-L-valine ethyl ester, were substrates for transglutaminase⁷⁴. Further, D-glutamine was dramatically less reactive than the L-form, and substitutions at the valyl site gave variations in activity⁷⁴. Folk and Cole performed what may be called the first quantitative work on defining the attributes of the amine acceptor substrate. They found that for L-glutamine-containing peptides, Z-L-glutaminyl-glycine (ZQG), ZQ and GGQG were substrates for TG but Q, QG and GQG were not^{75, 76}. This established the importance of distancing the amine terminus from the glutamine residue. The proximity of the glutamine to the carboxylate terminus was also found to be consistent with decreased activity, but to a smaller degree^{75, 76}. Curiously, replacing the Z-group in ZQG with other protecting groups such as methyloxycarbonyl, formyl, acetyl, propionyl, benzoyl and p-toluenesulfonyl reduced the reactivity by 2 to 20 times, underscoring the specificity of TG⁶⁵.

Detailed aspects of the glutamine binding pocket are described in detailed review⁷⁷. Experimental evidence points to a model of the glutamine binding site as a hydrophobic pocket of limited dimensions. Branching at either the β - or the γ -position relative to the carboxamide function precludes enzyme activity^{77, 78}. Further, it seems that the γ -position extends beyond the pocket, as hydrophobic substitutions at this site can actually enhance activity⁷⁸. Indeed this is the structure of glutamine where the so-called α -carbon of glutamine corresponds to the γ -position relative the carboxamide end-group. Observations of reactivities of a variety of model carboxamide compounds suggest a pocket dimension of approximately 2.5Å deep by 4.5-5.5Å in width⁷⁷, however these dimensions do not seem to define a fixed cylinder since both α -methylpropionamide and β -methylbutyramide act as competitive inhibitors⁷⁸. A flexible-pocket model is also consistent with the ultimate release of the acyl-transfer reaction product.

Interactions outside the binding pocket are important, but have proven difficult to precisely characterize. It is thought that both amide bonds on either side of glutamine residue contribute to productive binding and thereby higher kinetics, but are not essential⁷⁷. Structures even further removed from the active glutamine can strongly influence the reaction kinetics^{61, 67, 79}. One of the first systematic attempts to characterize the kinetic effects of the local peptide sequence on glutamine activity focused on substitutions of a single L-leucine (L) for the various glycines in N-formyl-gly₃-L-gln-gly₃ (fGGGQGGG)⁷⁹. It was found that methylamine and hydroxylamine incorporation was enhanced for fGGGQLGG and decreased for fGGLQGGG relative to fGGGQGGG.

All other substitution sites were found to be equivalent to fGGGQGGG. Another, more recent approach has been to examine variations of sequences from known protein substrates of high activity such as β -casein. Peptide variants of 15⁶⁷ and 10⁶⁸ amino acids in length on the local sequence of the TG-substrate glutamine in β -casein showed order of magnitude differences in the measured catalytic rate constant (k_{cat}) and substrate binding (K_{m}). Although there is only a tenuous link between the 3D conformation of β -casein and these short peptides the large differences in reactivity underscores the importance of 3^o structure in determining glutamine activity. Larger variability was measured for Factor XIII than for TG_{II}, but relative activities failed to correlate between Factor XIII and TG_{II} illustrating the differences in substrate specificity.

The amine substrate has a less restrictive specificity profile. In contrast to the strong specificity observed for glutamine substrates in particular peptides, a variety of amines can act as substrates. A number of small poly-functional amines are known substrates of TG *in vivo* with the notable exception of free peptides⁷².

Unfortunately much of what is known about the amine substrate specificity is based on extrapolations from inhibitor studies⁷⁷. These data indicate that the amine substrate binds in a somewhat geometrically restricted pocket akin to the glutamine binding pocket. In inhibitor studies with straight-chain and isobranched amines suggest that inhibitor potency drops off with the branch unit proximity to the primary amine⁷⁰. This trend continues until the ϵ -carbon where branching is inconsequential, similar to the

structure of lysine⁷⁰. Some advantage is also conferred by the L-configuration, again confirming the substrate specificity of peptide-bound L-lysine⁷⁰.

It has been suggested that two of the most important requirements for amine substrates are the amine pK_a and a hydrophobic region somewhat removed from the primary amine. Evidence for these effects is given by an elegant study by Lorand et al.⁶⁰ where a variety of straight chain substrates were assayed for activity by competition with monodansyl cadaverine (mdc). For example, dansyl-CH₂CH₂CH₂-S-CH₂NH₂ was found to be 7.7 times more active than mdc (dansyl-CH₂CH₂CH₂CH₂CH₂NH₂). This excess activity can be explained by the higher pK_a of mdc, with a slight (20%) correction for the girth of the sulfur. The importance of the hydrophobic pocket is exemplified in the effects of subtle modifications on the dansyl group of mdc (R-C₁₀H₆-SO₂NHC₃H₁₀NH₂, R=-NMe₂). Changing the R-group to R=H or R=-CH₂NMe₂ causes a 63% and 59% reduction in activity, respectively.

In an attempt to characterize an extended binding site, a series of pentapeptides were synthesized similar to the set discussed above for the amine acceptor site⁷⁰. A single leucine was substituted for one of each glycine in N-acetyl-gly₃-L-Lys-gly₃ (aGGGKGGG). The opposite positional relationship was found for lysyl-inhibition as was found for the amine acceptor binding site. The peptide aGGLKGGG was found to be a more potent inhibitor, and aGGGKLGG a less potent inhibitor than aGGGKGGG. This was found for both TG_{II} and Factor XIII.

Certain amides and esters can act as substrates for the reverse reaction. The reverse reaction, via acyl transfer as well as hydrolysis of transglutaminase has been

studied primarily with amides of ZQG⁶⁶ and esters of p-nitrophenyl^{64, 80, 81}, respectively. Both of these reactions tend to be one or two orders of magnitude smaller than the corresponding forward reaction for amide formation. Interestingly, the rate of TG-mediated amide hydrolysis is similar to the rate of ester hydrolysis, implicating the binding specificity as a more important factor than the hydrolytic stability of the bond itself.

1.5.5 Cofactors

Calcium is required for activity in all transglutaminases. By equilibrium dialysis, TG_{II} binds four calcium ions per molecule⁸¹. A calcium-induced conformational change is suggested by multiple lines of evidence. In the total absence of calcium, the active site sulfhydryl of TG_{II} is protected from inactivation by iodoacetamide³² and p-mercuribenzoate⁸². Exposure to calcium also alters the UV absorbance of TG_{II} at similar calcium concentrations⁸³. There is also suggestive evidence that calcium binding makes TG_{II} susceptible to calpain-mediated proteolysis⁵⁴.

Calcium binds to TG_{II} with two K_D values. The apparent TG_{II} calcium K_D as determined by spectral change and inactivation studies cited above is approximately 8mM. The K_D determined by spectral change⁸¹ gave constant values over the pH range of 5.6 to 9.0. However when measured by equilibrium dialysis⁸¹ the K_D was found to be 1mM, although the concentrations used were likely insensitive to higher K_D values as pointed out in a review by J. E. Folk and S. I. Chung⁶⁵. When measured by TG_{II} reactivity, two K_D values are apparent, consistent with the above results. The K_D as

measured by hydrolysis and esterase activity was measured to be 1-2mM^{32, 81}. For acyl transfer reactions, the calcium K_D was found to be 7mM⁸³.

Table 1-1: Transglutaminase FamilyAdapted from reference³³

Designation	Alternate Name	MW(kD)	Zymogen
Plasma Transglutaminase	Factor XIIIa, fibrin stabilizing factor, fibrinolygase, Laki-Lorand factor	83	a ₂ b ₂ tetramer b=80kD
Tissue Transglutaminase	TG _{II} , TG _c , type II-, cytosolic-, endothelial-, erythrocyte-, liver transglutaminase	77	no
Keratinocyte Transglutaminase	TG _K , type I-, particulate transglutaminase	90-membrane bound 80-soluble	no
Epidermal Transglutaminase	TG _E , type III-, bovine snout-, callus-, hair follicle transglutaminase	77	yes
Prostate Transglutaminase	TG _F , dorsal prostate protein I, major androgen-regulated prostate secretory protein, vesiculase	150-dimer	no
Hemocyte Transglutaminase	TG _H , Limulus transglutaminase	86	no

Table 1-2: Amine Acceptor Substrates

Substrate^a	Enzyme	k_{cat}(min⁻¹)	K_m(mM)^b	Conditions and Ref.
β-casein	TG _{II}	3.4	0.04	1
"	Factor XIII	98	0.03	1
Ser-Val-Leu-Ser-Leu-Ser-Gln-Ser-Lys-Val-Leu-Pro-Val-Pro-Glu	TG _{II}	87	0.4	1
"	Factor XIII	475	1.8	1
Ser-Gly-Leu-Ser-Leu-Ser-Gln-Ser-Lys-Val-Leu-Pro-Val-Pro-Glu	TG _{II}	158	1.4	1
"	Factor XIII	428	2.4	1
Ser-Val-Gly-Ser-Leu-Ser-Gln-Ser-Lys-Val-Leu-Pro-Val-Pro-Glu	TG _{II}	152	0.9	1
"	Factor XIII	654	12.9	1
Ser-Val-Leu-Ser-Gly-Ser-Gln-Ser-Lys-Val-Leu-Pro-Val-Pro-Glu	TG _{II}	210	1.8	1
"	Factor XIII	605	1.7	1
Ser-Val-Leu-Ser-Leu-Ser-Gln-Ser-Gly-Val-Leu-Pro-Val-Pro-Glu	TG _{II}	168	1.6	1
"	Factor XIII	47.6	23.8	1
Ser-Val-Leu-Ser-Leu-Ser-Gln-Ser-Lys-Gly-Leu-Pro-Val-Pro-Glu	TG _{II}	125	0.44	1
"	Factor XIII	124	1.4	1
Ser-Val-Leu-Ser-Leu-Ser-Gln-Ser-Lys-Val-Gly-Pro-Val-Pro-Glu	Factor XIII	141	2.5	1
Ser-Val-Leu-Ser-Leu-Ser-Gln-Ser-Lys-Val-Leu-Pro-Gly-Pro-Glu	TG _{II}	91	0.4	1
"	Factor XIII	401	1.8	1

Table 1-2 Continued: Amine Acceptor Substrates

Substrate^a	Enzyme	k_{cat}(min⁻¹)	K_m(mM)^b	Conditions and Ref.
Ser-Val-Leu-Ser-Leu-Ser-Gln-Ser-Lys-Gly-Gly-Pro-Gly-Pro-Glu	TG _{II}	159	5.2	1
"	Factor XIII	2.8	10.1	1
Ser-Val-Leu-Ser-Leu-Ser-Gln-Ser-Lys-Gly-Gly-Gly-Val-Pro-Glu	TG _{II}	167	1.9	1
"	Factor XIII	3.4	3.1	1
Ser-Val-Leu-Ser-Leu-Ser-Gln-Ser-Lys-Val-Leu	TG _{II}	23.4	3.5	1
"	Factor XIII	25.4	0.64	1
Ser-Leu-Ser-Gln-Ser-Lys-Val-Leu-Gly-Val-Pro-Glu	TG _{II}	162	1.5	1
"	Factor XIII	156	3.5	1
Gly-Gly-Gly-Gln-Gly-Lys(TFA) ^c -Val-Leu-Gly	TG _{II}	197	2.4	1
"	Factor XIII	93.7	6.1	1
Gly-Gly-Gly-Gln-Gly-Lys(TFA) ^c -Val-Leu-Gly-Gly	TG _{II}	210	3.1	1
"	Factor XIII	121	11.9	1
Leu-Gly-Leu-Gly-Gln-Gly-Lys-Val-Leu-Gly-NH ₂	TG _{II}	108	0.6	2
"	Factor XIII	377	1.0	2
Leu-Ser-Leu-Ser-Gln-Ser-Lys-Val-Leu-Gly-NH ₂	TG _{II}	181	1.2	2
"	Factor XIII	427	4.2	2
(Suc)Leu ^d -Gly-Leu-Gly-Gln-Gly-Lys-Val-Leu-Gly-NH ₂	TG _{II}	88	0.9	2
"	Factor XIII	433	3.5	2
(Suc) ^d Leu-Gly-Leu-Gly-Gln-Gly-Lys(Suc) ^c -Val-Leu-Gly-NH ₂	TG _{II}	257	1.5	2
"	Factor XIII	516	9.1	2

Table 1-2 Continued: Amine Acceptor Substrates

Substrate^a	Enzyme	k_{cat}(min⁻¹)	K_m(mM)^b	Conditions and Ref.
(Suc) ^d Leu-Gly-Gly-Gly-Gln-Gly-Lys(Suc) ^e -Val-Leu-Gly-NH ₂	TG _{II}	145	1.5	2
"	Factor XIII	734	5.3	2
Leu-Gly-Leu-Gly-Gln-Gly-Gly-Val-Leu-Gly-NH ₂	TG _{II}	302	3.7	2
"	Factor XIII	23.4	22.7	2
Leu-Gly-Leu-Gly-Gln-Gly-Ala-Val-Leu-Gly-NH ₂	TG _{II}	186	2.0	2
"	Factor XIII	173	4.8	2
(Suc) ^d Leu-Gly-Leu-Gly-Gln-Gly-Ala-Val-Leu-Gly-NH ₂	TG _{II}	351	1.7	2
"	Factor XIII	182	5.6	2
Leu-Gly-Leu-Gly-Gln-Gly-Arg-Val-Leu-Gly-NH ₂	TG _{II}	333	2.7	2
"	Factor XIII	278	3.7	2
(Suc) ^d Leu-Gly-Leu-Gly-Gln-Gly-Arg-Val-Leu-Gly-NH ₂	TG _{II}	104	1.7	2
"	Factor XIII	253	4.3	2
Leu-Gly-Leu-Gly-Gln-Gly-His-Val-Leu-Gly-NH ₂	TG _{II}	350	1.6	2
"	Factor XIII	263	4.2	2
Leu-Gly-Leu-Gly-Gln-Gly-Leu-Val-Leu-Gly-NH ₂	TG _{II}	115	0.9	2
"	Factor XIII	213	1.6	2
Leu-Gly-Leu-Gly-Gln-Gly-Lys-Ala-Leu-Gly-NH ₂	TG _{II}	115	3.1	2
"	Factor XIII	43.8	4.6	2
Leu-Gly-Leu-Gly-Gln-Gly-Lys-Val-Ala-Gly-NH ₂	TG _{II}	95	2.2	2
"	Factor XIII	21.3	5.5	2

Table 1-2 Continued: Amine Acceptor Substrates

Substrate^a	Enzyme	k_{cat}(min⁻¹)	K_m(mM)^b	Conditions and Ref.
Leu-Gly-Leu-Gly-Gln-Gly-Lys-Ala-Ala-Gly-NH ₂	TG _{II}	57.3	4.4	2
Leu-Gly-Leu-Gly-Gln-Gly-Lys-Leu-Val-Gly-NH ₂	TG _{II}	273	1.8	2
"	Factor XIII	104	3.3	2
Benzyloxycarbonyl-Gln-Gly	TG _{II}	200	7	3
Benzyloxycarbonyl-D-Gln-Gly	TG _{II}	0.21	36	3
Benzyloxycarbonyl-DL-β-methylGln-Gly	TG _{II}	-- ^f	-- ^f	3
Benzyloxycarbonyl-DL-γ-methylGln-Gly	TG _{II}	-- ^f	-- ^f	3
Formamide	TG _{II}	-- ^f	-- ^f	3
Acetamide	TG _{II}	0.5	1.7*10 ³	3
Propionamide	TG _{II}	1.9	0.9*10 ³	3
α-Methylpropionamide	TG _{II}	-- ^f	-- ^f	3
n-Butyramide	TG _{II}	3.3	2.8*10 ³	3
β-Methylbutyramide	TG _{II}	-- ^f	-- ^f	3
n-Valeramide	TG _{II}	1.9	0.6*10 ³	3
γ-Methylvaleramide	TG _{II}	13.4	1.5*10 ³	3
n-caproamide	TG _{II}	0.6	130	3

^a All peptide substrates are of the L configuration unless otherwise noted.

^b refers to apparent K_m

^c trifluoroacetyl-lysine

^d N-α-succinyl-leucine

^e N-ε-succinyl-lysine

^f No activity was detected after 24 hours.

Conditions and References:

1 - pH 7.45, 25°C, 0.1M Tris-Cl, 30mM NaCl, 1mM EDTA, 50mM CaCl₂, 1.5mM monodansyl cadaverine⁶⁷

2 - pH 7.45, 25°C, 0.1M Tris-Cl, 30mM NaCl, 1mM EDTA, 50mM CaCl₂, 1.5mM monodansyl cadaverine⁶⁸

3 - pH 7, 30°C, 0.1M Tris-Cl, 1mM EDTA, 50mM CaCl₂, 1mM methylamine⁶⁵

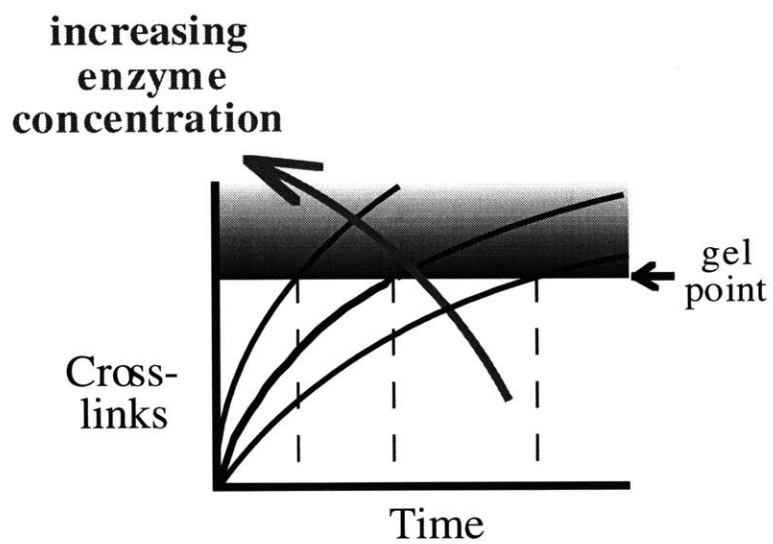


Figure 1-1. With enzymatic crosslinking gelation time can be controlled by modulating the enzyme concentration.

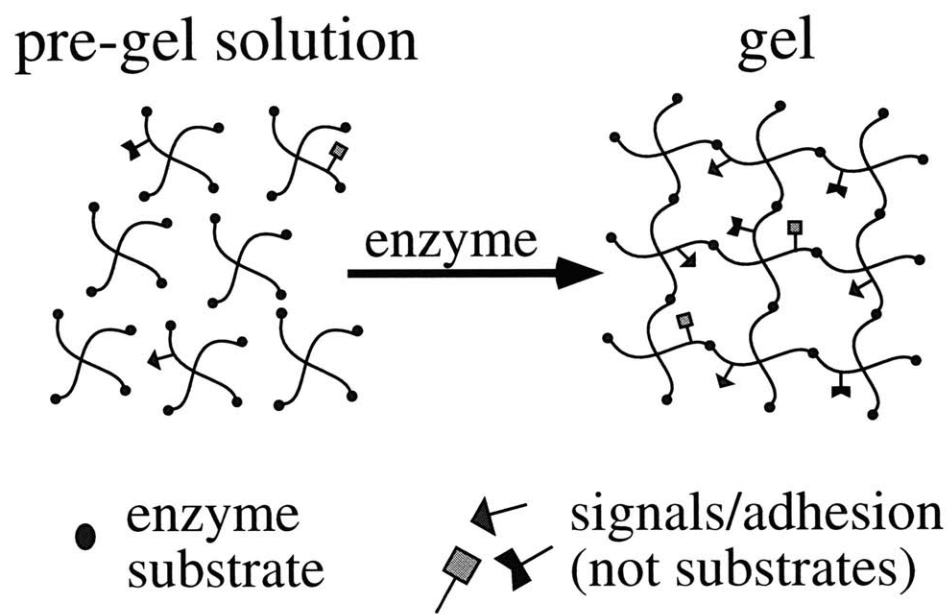


Figure 1-2. A crosslinking reaction that is specific for a particular substrate (circles) will leave other moieties free to interact with cells.

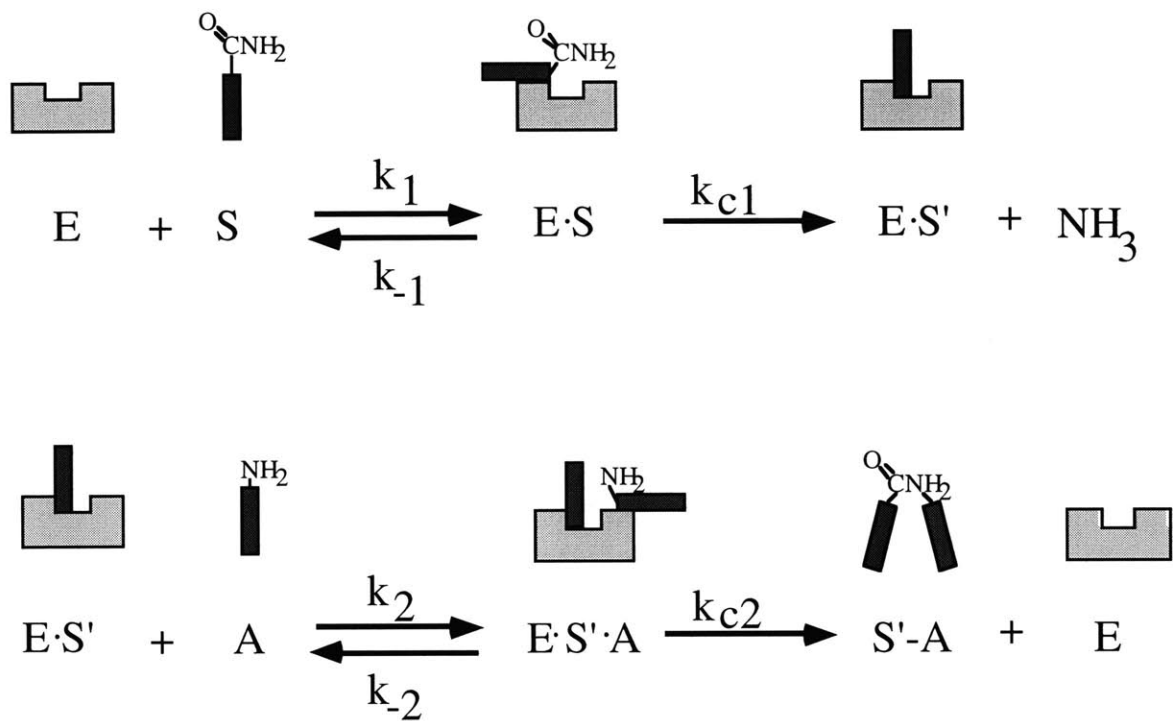


Figure 1-3. Kinetic mechanism for transglutaminase (E) crosslinking of an amine acceptor (S) to an amine donor (A).

1.6 References

1. Griffith, L.G., *et al.*, *Bioart. Org.*, "In vitro organogenesis of liver tissue," **831**: 382-397 (1997).
2. Kim, S.S., *et al.*, *Ann. Surg.*, "Survival and function of hepatocytes on a novel three-dimensional synthetic biodegradable polymer scaffold with an intrinsic network of channels," **228**(1): 8-13 (1998).
3. Falorni, A., Basta, G., Santeusanio, F., Brunetti, P. & Calafiore, R., *Pancreas*, "Culture maintenance of isolated adult porcine pancreatic islets in three-dimensional gel matrices: morphologic and functional results," **12**(3): 221-229 (1996).
4. Aebischer, P., *et al.*, *Nat. Med.*, "Intrathecal delivery of CNTF using encapsulated genetically modified xenogeneic cells in amyotrophic lateral sclerosis patients," **2**(6): 696-699 (1996).
5. Aebischer, P., *et al.*, *Transplantation*, "Transplantation in humans of encapsulated xenogeneic cells without immunosuppression - a preliminary report," **58**(11): 1275-1277 (1994).
6. Bellamkonda, R., Ranieri, J.P., Bouche, N. & Aebischer, P., *J. Biomed. Mater. Res.*, "Hydrogel-based three-dimensional matrix for neural cells," **29**: 663-671 (1995).
7. Yannas, I.V., *Adv. Polym. Sci.*, "Tissue regeneration templates based on collagen-glycosaminoglycan copolymers," **122**: 219-244 (1995).
8. Ishaug-Riley, S.L., Crane-Kruger, G.M., Yaszemski, M.J. & Mikos, A.G., *Biomaterials*, "Three-dimensional culture of rat calvarial osteoblasts in porous biodegradable polymers," **19**(15): 1405-1412 (1998).
9. Toolan, B.C., Frenkel, S.R., Pachence, J.M., Yalowitz, L. & Alexander, H., *J. Biomed. Mater. Res.*, "Effects of growth-factor-enhanced culture on a chondrocyte-collagen implant for cartilage repair," **31**: 273-280 (1996).
10. Dunnen, W.F.A.d., *et al.*, *J. Biomed. Mater. Res.*, "Biological performance of a degradable poly(lactic acid-ε-caprolactone) nerve guide: influence of tube dimensions," **29**: 757-766 (1995).
11. MacKay, S.M., Funke, A.J., Buffington, D.A. & Humes, H.D., *ASAIO J.*, "Tissue engineering of a bioartificial renal tube," **44**(3): 179-183 (1998).

12. Parenteau, N., *et al.*, *Biotech. Bioeng.*, "Biological and physical factors influencing the successful engraftment of a cultured human skin substitute," **52**(1): 3-14 (1996).
13. Brittberg, M., *et al.*, *New Engl. J. Med.*, "Treatment of deep cartilage defects in the knee with autologous chondrocyte transplantation," **331**(15): 889-895 (1994).
14. Aebischer, P., Goddard, M. & Tresco, P. in *Fundamentals of cell encapsulation and immobilization* (ed. Goosen, M.F.A.) 197-224 (CRC Press, Boca Raton, FL, 1993).
15. Hubbell, J.A., *Curr. Opin. Solid St. & Mat. Sci.*, "Synthetic biodegradable polymers for tissue engineering and drug delivery," **3**: 246-251 (1998).
16. Hubbell, J.A. & Langer, R., *Chem. Eng. News*, "Tissue engineering," **73**(11): 42-54 (1995).
17. Peppas, N.A. & Langer, R., *Science*, "New challenges in biomaterials," **263**: 1715-1720 (1994).
18. Ratner, B.D., *J. Biomed. Mater. Res.*, "The blood compatibility catastrophe," **27**: 283-287 (1993).
19. Courtney, J.M., Lamba, N.M.K., Sundaram, S. & Forbes, C.D., *Biomaterials*, "Biomaterials for blood-contacting applications," **15**(10): 737-744 (1994).
20. Merrill, E.W. in *Poly(ethylene glycol) chemistry, biotechnical and biomedical applications* (ed. Harris, J.M.) 199-220 (Plenum Press, New York, 1992).
21. Cima, L.G., Ingber, D.E., Vacanti, J.P. & Langer, R., *Biotech. Bioeng.*, "Hepatocyte culture on biodegradable polymeric substrates," **38**(2): 145-158 (1991).
22. Sawhney, A.S., Pathak, C.P. & Hubbell, J.A., *Macromol.*, "Bioerodible hydrogels based on photopolymerized poly(ethylene glycol)-co-poly(alpha-hydroxy acid) diacrylate macromers," **26**: 581-587 (1993).
23. Han, D.K., Park, K.D., Hubbell, J.A. & Kim, Y.H., *J. Biomater. Sci. Polym. Ed.*, "Surface characteristics and biocompatibility of lactide-based poly(ethylene glycol) scaffolds for tissue engineering," **9**(7): 667-680 (1998).
24. Zhao, X. & Harris, J.M. in *Poly(ethylene glycol)* (ed. Harris, J.M.) 458-472 (Am. Chem. Soc., Washington, 1997).

25. Smith-Mungo, L.I., *Matrix Biol.*, "Lysyl oxidase: Properties, regulation and multiple functions in biology," **16**(7): 387-398 (1998).
26. F E Bailey, J. & Koleske, J.V. *Poly(ethylene oxide)*, **1976**, Academic Press, New York.
27. Nagaoka, S., *et al.* in *Polymers as biomaterials* (eds. Shalaby, S.W., Hoffman, A.S., Ratner, B.D. & Horbett, T.A.) (Plenum Press, New York, 1985).
28. Prime, K.L. & Whitesides, G.M., *J. Am. Chem. Soc.*, "Adsorption of proteins onto surfaces containing end-attached oligo(ethylene oxide) - a model system using self-assembled monolayers," **115**(23): 10714-10721 (1993).
29. Pierschbacher, M.D. & Ruoslahti, E., *Nature*, "Cell attachment activity of fibronectin can be duplicated by small synthetic fragments of the molecule," **309**(3): 30-33 (1984).
30. Kuhl, P.R. & Griffith-Cima, L.G., *Nat. Med.*, "Tethered epidermal growth factor as a paradigm for growth factor-induced stimulation from the solid phase," **2**(9): 1022-1027 (1996).
31. Yee, V.C., *et al.*, *Proc. Natl. Acad. Sci. USA*, "Three-dimensional structure of a transglutaminase: human blood coagulation factor XIII," **91**: 7296-7300 (1994).
32. Folk, J.E., Cole, P.W. & Moolooly, J.P., *J. Biol. Chem.*, "Mechanism of action of guinea pig liver transglutaminase: V. the hydrolysis reaction," **243**(2): 418-427 (1968).
33. Aeschlimann, D. & Paulsson, M., *Thrombosis and Haemostasis*, "Transglutaminase: protein cross-linking enzymes in tissues and body fluids," **71**(4): 402-415 (1994).
34. Amendola, A., *et al.*, *P. Natl. Acad. Sci. USA*, "Induction of "tissue" transglutaminase in HIV pathogenesis: Evidence for high rate of apoptosis of CD4(+) T lymphocytes and accessory cells in lymphoid tissues," **93**(20): 11057-11062 (1996).
35. Hand, D., Campoy, F.J., Clark, S., Fisher, A. & Haynes, L.W., *J. Neurochem.*, "Activity and distribution of tissue transglutaminase in association with nerve muscle synapses," **61**(3): 1064-1072 (1993).
36. Gentile, V., Thomazy, V., Piacentini, M., Fesus, L. & Davies, P.J.A., *J. Cell Biol.*, "Expression of tissue transglutaminase in balb-c 3T3 fibroblasts - effects on cellular morphology and adhesion," **119**(2): 463-474 (1992).

37. Borge, L., Demignot, S. & Adolphe, M., *Biochim. Biophys. Acta - Mol. Cell Res.*, "Type II transglutaminase expression in rabbit articular chondrocytes in culture: Relation with cell differentiation, cell growth, cell adhesion and cell apoptosis," **1312**(2): 117-124 (1996).
38. Raghunath, M., *et al.*, *J. Clin. Invest.*, "Cross-linking of the dermo-epidermal junction of skin regenerating from keratinocyte autografts - Anchoring fibrils are a target for tissue transglutaminase," **98**(5): 1174-1184 (1996).
39. Zhang, W., Johnson, B.R., Suri, D.E., Martinez, J. & Bjornsson, T.D., *Acta Neuropathol.*, "Immunohistochemical demonstration of tissue transglutaminase in amyloid plaques," **96**(4): 395-400 (1998).
40. Johnson, T.S., *et al.*, *Oncogene*, "Transfection of tissue transglutaminase into a highly malignant hamster fibrosarcoma leads to a reduced incidence of primary tumor-growth," **9**(10): 2935-2942 (1994).
41. Hettasch, J.M., *et al.*, *Lab. Invest.*, "Tissue transglutaminase expression in human breast cancer," **75**(5): 637-645 (1996).
42. Chiocca, E.A., Davies, P.J.A. & Stein, J.P., *J. Cell. Biochem.*, "Regulation of tissue transglutaminase gene expression as a molecular model for retinoid effects on proliferation and differentiation," **39**: 293-304 (1989).
43. Lichti, U., Ben, T. & Yuspa, S.H., *J. Biol. Chem.*, "Retinoic acid induced transglutaminase in mouse epidermal cells is distinct from epidermal transglutaminase," **264**: 19308-19312 (1985).
44. Suedhoff, T., Birckbichler, P.J., Lee, K.N., Conway, E. & M K Paterson, J., *Cancer Res.*, "Differential expression of transglutaminase in human erythroleukemia cells in response to retinoic acid," **50**: 7830-7834 (1990).
45. Rubin, A.L. & Rice, R.H., *Cancer Res.*, "Differential regulation by retinoic acid and calcium of transglutaminases in cultured neoplastic and normal human keratinocytes," **46**: 2356-2361 (1986).
46. George, M.D., Vollberg, T.M., Floyd, E.E., Stein, J.P. & Hetten, A.M., *J. Biol. Chem.*, "Regulation of transglutaminase type II by transforming growth factor-beta 1 in normal and transformed human epidermal keratinocytes," **265**: 11098-11104 (1990).
47. Birckbichler, P.J., *et al.*, *Biochim. Biophys. Acta*, "Enhanced transglutaminase activity in transformed human lung fibroblast cellser exposure to sodium butyrate," **723**: 27-34 (1983).

48. Greenberg, C.S., Birckbichler, P.J. & Rice, R.H., *FASEB*, "Transglutaminases: multifunctional cross-linking enzymes that stabilize tissues," **5**: 3071-3077 (1991).
49. Borsook, H., Deasy, C.L., Haagen-Smit, A.J., Keighley, G. & Lowy, P.H., *J. Biol. Chem.*, "The incorporation of labeled lysine into the proteins of guinea pig liver homogenate," **179**: 689-705 (1949).
50. Folk, J.E. & Finlayson, J.S., *Adv. Protein Chem.*, "The epsilon-(gamma-glutaminy)lysine cross-link and the catalytic role of transglutaminases," **31**: 1-133 (1977).
51. Nakanishi, K., *et al.*, *Eur. J. Biochem.*, "Cloning and sequence analysis of cDNA clones for bovine aortic-endothelial-cell transglutaminase," **202**: 15-21 (1991).
52. Eitan, S. & Schwartz, M., *Science*, "A transglutaminase that converts interleukin-2 into a factor cytotoxic to oligodendrocytes," **261**(5117): 106-108 (1993).
53. Nunes, I., Gleizes, P.E., Metz, C.N. & Rifkin, D.B., *J. Cell Biol.*, "Latent transforming growth factor-beta binding protein domains involved in activation and transglutaminase-dependent cross-linking of latent transforming growth factor-beta," **136**(5): 1151-1163 (1997).
54. Zhang, J., Lesort, M., Guttmann, R.P. & Johnson, G.V.W., *J. Biol. Chem.*, "Modulation of the in situ activity of tissue transglutaminase," **273**(4): 2288-2295 (1998).
55. Takahashi, N., Takahashi, Y. & Putnam, F.W., *Proc. Natl. Acad. Sci. USA*, "Primary structure of blood coagulation factor XIIIa (fibrinolygase, transglutaminase) from human placenta," **83**: 8019-8023 (1986).
56. Grundmann, U., Amann, E., Zettlmeissl, G. & Kupper, H.A., *Proc. Natl. Acad. Sci. USA*, "Characterization of cDNA coding for human factor XIIIa," **83**: 8024-8028 (1986).
57. Ichinose, A., Hendrickson, L.E., Fujikawa, K. & Davie, E.W., *Biochem.*, "Amino acid sequence of the a-subunit of human factor XIII," **25**: 6900-6906 (1986).
58. Ichinose, A., McMullen, B.A., Fujikawa, K. & Davie, E.W., *Biochem.*, "Amino acid sequence of the b-subunit of human factor XIII, a protein composed of ten repetitive segments," **25**: 4633-4638 (1986).
59. Chung, S.I. & Folk, J.E., *J. Biol. Chem.*, "Kinetic studies with transglutaminases: the human blood enzymes (activated coagulation factor XIII) and the guinea pig hair follicle enzyme," **247**(9): 2798-2807 (1972).

60. Lorand, L., *et al.*, *Biochem.*, "Specificity of guinea pig liver transglutaminase for amine substrates," **18**(9): 1756-1765 (1979).
61. Gorman, J.J. & Folk, J.E., *J. Biol. Chem.*, "Structural features of glutamine substrates for human plasma factor XIIIa (activated blood coagulation factor XIII)," **255**(2): 419-427 (1980).
62. Maticic, S. & Loewy, A.G., *Biochem. Biophys. Res. Commun.*, "Transglutaminase activity of the fibrin crosslinking enzyme," **24**(6): 858-866 (1966).
63. Folk, J.E., *J. Biol. Chem.*, "Mechanism of action of guinea pig liver transglutaminase: VI. order of substrate addition," **244**(13): 3707-3713 (1969).
64. Chung, S.I., Shranger, R.I. & Folk, J.E., *J. Biol. Chem.*, "Mechanism of action of guinea pig liver transglutaminase: VII. Chemical and stereochemical aspects of substrate binding and catalysis," **245**(23): 6424-6435 (1970).
65. Folk, J.E. & Chung, S.I., *Adv. Enz.*, "Molecular and catalytic properties of transglutaminases," **38**: 109-191 (1973).
66. Gross, M. & Folk, J.E., *J. Biol. Chem.*, "Activity of guinea pig liver transglutaminase toward ester analogs of amide substrates," **249**(10): 3021-3025 (1973).
67. Gorman, J.J., *J. Biol. Chem.*, "Structural features of glutamine substrates for transglutaminases: specificities of human plasma factor XIIIa and the guinea pig liver enzyme toward synthetic peptides," **256**: 2712-2715 (1981).
68. Gorman, J.J. & Folk, J.E., *J. Biol. Chem.*, "Structural features of glutamine substrates for transglutaminases: role of extended interactions in the specificity of human plasma factor XIIIa and the guinea pig liver enzyme," **259**: 9007-9010 (1984).
69. Schrode, J. & Folk, J.E., *J. Biol. Chem.*, "Stereochemical aspects of amine substrate attachment to acyl intermediates of transglutaminases: human blood plasma enzyme (activated coagulation factor XIII) and guinea pig liver enzyme," **254**(3): 653-661 (1979).
70. Gross, M., Whetzel, N.K. & Folk, J.E., *J. Biol. Chem.*, "Amine binding sites in acyl intermediates of transglutaminases," **252**(11): 3752-3759 (1977).
71. Clarke, D.D., Neidle, A., Sarkar, N.K. & Waelsch, H., *Arch. Biochem. Biophys.*, "Metabolic activity of protein amide groups," **71**: 277-279 (1957).

72. Clarke, D.D., Mycek, M.J., Neidle, A. & Waelsch, H., *Arch. Biochem. Biophys.*, "The incorporation of amines into protein," **79**: 338-354 (1959).
73. Mycek, M.J., Clarke, D.D., Neidle, A. & Waelsch, H., *Arch. Biochem. Biophys.*, "Amine incorporation into insulin as catalyzed by transglutaminase," **84**: 528-540 (1959).
74. Neidle, A. & Acs, G., *Fed. Proc.*, "Substrate requirements of transglutaminase," **20**: 234 (1961).
75. Folk, J.E. & Cole, P.W., *Biochim. Biophys. Acta*, "Transglutaminase: mechanistic features of the active site as determined by kinetic and inhibitor studies," **122**: 244-264 (1966).
76. Folk, J.E. & Cole, P.W., *J. Biol. Chem.*, "Structural requirements of specific substrates for guinea pig liver transglutaminase," **240**(7): 2951-2960 (1965).
77. Folk, J.E., *Adv. Enz.*, "Mechanism and basis for specificity of transglutaminase-catalyzed epsilon-(gamma-glutamyl) lysine bond formation," **54**: 1-56 (1983).
78. Gross, M. & Folk, J.E., *J. Biol. Chem.*, "Mapping of the active site of transglutaminase," **248**(4): 1301-1306 (1973).
79. Gross, M., Whetzel, N.K. & Folk, J.E., *J. Biol. Chem.*, "The extended active site of guinea pig liver transglutaminase," **250**(12): 4648-4655 (1975).
80. Folk, J.E., Cole, P.W. & Mullooly, J.P., *J. Biol. Chem.*, "Mechanism of action of guinea pig liver transglutaminase," **242**(19): 4329-4333 (1967).
81. Folk, J.E., Cole, P.W. & Mullooly, J.P., *J. Biol. Chem.*, "Mechanism of action of guinea pig liver transglutaminase: III the metal-dependent hydrolysis of p-nitrophenyl acetate; further observations on the role of metal in enzyme activation," **242**(11): 2615-2621 (1967).
82. Connellan, J.M., Chung, S.I., Whetzel, N.K., Bradley, L.M. & Folk, J.E., *J. Biol. Chem.*, "Structural Properties of guinea pig liver transglutaminase," **246**(4): 1093-1098 (1971).
83. Folk, J.E., Mullooly, J.P. & Cole, P.W., *J. Biol. Chem.*, **242**: 1838 (1967).

2 TRESYL-MEDIATED SYNTHESIS

2.1 Background

Covalent linkage of peptides and small molecules to poly(ethylene glycol) end groups is a core synthetic method used in this work. To avoid the introduction of superfluous chemical moieties, zero-length crosslinking agents were desired. From the family of potential chemistries, tresyl chloride (2,2,2-trifluoroethanesulfonyl chloride) was chosen on the basis of reported high conversions in aqueous media as well as ideal reactivity, reported as moderate coupling rates with only slow hydrolysis of the tresyl group under the appropriate conditions¹. During the course of this work the definition of ‘appropriate conditions’ had become less certain, as it has become apparent that a second side reaction can reduce yields via an addition/elimination at the carbon β to the trifluoro group²⁻⁴. In light of this new information a comprehensive study of tresyl-mediated synthesis was undertaken.

Nearly two decades ago, 2,2,2-trifluoroethanesulfonyl chloride (tresyl chloride) was introduced as a more reactive alternative to p-toluenesulfonyl chloride (tosyl chloride) in activating hydroxyl groups to covalent modification for the preparation of affinity chromatography supports¹. Tresyl chloride is widely used in solid support activation as well as in poly(ethylene glycol) (PEG) activation for PEG-modification of small drugs and proteins for biological stabilization and immuno-modulation⁵.

It had long been assumed that the reaction mechanism for tresyl-mediated coupling was identical to that of tosyl chloride and other sulfonyl chlorides where the substituted sulfonyl acts as a leaving group. Recently it has been suggested that alternative mechanisms may prevail. Demiroglou et al.⁶ proposed a mechanism in which the sulfonyl sulfur is retained throughout the entire coupling reaction. On the basis of experimental evidence, Gais and Ruppert² as well as King and Gill^{3, 4} corrected this postulated mechanism to include nucleophile addition by an β -elimination/Michael-type addition reaction. The present understanding of tresyl reactions in aqueous media include three pathways (Figure 2-1): hydrolysis, nucleophilic displacement, and β -elimination / addition.

The studies described here were carried out with the objective of developing predictive kinetic models to optimize coupling reaction yield as a function of substrate properties and reaction conditions.

2.2 Experimental Design

Experimental work regarding tresyl chloride-mediated coupling has been focused on determining the molecular structure of reaction products, yet for practical application of tresyl-mediated coupling it is necessary to know how reaction conditions may affect the coupling yield. To optimize the amount of secondary amine linkages, it is necessary to formulate a model that is at least empirically valid, that accurately predicts yields in a useful rate of reaction conditions. In elucidating the effects of pH, temperature and steric

effects, Figure 2-1 has been taken as a starting point in defining effective rate constants that govern the reaction network for tresylate reactions. These rates may not represent elementary rate constants in all cases, but if tempered across an experimental space of temperature, reaction pH, nucleophile steric factors and nucleophile pK_a , should provide the necessary information to reliably predict ideal synthesis conditions.

A number of reaction pathways for tresylated species have recently been elucidated, yet kinetic data which could be used to maximize desired products is somewhat limited. The goal of this work is to measure apparent rate constants for a reaction network that describes the set of possible reactions for the displacement of tresyl groups by primary amines in an aqueous environment as a function of pH temperature and steric factors. This has been undertaken in two steps. First, in the absence of an amine nucleophile, rate constants for hydrolysis and hydroxyl-mediated tresylate conversion were measured. Second, with knowledge of the solvent-mediated reactions, rate constants for coupling of various primary amine species were measured by fitting to a kinetic model consistent with known reaction mechanisms.

Tresylated poly(ethylene glycol) (PEG-Tr) has been used as a model in these studies. This offers the advantage of being identical or a close approximation of the synthesis product of interest. There is an analytical advantage in coupling small molecules to a larger polymer such as PEG in that the reaction progress can be readily monitored by size-based separation methods such as size exclusion chromatography. However analysis of the end products becomes that much more difficult as the presence of the PEG chain dilutes any measurement of end groups. Since work to date found in

the literature has focus almost entirely on end group structure, as noted above, the use of PEG-Tr as a model seemed an obvious choice.

2.3 Experimental Methods

Synthesis of tresylated PEG. Tresylation was performed by a method similar to that of Nilsson and Mosbach⁷, as detailed in Appendix A1. In the present study, dihydroxyl PEG (6000MW) (Fluka) was used as the starting material. As trace amounts of residual base may have a significant effect on the outcome of tresyl-mediated reactions, the amount of residual base following purification was assayed by ¹H-NMR. Residual triethylamine was found to be 0.02wt%. Based on sulfur elemental analysis, tresylation was approximately 100%, with 3.08 g/mmolTr [52.2%C, 8.54%H, 1.04%S]. Each tresyl group (= [1], see Figure 2-1) of PEG-Tr₂ is assumed to react independently, therefore designations 'PEG-Tr' and 'PEG-Tr₂' are used interchangeably.

Measurement of Isolated Hydrolysis Reaction. Progress of the hydrolysis reaction was monitored by continuous titration. A weighed amount of PEG-Tr₂ (about 50mg) was added to a measured volume (about 100mL) of Milli-Q water. The solution was stirred continuously. Dilute potassium hydroxide (20mM) was added as needed to maintain the pH within 0.05 units of desired pH as measured by a standard calomel electrode. The amount and time of addition of each acid aliquot was recorded. Continuous titration experiments were run at 22 ± 1 °C with pH 6.0, 7.0, 7.5, 8.0, 8.5, 9.0, and at 4 ± 0.2 °C with pH 8.0, 8.5, 9.0. Each continuous titration reaction was monitored for 80 minutes.

For slower reactions at 4 ± 0.2 °C with pH 5.0, 6.0 and 7.0, base was required much less often to maintain the desired pH. In these three conditions, the rate of acid evolution was measured by the rate of pH change, where the pH was always maintained within ± 0.1 pH units of the desired level. These three slower reactions were run at higher PEG-Tr₂ concentrations (about 2mg/mL) and were maintained over a number of days, with frequent recalibration of the pH meter.

The measurement of moles of base added to maintain constant pH was used to calculate moles of tresyl groups consumed. By reaction stoichiometry four moles of base are required to neutralize the acid evolved by the conversion of R-Tr to R-OSO₂CH₂COO⁻, and one mole of base is required to neutralize the hydrolysis of R-Tr to R-OH and ⁻OSO₂CH₂CF₃. The fractional conversion of tresyl groups (X_{Tr}) was calculated on the basis of the weight of PEG-Tr₂ used in each experiment (measured to $\pm 0.1\%$), using the value of 3.08 gPEG/mmolTr noted above, confirmed by total hydrolysis of PEG-Tr₂.

Measurement of Simultaneous Coupling/Hydrolysis Reaction. A measured amount of PEG-Tr to make a final concentration of 40mM in tresyl was added to a solution 100mM in primary amine and 400mM in potassium phosphate at the desired pH. The extent of the coupling reaction was measured as a function of time by periodic sampling of the reaction solution by a HPLC Hitachi L-7200 autosampler. The aliquot was immediately injected onto one TSK G4000PW and one TSK G2000PW column in series. The mobile phase was 0.50M sodium chloride with 10mM potassium phosphate

and 4% acetonitrile at pH 4 delivered by a Hitachi L-7100 pump. Detection was by a Hitachi L-7420 UV-vis detector at 260nm where PEG-Tr has an insignificant absorbance. For each measurement the fraction of amine bound to PEG was calculated as the integral of absorbance at 260nm for the PEG peak (first to elute) divided by the total integral (PEG peak + free amine peak). Amines examined (Figure 2-2) include glycyL-DL-phenylalanine (Gly-Phe from Sigma), L-phenylalanine (Phe from Aldrich), and N²-(Carbobenzyloxy)-L-lysine (α CBZ-Lys from Aldrich). All amines were examined at 4°C and 22°C.

Algorithm for Rate Constant Fitting. Whereas analytical solutions to rate equations were unavailable, rate constants were fit using standard Fortran models extracted from Numerical Recipes⁸ as given in Appendix C.

The data was separated for rate constant analysis by nucleophile (n=3) and by temperature (n=2). For each of these six data groups rate constants were optimized by the LM method for all pH's simultaneously.

2.4 Results and Discussion

2.4.1 Rate Constants for Hydrolytic Processes

Hydrolysis is an unavoidable side effect of aqueous tresyl-mediated synthesis. Attempts have been made to utilize the tresyl leaving group in non-aqueous conditions to side step this issue. Unfortunately, even at 70°C in one of the most polar solvents, dimethylformamide, typical rates were on the order of ~1% per day, or a half-life of

about 70 days, an unacceptable rate for our purposes. Therefore tresyl-mediated syntheses are most appropriately conducted in aqueous conditions, optimally where hydrolysis is minimized.

King and Gill have shown that the ethyl trifluoroethanesulfonate in the absence of a nucleophile will hydrolyze to different species depending on the solution pH⁴ as can be inferred from Figure 2-3. They reported data at 25°C supporting a traditional sulfonate ester hydrolysis pathway (first order rate constant = k_w) at low pH and reversible E1cB reaction at high pH (pseudo-first order rate constant = $k_{OH}[OH^-]$) in which the first step is rate limiting. Given the set of reactions in Figure 2-3, the disappearance of PEG-Tr (1), can be written as:

$$-\frac{d[\text{PEG} - \text{Tr}]}{dt} = (k_w + k_{OH}[OH^-]) \cdot [\text{PEG} - \text{Tr}]$$

$$\text{where, } k_{OH} = \frac{k_{E1}^{\text{fwd}} k_{E1,2}}{k_{E1}^{\text{rev}}[H_2O] + k_{E1,2}}$$

The integrated form of this equation in terms of conversion ($\equiv X_{Tr}$) is

$$-\ln(1 - X_{Tr}) = (k_w + k_{OH}[OH^-]) \cdot t = k_{h,app} \cdot t$$

$$\text{where, } X_{Tr} = 1 - \frac{[\text{PEG} - \text{Tr}]}{[\text{PEG} - \text{Tr}]_0}$$

This equation implies that a plot of $-\ln(1-X_{Tr})$ versus time would be linear, with the slope equal to $(k_w + k_{OH}[OH^-])$. By varying the pH, unique values for k_w and k_{OH} can be computed. Data for hydrolysis reactions is plotted in Figure 2-4 at 4°C for pH 8-9 and 22°C for pH 6-9.

Our data for the hydrolysis of tresylated PEG at 4°C and 22°C supports the model given in Figure 2-3. Linearity of the $\ln(1 - X_{Tr})$ plot (Figure 2-4) confirms that the first hydrolysis step is rate limiting under almost all conditions studied. The pH9.0 22°C reaction deviates somewhat from linearity, indicating that one or more of the multiple steps between (3) and (4) of Figure 2-1 may be limiting in the high pH regime.

To derive rate constants, k_w and k_{OH} , the apparent hydrolysis rate, $k_{h,app}$, was fit by a least-squares method to $k_{h,app} = k_w + k_{OH}[OH^-]$ separately for 4°C and 22°C as shown in Figure 2-5. Table 2-1 shows the rate constants fit to the data in Figure 2-5.

The hydrolysis rate constant, k_w , was found to be a stronger function of temperature than k_{OH} , the apparent rate constant for the addition-elimination pathway. The low temperature dependence of k_{OH} may point to a significant influence of k_{E1}^{rev} , consistent with a reversible E1cB mechanism. Because k_w is of a similar order of magnitude as $k_{OH}[OH^-]$ around room temperature and slightly basic pH's, this difference in temperature dependence might allow for the control of the distribution of products by manipulating pH and temperature. This will depend on the kinetics of S_N2 nucleophilic displacement discussed below.

2.4.2 Development of a Tresyl-Mediated Coupling Model

It has been suggested that there are at least two pathways by which nucleophilic amines can couple to tresylated species (Figure 2-1)²⁻⁴. The first pathway involves a S_N2 nucleophilic displacement, similar to that which is observed for other sulfonate leaving groups. This S_N2 pathway is thought to be minor or undetectable at very high pH⁴. At high pH, the second pathway has been observed that is thought to go through an addition-elimination intermediate (3)³. This intermediate can undergo further modifications to an inactive product (4), or it can react with an amine to give a coupled product (6).

The apparent first order rate dependence of the addition-elimination pathway for hydrolysis suggests that $k' \gg k_{OH}[OH^-]$. This implies that as (3) is formed it is rapidly converted to a mixture of (4) and (6), such that $[3] \ll [1]$. We can describe the fraction of (3) that becomes (6) as α , given by the following approximation:

$$\frac{d[6]}{dt} \sim \alpha \cdot (k_1[OH^-][1])$$

$$\text{where, } \alpha = \frac{k_2[N:]}{k_2[N:] + k'} ; [N:] \equiv \text{unprotonated amine}$$

As suggested by the hydrolysis experiments, the above assumption should hold at least for $pH \leq \sim 9.0$. Because reactions governed by k_2 and k' are downstream of the rate limiting step, (1 \rightarrow 3), the absolute magnitudes of k_2 and k' cannot be measured independently. Only the ratio k_2/k' can be calculated.

The rate constants k_w and k_{OH} are known from the previous section (Table 2-1). Here we will fit k_1 and k_2/k' for each amine species at each temperature, based on measured coupling data for a set of model amines. Based on Figure 2-1 and the above approximation, we can write the following differential equations that describe the concentrations of the reaction components as a function of time:

$$\frac{d[1]}{dt} = -(k_w + k_{OH}[OH^-] + k_1[N :]) \cdot [1]$$

$$\frac{d[2]}{dt} = k_w[1]$$

$$\frac{d[4]}{dt} = (1 - \alpha)k_{OH}[OH^-][1]$$

$$\frac{d[5]}{dt} = k_1[N :][1]$$

$$\frac{d[6]}{dt} = \alpha k_{OH}[OH^-][1]$$

$$\frac{d[N]_{total}}{dt} = -(k_1[N :] + \alpha k_{OH}[OH^-]) \cdot [1]$$

The $[OH^-]$ concentration was calculated using the measured pH and the ion product of water, K_w , at the appropriate temperature (see Table 2-2):

$$[OH^-] = K_w(T) \cdot 10^{pH}$$

The concentration of unprotonated amine was calculated from an algebraic variant of the Henderson-Hasselbach equation as:

$$[N:] = [N]_{\text{total}} \cdot \frac{10^{\{\text{pH} - \text{pK}_a(T)\}}}{1 + 10^{\{\text{pH} - \text{pK}_a(T)\}}}$$

Both K_w and the pK_a for each amine species vary with temperature (Table 2-2). The pK_a 's for the various amine species were adjusted for temperature based on the van't Hoff equation by:

$$\text{pK}_a(T_2) = \text{pK}_a(T_1) - \log \left\{ \exp \left[-\frac{\Delta H^\circ}{R} \left(\frac{1}{T_1} - \frac{1}{T_2} \right) \right] \right\}$$

The temperature adjustments to the pK_a is significant, yet small enough to allow for use of approximate values for ΔH° . For example, variations in ΔH° on the order of 10kJ/mol imply differences in pK_a of only 0.1 pH unit at 4°C. The heat of ionization for the α -amine of phenylalanine was taken as 44 kJ/mol⁹. The heat of ionization for the α -amine of glycyl-phenylalanine was also approximated as 44 kJ/mol based on the observation that chemical substituents removed from the α -amine have little effect on the ΔH° . For example, enthalpy literature values for similar molecules such as glycine¹⁰, glycylglycine¹¹ and phenylalanine (above) were all given as 44 kJ/mol. The heat of

ionization for the α -amine of α -CBZ-lysine was assumed to be similar to α -dimethyl-lysine¹² at 52 kJ/mol. Heat capacities, defined as the change in ΔH° with temperature, were assumed to be insignificant based on typical literature values. For example, the heat capacity for a prototypical α -amine of glycine¹⁰, predicts only a 0.2kJ/mol difference in ΔH° between 4°C and 22°C.

To test the robustness of this tresyl reaction network model, we chose to experimentally study three model amine compounds (Figure 2-2) -- a high pK_a species, α CBZ-lysine; a low pK_a species, glycyL-phenylalanine; and a more sterically hindered amine of intermediate pK_a , phenylalanine -- to probe for possible steric inhibition. Based on the results from the hydrolysis experiments, a pH range of 7.5-8.5 was chosen for study so that $k_{OH}[OH^-]$ is of the same order as k_w for maximum resolution of the various pathways. Experiments at room temperature (22°C) and in a 4°C cold room were conducted to measure the effects of temperature.

Figure 2-6 shows measured reaction time courses and curves predicted by the model for the three model amines at three pH's and two temperatures. The best-fit rate constants from the chi-squared minimization fitting routine are given in Table 2-3. The model reaction network (Figure 2-1) was able to fit the observed data quite well considering that a single set of rate constants were fit to all pH values simultaneously. In all cases, the model was able to capture the long time behavior trend as a function of reaction pH, as well as the final conversion. The transient behavior was also fit acceptably well in all cases, with the exception of phenylalanine at 22°C (Figure 2-6c).

The transient portion of Figure 2-6c suggest a weaker dependence on pH than predicted with [N:] as the driving force, possibly due to an effect of the proximity of the carboxylate group to the nucleophilic amine.

2.4.3 Temperature Effects

The reaction temperature can have a profound influence on the kinetics and product distribution in tresyl-mediated reactions as illustrated in Figure 2-6. In general it can be said that room temperature reactions lead to higher total coupling yields. Yet, our data suggest that the distribution of the coupled products, (5) and (6), can also be affected by temperature.

Our data suggest that lower temperatures, a higher proportion of (5) is formed relative to (6). This is evident from the temperature influence on the initial step of the reaction. Whereas k_w and k_{OH} appear to have significant temperature dependencies, k_1 appears to be only slightly affected by temperature. This suggests that lowering the temperature serves to increase the relative yield of (5). The ratio of k_2/k' is also a function of temperature. The apparent activation energy of k_2 is higher than that of the hydrolysis rate constant, k' , as suggested by our data (Table 2-3). Thus, our data indicate that higher temperatures yield more (6) relative to (4). It should be noted that higher temperatures also contributes to increased hydrolysis through the (1→2) pathway.

Temperature also has a small, but significant effect on pK_w and the pK_a 's of the amines as shown in Table 2-2.

2.4.4 pH Effects

Increasing the pH of the reaction solution increases the rate of conversion of tresyl species, through the addition-elimination pathway as well as the amine-nucleophilic displacement pathway shown in Figure 2-1. Increasing the hydroxyl concentration increases the flux through the addition-elimination pathway (1 → 3). Increasing the pH also has the effect of creating a larger concentration of unprotonated amines, increasing the amine-nucleophilic displacement as well as the conversion of (3) to (6).

The reaction pH has an especially strong influence on the initial fate of (1). A detailed analysis and discussion of similarly competing pH-dependent reactions can be found in the literature^{13, 14}. In the present case, the relative values of k_w , $k_{OH}[OH^-]$ and $k_1[N:]$ must be considered to optimize the amount of (5) formed relative to (2) and (3). This can be quantified as,

$$\frac{\text{rate}_{1 \rightarrow 5}}{\text{rate}_{1 \rightarrow 2} + \text{rate}_{1 \rightarrow 3}} = \frac{k_1[N:]}{k_w + k_{OH}[OH^-]} = k_1[N]_{\text{total}} \Phi$$

where, $\Phi = \frac{[N:]}{[N]_{\text{total}} + k_w + k_{OH}[OH^-]}$

The parameter Φ then expresses the relative rates as a function of pH, regardless of the absolute concentration of amine and the particular value of k_1 and $[N]_{\text{total}}$. In Figure 2-7

we show a plot of $\log(k_1\Phi)$ versus pH for the three model amines at 4°C and 22°C. By solving for $\partial\Phi/\partial\text{pH}=0$, the pH that maximizes Φ is found to be:

$$\text{pH}|_{\max\Phi} = \frac{\text{pK}_w + \text{pK}_a + \log\left(\frac{k_w}{k_{\text{OH}}}\right)}{2}$$

This defines the optimal pH for (1→5)-type coupling. It can be seen from Figure 2-7 that $\Phi(\text{pH}|_{\max\Phi})$ increases with decreasing pK_a , predicting a lower required amine concentration, but longer reaction times. Decreasing temperature has the effect of somewhat increasing $\Phi(\text{pH}|_{\max\Phi})$ as well as $\text{pH}|_{\max\Phi}$.

Based on Figure 2-1, the interplay of the pH effect on hydroxyl and unprotonated amine concentration can be separated into three regimes: $[\text{OH}^-] \ll k_w/k_{\text{OH}}$, $[\text{OH}^-] \sim k_w/k_{\text{OH}}$, $[\text{OH}^-] \gg k_w/k_{\text{OH}}$. At low pH's, only hydrolysis (1→2) and nucleophilic substitution (1→5) are significant, yet a large concentration of the amine species will be needed to favor addition over hydrolysis due to the low fraction of unprotonated amines at low pH. In the intermediate regime, all three pathways can be significant, however, the (1→5) pathway can be made dominant with a lower amine concentration than is needed for the later low pH regime. In the high pH regime, hydrolysis is insignificant relative to the first step in the addition-elimination pathway (1→3). This regime can prove to be impractical because $[\text{OH}^-]$ increases faster than $[\text{N:}]$ with increasing pH, requiring a large excess of amines.

In our model, we have attempted to represent all reactions in terms of possible elementary reactions. However, in the case of k_1 in particular, our data suggests that there might be a dependence on the amine pK_a that would not be consistent with the assertion that k_1 is an elementary reaction. It can be seen from Table 2-3 that k_1 increases with pK_a . This trend acts in the opposite direction but with a smaller magnitude than the pK_a dependence imposed by using $[N:]$ as the effective amine dependence. Attempts to fit the data with $k_1[N]_{total}$ as the driving force failed to yield a fit comparable to that of $k_1[N:]$ as the driving force.

In an attempt to fit all the data for k_1 to a single rate relation, an empirical model was developed for the S_N2 reaction as shown in Figure 2-8. This empirical rate equation fits the data of all temperatures, reaction pH's, and amines except for the phenylalanine 4°C reaction, possibly for steric reasons. The correlation of the empirical rate equation with the measured values for k_1 is illustrated in Figure 2-9. It is interesting to note that the k_1 dependence on $K_a^{-0.63}$ is invariant with temperature, although only limited data is available at 4°C. The consistency of this empirical relation across the variety of amines may indicate a slightly different dependence than the concentration of unprotonated amine, $[N:]$.

2.4.5 Steric Effects

Phenylalanine was expected to be the most sterically inhibited. The effect was most noticeable at 4°C (Figure 2-6d). This is best illustrated in Figure 2-9, where the phenylalanine 4°C reaction is well removed from the trends established by all other rate

constants. It is also possible that steric factors rather than the pK_a dependence supported above may account for the higher values of k_1 for α CBZ-Lys as compared to glycyl-phenylalanine 4°C.

2.4.6 Control of Product Distribution

It could be argued that the relative amount of (5)-type, 2° amine linkages and (6)-type, sulfonyl linkages may be more important than total yields, especially since (6)-type linkages may be subject to slow hydrolytic cleavage. In general, it would be desirable to maximize the number of (5)-type, secondary amine linkages. Our model predicts that reactions run at 4°C would have more secondary amine bonds than at 22°C for a given amine concentration. In general the fraction of secondary amine linkages increases with increasing amine concentration by increasing the rate of (1)→(5) relative to (1)→(2)+(3).

The distribution of (4) and (6) from (3) is best described by α . At any given time, α is the instantaneous fraction of (3) that will become (6):

$$\alpha = \frac{k_2[N :]}{k_2[N :] + k'} = \frac{d[6]/dt}{d[4]/dt + d[6]/dt}$$

Because α is a function of $[N:]$ its value changes as the reaction progresses. To compare values of k_2 for the three model amines at both temperatures it is instructive to compare the initial value of α . Alpha will tend to decrease somewhat from its initial value as free

amines are consumed. Figure 2-10 shows $\alpha(t=0)$ for the 18 curves examined. The value of α was found to be consistently larger at 22°C than at 4°C. For any given amine, the initial value of α is an increasing function of reaction pH through the dependence of [N:] on the solution pH. Alpha was found to be a decreasing function of pK_a , with a value approaching unity for 100mM glycyl-phenylalanine at 22°C, suggesting that the driving force for this coupling pathway has a stronger dependence on solution pH than is exerted through [N:].

2.5 Conclusions

With the judicious choice of reaction temperature and pH, tresyl-mediated couplings can be achieved with high yields. To maximize the total yield and the fraction of secondary amine linkages, our model predicts that it is desirable to run tresyl coupling reactions at lower temperatures around pH8, depending on the amine pK_a as specified by the above equation for $pH|_{\max\Phi}$ and illustrated in Figure 2-7. Although total yields ($[5]+[6]$) may be higher at elevated pH levels (Figure 2-6), (6)-type amide linkages may be unstable over prolonged periods in aqueous environments. Where reactions must be run at higher temperatures due to solubility limitations, maximal secondary amine linkages are predicted at slightly higher pH levels to overcome the higher rate of hydrolysis (k_w).

Where the choice of nucleophilic amine is possible, it is advantageous to use an amine of low pK_a to maximize the concentration of the unprotonated species. This points

to an advantage of coupling peptides via an N-terminal glycine rather than through an ϵ -amine group of a lysine residue.

When coupling to tresylated species via a lysyl ϵ -amine is necessary, as may be the case with certain proteins, low temperature at pH~8.8 is indicated (Figure 2-7). In this case high concentrations of amine are necessary, even beyond the 100mM amine used here, to achieve high yields of secondary amine linkages. Beyond pH~8.8, additional tresyl conversion (Figure 2-6) is predicted to be largely through (6)-type amide linkages.

In some applications, it may be the nucleophilic amine that is limiting, rather than the tresyl-activated species. Such a case is encountered in attaching pendant PEG chains to proteins or small molecules. When the tresylated species is used in large excess, it can be seen from Scheme I that the (1) \rightarrow (3) pathway (\sim [Tr]) can quickly become dominant over the (1) \rightarrow (5) pathway (\sim [N:][Tr]). This raises the concern that the limited number of amines might be consumed in a (3) \rightarrow (6) reaction, disfavoring (1) \rightarrow (5). To maximize secondary amine linkages in this case it is advantageous to run under conditions where α is small (Figure 2-10), i.e. at a somewhat lower pH than prescribed by Figure 2-7.

TABLE 2-1
HYDROLYSIS RATE CONSTANTS

Temperature	k_w (10^{-6} sec^{-1})	k_{OH} ($10^3 \text{ sec}^{-1} \text{ M}^{-1}$)
4°C	0.22	68
22°C	17.0	78.3

TABLE 2-2
IONIZATION CONSTANTS

Temperature	pK_w¹⁵	pK_a Gly-Phe	pK_a Phe	pK_a αCBZ-Lys
4°C	14.78	8.6	9.6	11.3
22°C	14.08	8.1	9.1	10.7

The amine pK_a's at 4°C and 22°C were calculated as explained in the text from literature values at 25°C for glycyphenylalanine¹⁶ and phenylalanine¹⁷. The pK_a of the αCBZ-Lys was assumed to be similar to lysine¹⁸ and 6-aminohexanoic acid¹¹, which have similar pK_a's.

TABLE 2-3

TRESYL-MEDIATED COUPLING EFFECTIVE RATE CONSTANTS

Rate Constant	Gly-Phe		Phe		α CBZ-Lys	
	4°C	22°C	4°C	22°C	4°C	22°C
k_1 ($10^{-2} \text{ sec}^{-1} \text{ M}^{-1}$)	0.48(0.02)	0.69(0.05)	0.16(0.01)	3.1(0.2)	25(2)	29(2)
k_2/k' (10^2 M^{-1})	13(6)	-- ²	-- ¹	0.63(0.16)	12(6)	5.4(1.3)

Rate constants are given as value(standard deviation). The large standard deviation in the case of k_2/k' for α CBZ-Lys at 4°C reflects a relative insensitivity of the fit to this parameter.

¹ k_2 was found to be negligible as compared to k' under the conditions examined.

² k' was found to be negligible as compared to k_2 under the conditions examined.

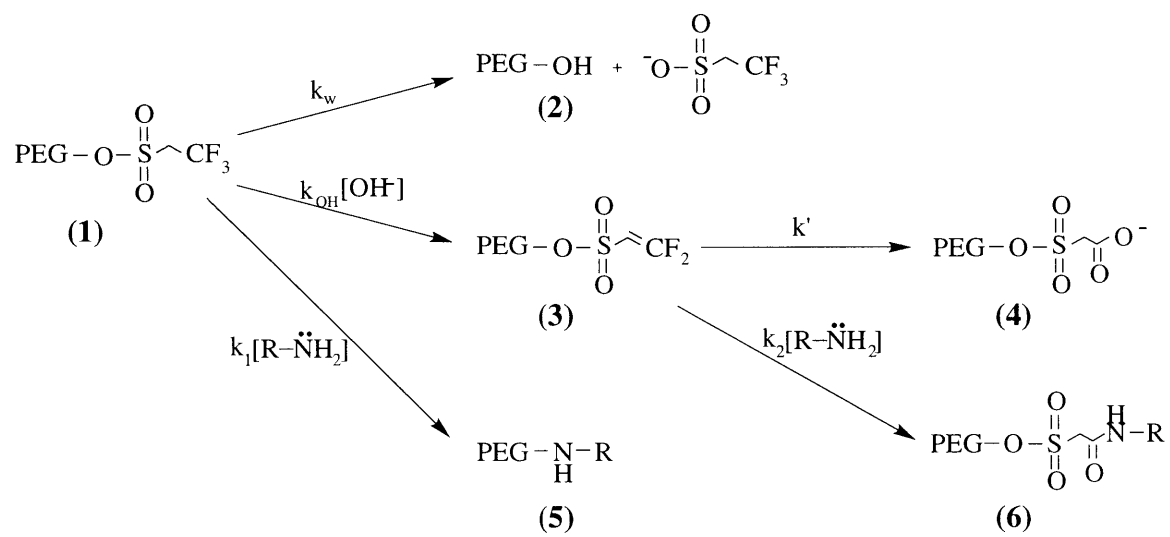
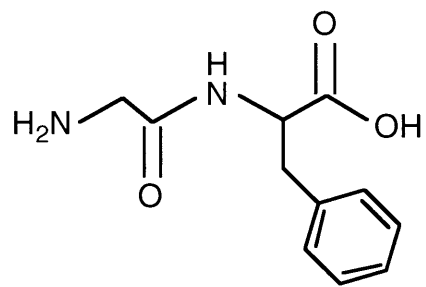
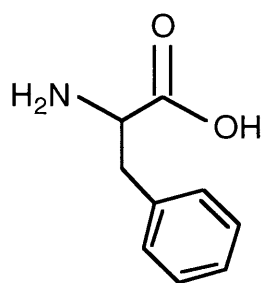


Figure 2-1. Reaction scheme for aqueous PEG-tresylate.

Glycine-Phenylalanine



Phenylalanine



N²-CBZ-Lysine

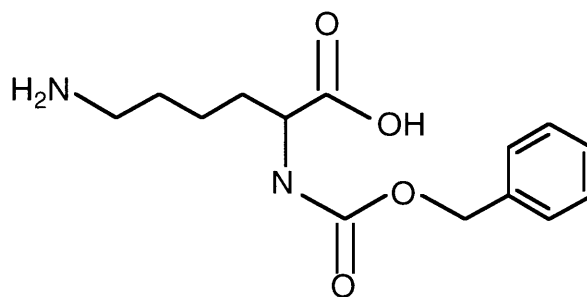


Figure 2-2. Model primary amines used in coupling studies. Compounds were chosen to span a range of pK_a's (see Table 2-2). Glycine-phenylalanine, phenylalanine and αCBZ-lysine were chosen as models for peptidyl N-termini, branched amines, and protein surface-presented lysines, respectively.

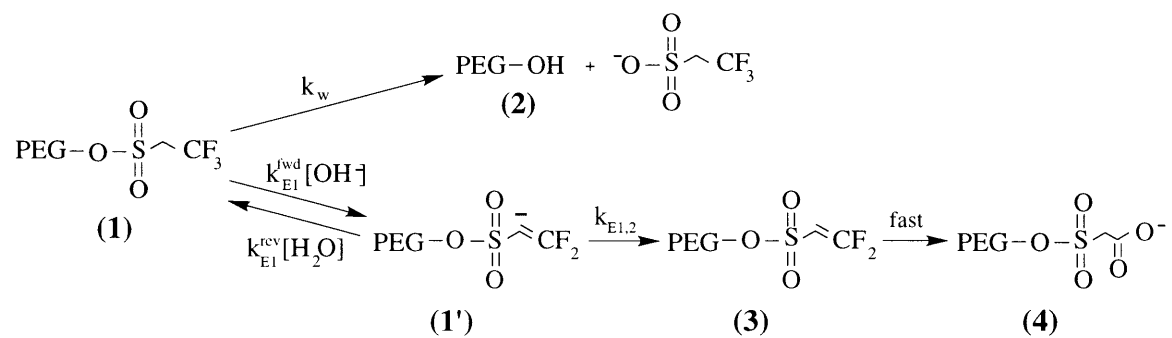


Figure 2-3. Hydrolysis model for PEG-tresyl in the absence of amine nucleophile.

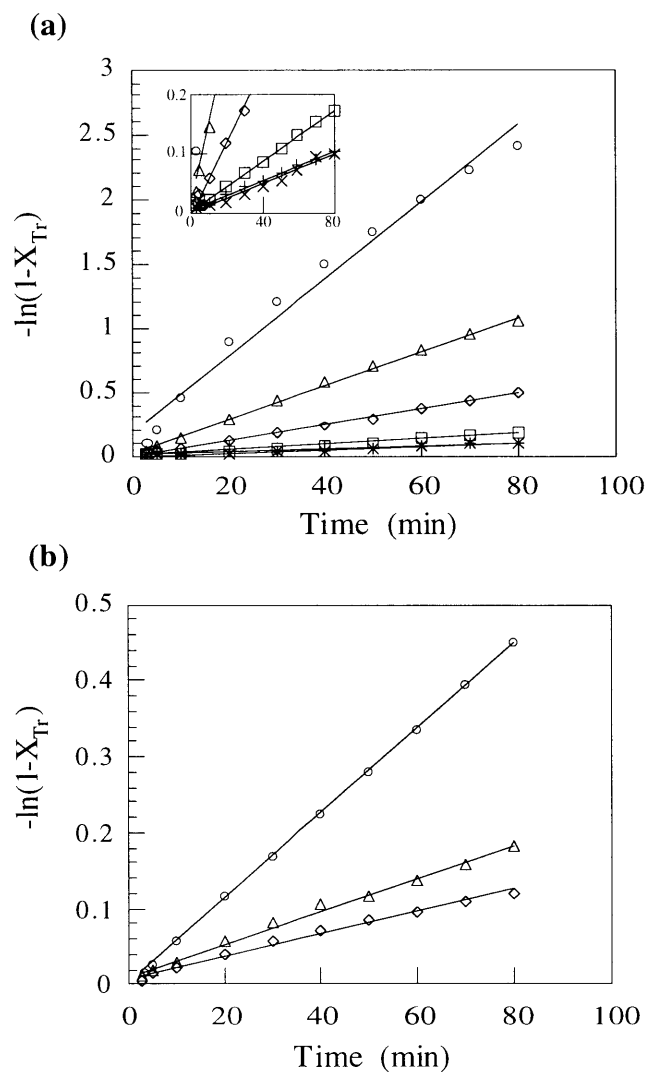


Figure 2-4. Hydrolysis reaction at 22°C (1a) at pH6.0 (×), pH7.0 (+), pH7.5 (□), pH8.0 (◇), pH8.5 (Δ), pH9.0 (o), and 4°C (1b) at pH8.0 (◇), pH8.5 (Δ) and pH9.0 (o). All reactions were followed by titration as detailed in Section 2.3. Conversion of tresyl groups ($X_{Tr} = 1 - [1]/[1]_0$) was calculated on the basis of the initial concentration of tresyl groups for each experiment.

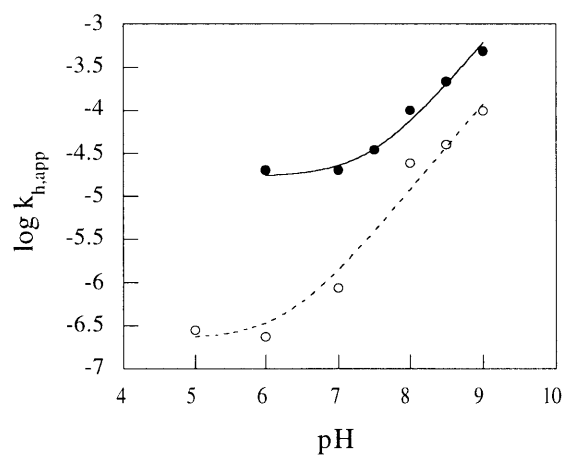


Figure 2-5. Least-squares fit for hydrolysis reaction ($k_{h,app} = k_w + k_{OH}[OH^-]$) for 22°C (●) and 4°C (○). Values of $k_{h,app}$ are taken from the slopes of curves in Figure 2-4 for faster reactions (points where $\log k_{h,app} > -5$) and from the rate of pH change (see Section 2.3) for slower reactions (points where $\log k_{h,app} < -5$).

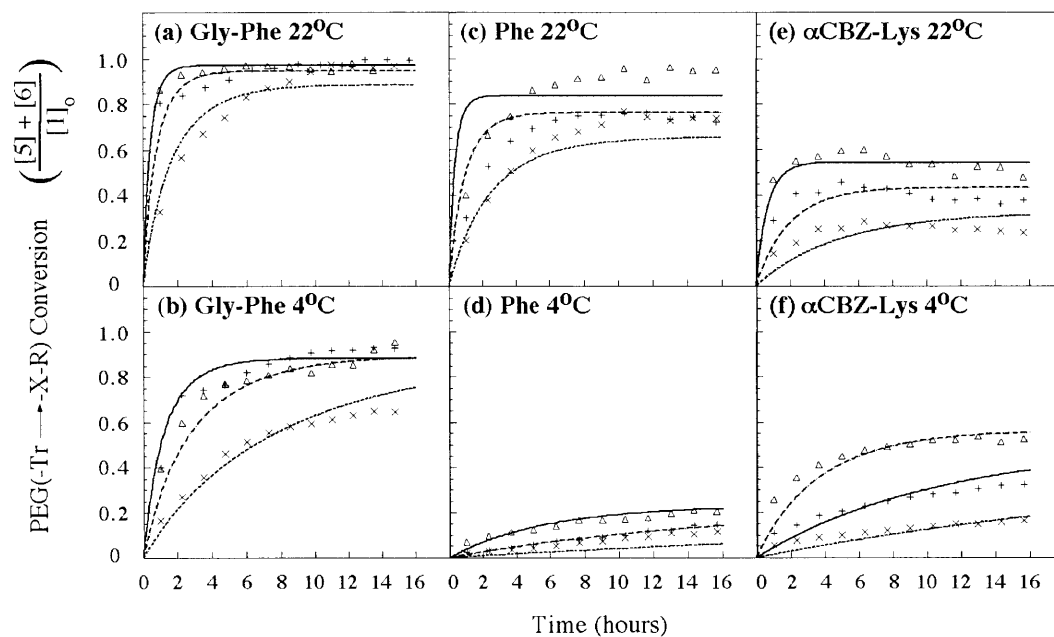


Figure 2-6. PEG(-Tr \rightarrow -X-R) conversion data and model fit for the reaction PEG-Tr + H_2N -R \rightarrow PEG-X-R where X=(NH) or (OSO₂CH₂C(O)NH). Each panel (a-f) is fit by a single set of rate constants to the mechanism prescribed in Figure 2-1. Data (symbols: (x) pH7.5, (+) pH8.0, (Δ) pH8.5) and model predictions (lines: pH7.5 (----), pH8.0(—), pH8.5 (—)) are given for Gly-Phe at 22°C (1a), Gly-Phe at 4°C (1b), Phe at 22°C (1c), Phe at 4°C (1d), α CBZ-Lys at 22°C (1e) and α CBZ-Lys at 4°C (1f). Conversion data ($= ([5]+[6]) / [1]_0$) was measured as the fraction of tresyl groups converted to PEG-N-R.

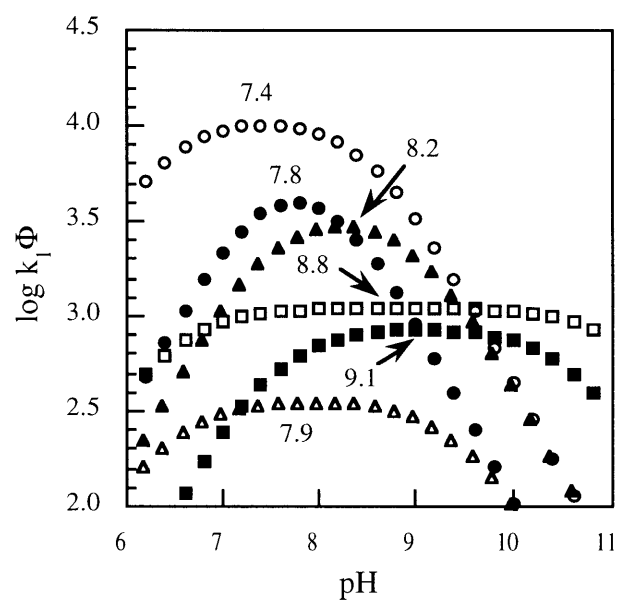


Figure 2-7. Plot of relative rates of reactions with PEG-Tr in terms of $k_1\Phi$ (see text). Curves are given at 4°C (open symbols) and 4°C (filled symbols) for Gly-Phe (o/●), Phe (Δ/▲) and αCBZ-Lys (□/■). The pH where $k_1\Phi$ is a maximum is indicated (numeral) for each curve. Maximal $k_1\Phi$ predicts an optimal pH for (1→5)-type coupling.

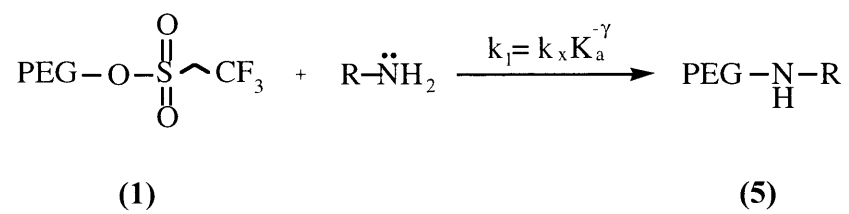


Figure 2-8. Empirical rate equation for amine/tresyl coupling.

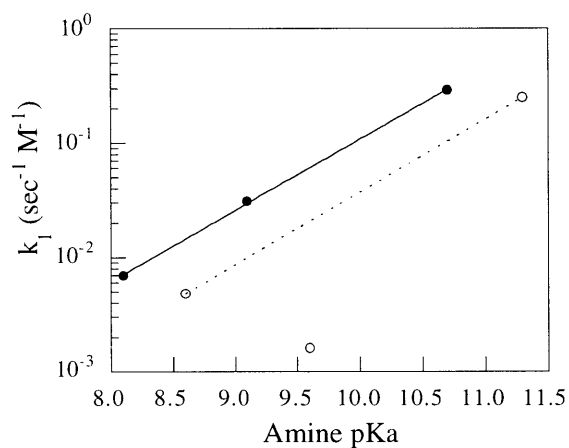


Figure 2-9. Empirical correlation (see Figure 2-8) for rate constant k_1 at 22°C (●) and 4°C (○) with the amine pK_a (see Table 2-2) fit to $k_1 = k_x K_a^{-\gamma}$ where $k_x(22^\circ\text{C}) = 6.4 \times 10^{-8} \text{ M}^{-1} \text{ sec}^{-1}$, $k_x(4^\circ\text{C}) = 1.6 \times 10^{-8} \text{ M}^{-1} \text{ sec}^{-1}$, $\gamma(22^\circ\text{C}) = 0.62$ and $\gamma(4^\circ\text{C}) = 0.63$. Fit at 4°C (----) is included to illustrate the similarity in γ to the fit at 22°C (—) even though the data point at $pK_a=9.6$ is omitted due to suspicion of steric influences.

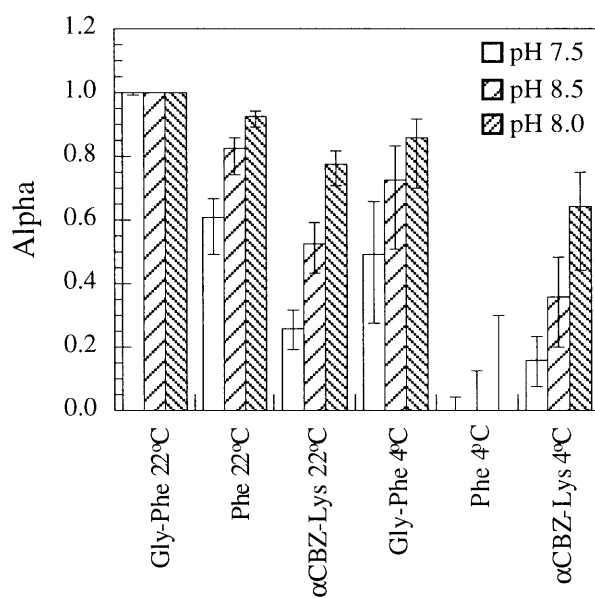


Figure 2-10. Plot of the initial distribution of products from (3), given as α ($= \text{rate}_{3 \rightarrow 6} / \text{rate}_{3 \rightarrow 4+6}$), based on Scheme I and measured rate constants, k_2/k' . Because α is a function of the concentration of the nucleophilic species $[N:]$, α is expected to be a function $[N:]$, and will decrease with time proportional to the depletion of $[N:]$. Error bars are 95% confidence intervals.

2.6 References

1. Nilsson, K. & Mosbach, K., *Biochem. Biophys. Res. Commun.*, "Immobilization of enzymes and affinity ligands to various hydroxyl group carrying supports using highly reactive sulfonyl chlorides," **102**(1): 449-457 (1981).
2. Gais, H.-J. & Ruppert, S., *Tet. Lett.*, "Modification and immobilization of proteins with polyethylene glycol tresylates and polysaccharide tresylates: evidence suggesting a revision of the coupling mechanism and the structure of the polymer-polymer linkage," **36**(22): 3837-3838 (1995).
3. King, J.F. & Gill, M.S., *Angew. Chem. Int. Ed. Engl.*, "Reactions of Neopentyl 2,2,2-trifluoroethanesulfonate (tresylate) with nucleophiles: a model study for the coupling of nucleophiles with tresyl agarose," **34**(15): 1612-1613 (1995).
4. King, J.F. & Gill, M.S., *J. Org. Chem.*, "Alkyl 2,2,2-trifluoroethanesulfonates (tresylates): elimination-addition vs bimolecular nucleophilic substitution in reactions with nucleophiles in aqueous media," **61**(21): 7250-7255 (1996).
5. Harris, J.M. (ed) (1992) *Poly(ethylene glycol) Chemistry*. Topics in Applied Chemistry. Edited by Katritzky, A.R. & Sabongi, G.J., Plenum Press, New York
6. Demiroglou, A., Bandel-Schlesselmann, C. & Jennissen, H.P., *Angew. Chem. Int. Ed. Engl.*, "A novel reaction sequence for the coupling of nucleophiles to agarose with 2,2,2-trifluoroethanesulfonyl chloride," **33**(1): 120-123 (1994).
7. Nilsson, K. & Mosbach, K., *Meth. Enzymol.*, "Immobilization of ligands with organic sulfonyl chlorides," **104**: 56-69 (1984).
8. Press, W.H., Flannery, B.P., Teukolsky, S.A. & Vetterling, W.T. *Numerical Recipes*, **1986**, Cambridge University Press, Cambridge.
9. Izatt, R.M., Wrathall, J.W. & Anderson, K.P., *J. Phys. Chem.*, "Studies of the copper(II)-alanine and phenylalanine systems in aqueous solution. Dissociation and formation constants as a function of temperature," **65**: 1914-1915 (1961).
10. King, E.J., *J. Am. Chem. Soc.*, "The ionization constants of glycine and the effect of sodium chloride upon its second ionization," **73**: 155-159 (1951).
11. Smith, E.R.B. & Smith, P.K., *J. Biol. Chem.*, "Thermodynamic properties of solutions of amino acids and related substances," **146**: 187-195 (1942).
12. Marini, M.A., Berger, R.L., Lam, D.P. & Martin, C.J., *Anal. Biochem.*, "Thermal titrimetric evaluation of the heats of ionization of the commonly occurring amino acids and their derivatives," **43**: 188-198 (1971).

13. King, J.F., Rathore, R., Lam, J.Y.L., Guo, Z.R. & Klassen, D.F., *J. Am. Chem. Soc.*, "pH Optimization of Nucleophilic Reactions in Water," **114**: 3028-3033 (1992).
14. King, J.F., Guo, Z.R. & Klassen, D.F., *J. Org. Chem.*, "Nucleophilic Attack vs General Base Assisted Hydrolysis in the Reactions of Acetic Anhydride with Primary and Secondary Amines. pH-Yield Studies in the Recognition and Assessment of the Nucleophilic and General Base Reactions," **59**: 1095-1101 (1994).
15. Marshall, W.L. & Franck, E.U., *J. Phys. Chem. Ref. Data*, "Ion product of water substance, 0-1000C, 1-10,000 bars, new international formulation and its background," **10**(2): 295-304 (1981).
16. Biester, J.L. & Ruoff, P.M., *J. Am. Chem. Soc.*, "Structural influences on the stability of dipeptide-metal ion complexes," **81**: 6517-6521 (1959).
17. Nevenzel, J.C., Shelberg, W.E. & Niemann, C., *J. Am. Chem. Soc.*, "The apparent ionization constants and ultraviolet spectra of o-, m- and p-chloro and p-sulfamyl-DL-phenylalanine," **71**: 3024-3026 (1949).
18. Ellenbogen, E., *J. Am. Chem. Soc.*, "Dissociation constants of peptides. I. A survey of the effect of optical configuration," **74**: 5198-5201 (1952).

3 KINETICS OF TRANSGLUTAMINASE-CATALYZED REACTIONS FOR FREE & PEG-BOUND SUBSTRATES

3.1 Introduction

Use of the crosslinking enzyme transglutaminase for gel formation requires detailed knowledge of parameters that may affect gel formation. Although one of transglutaminase's primary function in nature is the building up of structure¹ from soluble units such as collagen² and fibronectin³, activity toward synthetic substrates and synthetic substrates bound to poly(ethylene glycol) (PEG) is by no means guaranteed. We therefore characterized the kinetics of transglutaminase-mediated reactions using both model substrates and substrates suitable for gel formation. We examined both side reactions that may inactivate transglutaminase as well as reaction kinetics involving PEG-bound substrates. We also characterized reactions leading to transglutaminase deactivation under the condition of gel formation.

3.2 Tissue Transglutaminase Self-Crosslinking

Tissue transglutaminase (TG_{II}) kinetics follow a modified double displacement mechanism, as discussed in Section 1.4.3. Because enzyme acylation is the rate-limiting step in crosslink formation under the conditions of saturating amine concentrations, TG_{II} kinetics can be adequately described by standard Michaelis-Menton kinetics. However in conditions where the enzyme concentration is relatively large (μM), TG_{II} is known to act as a substrate in its own reaction. Because the use of micromolar concentrations of TG_{II}

are required for most gel-forming applications, the kinetics of TG_{II} self-reaction must be considered to make predictions of the overall kinetics of gel formation (see Section 5.2).

Literature reports suggest that pure tissue transglutaminase isolated from guinea pig liver can act as a substrate in its own reaction³ and thereby crosslink itself to amines^{4, 5} and other TG_{II} molecules⁴ in the absence of another amine acceptor. This phenomena has not been reported for other forms of transglutaminases, and therefore could be unique to TG_{II}. Self-crosslinking has also been demonstrated in the presence of other TG_{II} substrates *in vitro* at 4°C with fibrinogen and fibronectin³, and at 37°C with laminin and nidogen⁶. It has further been observed that self-crosslinking may affect TGII activity as the resultant high molecular weight TG-conjugates exhibit reduced activity⁴.

Many enzymes, including TG_{II}, exhibit pH-dependent activity⁷. A pH dependence for inactivation of TG_{II} has been suggested as well based on a calcium-dependent susceptibility to oxidative inactivation in the presence of Cu(II)⁸, but it is unclear to what degree TG_{II} might be oxidized under physiologic conditions.

The possibility of multiple, pH-dependent routes to TG_{II} inactivation as well as activity dependence on calcium and GTP⁹ point to a complex control mechanism that would be expected for an enzyme with such diverse biological roles. Here we have undertaken a kinetic study of TG_{II} mediated self-crosslinking to quantify these processes.

3.2.1 Experimental Methods

Enzyme Storage. A discussion of transglutaminase storage conditions can be found in Appendix A3. Tissue transglutaminase (TG_{II}) was purchased from Sigma. TG

was dissolved in 0.5x Dulbecco's phosphate buffered saline (Life Technologies) (9mM phosphate) with 160mM potassium chloride and 1mM ethylenediaminetetraacetic acid in a 4°C cold room. Aliquots of 10μL and 20μL at a concentration of 10μM were stored at -70°C and thawed immediately prior to use.

Peptide Synthesis. The glutamine substrate (Gly-Pro-Leu-Gly-Ile-Ala-Gly-Gln-Ser-His-Gly) was synthesized on a Rainin PS2000 Peptide Synthesizer by standard Fmoc methods in dimethylformamide (DMF) as described in Appendix A2.

Enzyme Activity Assay. A protocol for measurement of amine acceptor substrate activity is given in Appendix A5. For each assay, 80μL of a solution of glutamine substrate with 10mM calcium chloride and 10mM monodansyl cadaverine (mdc) (Aldrich) in 100mM Tris was brought to the appropriate temperature in a constant temperature water bath. Dithiothreitol (Life Technologies) and glutathione (Sigma) were included in some experiments as reducing agents to inhibit enzyme oxidation. Experiments at pH 6.0 and below were also buffered with 100mM MES (2-[N-morpholino]-ethanesulfonic acid) (Sigma).

Kinetic Rate Constant Fitting Algorithm. Where analytical solutions to rate equations were unavailable, rate constants were fit using standard FORTRAN models extracted from Numerical Recipes¹⁰, as explained in Section 2.2.3. The FORTRAN code is included in Appendix C.

Transglutaminase Self-Crosslinking. The effects of temperature and calcium concentration were examined by incubating aliquots of transglutaminase (5μM) in 50mM

Tris at pH7.4 for 1 hour followed by characterization of protein products by gel electrophoresis. Incubations were performed at 4°C with (8mM) and without calcium. Incubations at 37°C were carried out with calcium (8mM), without calcium, and with calcium (8mM) in the presence of 5mM monodansyl cadaverine. Two additional conditions included one week at 4 °C with no calcium and a zero time case with analysis immediately following thawing from -70 °C. Reactions were terminated by the addition of buffer consisting of 0.5mg/mL bromophenol blue, 31mg/mL dithiothreitol, 0.10g/mL glycerol and 2.0% sodium dodecylsulfate (SDS) in 62.5mM Tris pH6.8.

Samples were run along with a fresh aliquot and molecular weight markers on a 7% SDS-poly(acrylamide) electrophoresis gel topped by a 3.5% stacking gel. Molecular weight markers (Biorad) consisted of a mixture of labeled proteins: myosin (208kD), β -galactosidase (127kD), bovine serum albumin (85kD), carbonic anhydrase (45kD), soybean trypsin inhibitor (32.8kD), lysozyme (18kD) and aprotinin (7.4kD). All molecular weights are 'apparent' as labeled.

Cytotoxicity of dithiothreitol. Balb/c 3T3 fibroblasts were cultured in a culture media of high glucose Dulbecco's Modified Eagle Medium (Gibco) supplemented with 200mM L-glutamine, 10% calf serum and 1% penicillin/streptomycin to inhibit bacterial growth (all products from Gibco). Various amounts of DTT was added 4 hours after cell plating. Cell numbers were counted after 24 hours in the presence of DTT. Experiments were run at 0mM, 0.30mM, 1.0mM and 3.0mM DTT.

3.2.2 Results

3.2.2.1 TG Self-Crosslinking Processes

Data which supports a transglutaminase self-crosslinking reaction are shown in Figure 3-1. Transglutaminase solutions were incubated at 4°C or 37°C for 1 hour (and 1 week for a calcium-free 4°C condition) with (8mM) and without calcium to examine the effects of these conditions on possible self-crosslinking processes. Monodansyl cadaverine, a potent amine donor substrate, was added to a calcium-containing aliquot at 37°C to assess crosslinking kinetics under conditions of amine competition for TG-expressed amine donor substrates. All samples were run on an SDS-PAGE gel to quantify crosslinking, using a sample added directly from -70 °C storage as a control. Results are shown in Figure 3-1.

Calcium was found to be required for the formation of high molecular weight aggregates. Aggregate formation was observed at 4°C but at a much lower level than at 37°C. Addition of 5mM monodansyl cadaverine effectively inhibited the crosslinking reaction. This is the first reported demonstration of self-crosslinking inhibition.

The degree of transglutaminase inactivation during the self-crosslinking experiments was characterized by monitoring the crosslinking of monodansyl cadaverine to a peptidyl amine acceptor substrate. This peptide was modeled on the structure of a known substrate for TG_{II}, N,N-dimethylcasein, as well other synthetic oligopeptide analogs of the active glutamine of N,N-dimethylcasein¹¹.

The kinetics of transglutaminase reactions have been shown to follow a modified double-displacement mechanism¹²⁻¹⁴, as discussed in Section 1.5.3. Under the conditions

of saturating amine substrate concentrations used in this study, the first catalytic step is limiting (see Figure 1-1). If the concentration of the active enzyme were invariant with time, a pseudo Michaelis-Menton¹⁵-type treatment would be appropriate:

$$\frac{d[\text{crosslink}]}{dt} = \frac{k_{\text{cat}}[\text{TG}]_t[\text{S}]}{K_{\text{m,app}} + [\text{S}]} \quad (3-1)$$

where [S] is the concentration of the amine acceptor substrate and [TG]_t is the total enzyme concentration. However, because the apparent enzyme concentration can in fact be a decreasing function of time due to inactivation, the kinetic mechanism describing the TG-mediated transamidation reaction must be represented as in Figure 3-2.

To verify that the reaction conditions were enzyme-limited and not substrate-limited, an activity assay was run (described above) with the enzyme being added in two separate aliquots as shown in Figure 3-3. After the addition of the first aliquot the reaction appeared virtually complete after 90 minutes (Figure 3-3). If one of the substrates was limiting, no further reaction would be observed upon addition of another aliquot of enzyme. Instead, with the addition of another aliquot of enzyme, the reaction re-initiated and followed the characteristic time-dependent activity exhibited upon addition of the first aliquot. This behavior is consistent with the hypothesis that the enzyme undergoes deactivation during the 90 minute reaction time.

Transglutaminase could become inactive by a number of possible mechanisms, as summarized in Figure 3-4. First, transglutaminase could participate in a reaction

unrelated to its activity such as spontaneous oxidation, hydrolysis or denaturation (Figure 3-4, Scheme A). Second, there is evidence that TG_{II} can become covalently linked to itself by disulfide bonds through known surface-accessible cysteines⁸ (Figure 3-4, Scheme B). Third, the enzyme could undergo some chemical reaction related to its crosslinking activity. Such self-crosslinking, with TG acting as a substrate in its own reaction, has been suggested in the literature^{3, 4}. In this type of reaction, TG_{II} may act as the amine donor (Figure 3-4, Scheme C), amine acceptor (Figure 3-4, Scheme D), or both.

Each of these mechanisms predict a unique type of kinetic dependence on the enzyme and substrate concentrations. By fitting the equations to measured data, it can be determined if the deactivation mechanism is consistent with any given deactivation mechanism. The reactions will be divided into four possible routes. The simplest mechanism is a first order ($\sim[TG]^1$) inactivation as shown in Figure 3-4, Scheme A. Contribution from this mechanism might be measured by experiments with antioxidants. More complex mechanisms that must be considered include second order ($\sim[TG]^2$) degradation where two TG_{II} molecules must come together to produce an inactive enzyme. This may be described by a second order rate constant if the enzyme acts independently of the two substrates as in Figure 3-4, Scheme B, or more complex behavior might result from TG crosslinking one of the substrates to itself to form the inactive enzyme as in Figure 3-4, Schemes C and D. These kinetic dependencies will provide strong evidence for a significant contribution to enzyme inactivation by Figure 3-

4, Scheme D in which TG_{II} expresses a glutaminyl TG_{II} substrate, when covalently linked to an amine donor serves to inactivate the enzyme.

Further evidence for the mechanism of inactivation might be gained from structural studies by circular dichroism. However alterations in structure could occur independently of self-crosslinking, through simple aggregation. Conversely, self-crosslinking resulting in inactivation would not necessarily produce an observable change in conformation. Steric inhibition could be solely responsible for inactivation. Therefore, while conformational changes associated with inactivation may be interesting from a structure/function point of view, measurement of this phenomena would not provide direct evidence of the role of self-crosslinking on transglutaminase inactivation.

3.2.2.2 Kinetic Model

A set of kinetic equations can be written to describe the formation of the crosslinked product as a function of time. The mechanism given in Figure 3-2 implies:

$$\frac{d[S' - A]}{dt} = k_{c1}[E \cdot S] \quad (3-2)$$

$$\frac{d[E \cdot S]}{dt} = k_1[E][S] - k_{-1}[E \cdot S] - k_{c1}[E \cdot S] \quad (3-3)$$

Two familiar Michaelis-Menton-type simplifications can be made to express these equations in terms of just [E] and [S]. By assuming the intermediate [E·S] is at pseudo-

steady state, $[E \cdot S]$ can be expressed in terms of $[E]$ and $[S]$. In (3-2), an assumption that $-d[S] \sim d[S' \cdot A]$ can be made based on the fact that the total enzyme concentration, $[E]_t$, is typically at least three orders of magnitude smaller than $[S]_o$. This gives:

$$-\frac{d[S]}{dt} = \frac{k_{c1}}{K_{m1}} [E][S] \quad (3-4)$$

$$\text{where, } K_{m1} = \frac{k_{-1} + k_{c1}}{k_1} \quad (3-5)$$

Equation (3-4) will apply for any $[E]=f(\text{time})$ and thereby for any inactivation mechanism.

As a first step in determining the mechanism or mechanisms of TG_{II} inactivation, it is useful to consider the reaction behavior at early times such that the amount of inactivated enzyme is approximately zero, $[E]_i \sim 0$. In this regime the mass balance for the total enzyme concentration, $[E]_t$ for Figure 3-4, Scheme A, B and C can be written as,

$$[E]_t = [E] + \frac{[E][S]}{K_{m1}} \quad (3-6)$$

where the pseudo-steady state condition for $[E \cdot S]$ has been applied. The concentrations of $[E \cdot S']$ and $[E \cdot S' \cdot A]$ are insignificant in (3-6) under conditions of saturating amine substrate. For Figure 3-4, Scheme D the concentration of $[E \cdot E]$ must be included.

Assuming pseudo-steady state for $[E \cdot E]$ as was done for $[E \cdot S]$ gives,

$$[E]_t = [E] + \frac{[E][S]}{K_{m1}} + 2 \frac{[E]^2}{K_{mi,a.d.}} \quad (3-7)$$

$$\text{where, } K_{mi,a.d.} = \frac{k_{-1,a.d.} + k_{i,a.d.}}{k_{1,a.d.}} \quad (3-8)$$

Comparison of (3-6) and (3-7) shows that the relationship between $[E]$ and $[E]_t$ are clearly different for the different kinetic schemes, implying a different dependence on $[E]_t$ of the initial rate of glutaminy substrate conversion by (3-4). By (3-6), the initial rate will depend on the first power of $[E]_t$, whereas by (3-7) the initial rate will be dependent on $[E]_t^\phi$, where $\phi = 0.5-1$ as a function of $[S]/K_{m1}$ and $K_{mi,a.d.}$. Thus, a dependence on $[E]_t$ of order between 0.5 and unity will imply a contribution by Figure 3-4, Scheme D.

Initial rates were measured as a function of $[E]_t$ to determine the value of ϕ . Data for initial rates at 37°C, pH 7.5 were taken as the conversion ($X_S \equiv 1 - [S]/[S]_0$) at 30 seconds. By (3-4), it can be seen that plotting the natural logarithm of the conversion at 30 seconds versus the natural logarithm of $[E]_t$ will give a line with the slope equal to ϕ . As shown in Figure 3-5, $\phi = 0.67$, implying that Figure 3-4, Scheme D is a significant contributor to TG_{II} inactivation, although not necessarily the *sole* contributor.

With the reaction of Scheme D describing the process by which TG_{II} become inactive, the following set of equations would be sufficient to describe the crosslinking reaction and simultaneous degradation of TG_{II} :

$$-\frac{d[S]}{dt} = \frac{k_{cl}}{K_{m1}} [E][S] \quad (3-4)$$

$$\frac{d[E]_i}{dt} = \frac{k_{i,a.d.}}{K_{mi,a.d.}} [E]^2 \quad (3-9)$$

$$[E] = \frac{K_{mi,a.d.}}{4} \left(\sqrt{\left(1 + \frac{[S]}{K_{m1}}\right)^2 + \frac{8}{K_{mi,a.d.}} ([E]_t - [E]_i)} - \left(1 + \frac{[S]}{K_{m1}}\right) \right) \quad (3-10)$$

Equation (3-10) is simply an algebraic variant of (3-7). The complex structure of (3-10) makes (3-4) and (3-9) inseparable, except in limiting cases. If $8 \cdot [E]_t / K_{mi,a.d.} \ll 1$, the free enzyme concentration $[E]$ would be linear with $[E]_t$ ($\phi=1$) yielding algebraic solutions to (3-4) and (3-9). Since $\phi=0.67$ the full expression must be considered. Solutions for $[S]$ and $[E]$ as a function of time can be found given a set of rate constants by the numerical methods discussed above.

From (3-10) and a particular value of ϕ an upper limit can be found for $K_{mi,a.d.}$ by the constraint that both $[S]$ and K_{m1} must be positive. For the conditions used for the experiments represented in Figure 3-5 and $\phi=0.67$, it can be shown that $K_{mi,a.d.} \leq 1.0 \mu\text{M}$.

Data obtained from measuring the conversion of the glutaminy substrate over 90 minutes were used to find values for the rate constants for the TG-glutaminy substrate model (Scheme D, Equations (3-4), (3-9) and (3-10)). A set of optimal rate constants was defined as the set that gave the smallest squared deviation from the data set. This was

done by standard differential equation integration techniques discussed above. Best fits were obtained for the TG-substrate model with $K_{m1} \gg [S]$ for the substrate concentrations used here ($\leq 4\text{mM}$). With $K_{m1} \gg [S]$ and the constraint of $\phi=0.67$, (3-10) requires $K_{mi,a.d.} \sim 1.0\mu\text{M}$. This leaves only $k_{i,a.d.}$ and the ratio k_{c1}/K_{m1} as unknowns. Separate rate constants were fit to data for cases of $0.50\mu\text{M}$, $1.00\mu\text{M}$ and $2.00\mu\text{M}$ transglutaminase concentrations. These rate constants were then compared for similarity as an assessment of the validity of using the TG-glutaminy substrate model (Scheme D) as the exclusive pathway for inactivation. Results are shown in Figure 3-6.

The values of k_{c1} were found to be consistent over the range of concentrations tested, yet the value of $k_{i,a.d.}$ varied inversely with the enzyme concentration. This indicates that the TG-substrate model under-predicts the rate of TG inactivation at low enzyme concentrations. It is possible that a contribution from another enzyme inactivating mechanism may account for this discrepancy. Inactivation by oxidation or disulfide bond formation as Figure 3-4, Scheme A would be an example a process that would be become evident relative to Figure 3-4, Scheme D at lower enzyme concentrations. To explore this possibility, a coupling experiment was conducted in the presence of an antioxidant (50mM DTT) at the same enzyme concentration ($2.00\mu\text{M}$) as a previous experiment. It was found that the presence of 50mM DTT significantly improved the apparent activity of TG_{II} at longer reaction times (Figure 3-7), consistent with a contribution by Figure 3-4, Scheme A.

Under conditions where oxidation may be important, (3-9) must be rewritten as,

$$\frac{d[E]_i}{dt} = \frac{k_{i,a.d.}}{K_{mi,a.d.}} [E]^2 + k_{i,ox} ([E]_t - [E]_i) \quad (3-11)$$

where $k_{i,ox}$ is a first-order rate constant describing the oxidative process inhibited by DTT.

Equations (3-4), (3-10) and (3-11) can be used to find values for all pertinent rate constants. Assuming $k_{i,am} \sim 0$ in the 50mM DTT case, it was found that describing the temporal loss of TG_{II} activity by (3-11), allowed all four data sets to be described by a single set of rate constants as shown in Figure 3-7. The consistency of the model supports the hypothesis that TG_{II} inactivation can be described as a combination of oxidation and TG-glutaminy substrate crosslinking.

To further test the robustness of the model described by (3-4), (3-10) and (3-11) inclusive of the rate constants collected here (Figure 3-7), we attempted to predict previously published observations and data of another laboratory⁵ using only their experimental conditions as an input to our model. Aeschlimann and Paulsson measured the incorporation of a radiolabeled primary amine, ³H-putrescine, into TG_{II} in the absence of another glutaminy substrate ($[S] = 0$ mM) at two concentrations of TG_{II}: 125nM and 750nM. Our model correctly predicts the rates of enzyme labeling as well as the relative final labeling levels measured at 125nM and 750nM TG_{II} (Figure 3-8).

3.2.2.3 Temperature, pH and Antioxidant Dependence

Experiments at a variety of temperatures and pH levels, with and without antioxidants were performed to elucidate the effects of these parameters on TG_{II} activity and rate of inactivation. To evaluate each time course individually, it is useful to invoke a simple empirical mechanism that may not rigorously reconcile with the mechanisms supported above, yet captures the essence of the kinetic behavior. If we chose to describe the inactivation mechanism by Figure 3-4, Scheme A, and further collapse the crosslinking into a pseudo-first order reaction (equivalent to $K_{m1} \gg [S]_0$), the concentration of uncoupled glutaminy substrate can be described by,

$$[S] = [S]_0 \exp\left[\frac{-k_{c1}[E]_t}{k_{i,app}K_{m1,app}}(1 - \exp(-k_{i,app}t))\right] \quad (3-12)$$

The apparent inactivation rate, $k_{i,app}$, will be affected by the true constants ($k_{i,a.d.}$, $K_{mi,a.d.}$, and $k_{i,ox}$), while the apparent crosslinking rate $k_{c1}/K_{m1,app}$ will be a function of $[E]_t$ and $[S]_0$. Table 3-1 shows apparent rate constants found for a variety of temperatures and pH values as well as conditions with antioxidants. Experiments shown in Figure 3-7 are included as experiments 1-4 for comparison.

To test the temperature dependence of these reactions, experiments were performed at 21°C with and without DTT. Additionally, a small amount of a less potent anti-oxidant, glutathione (GSH) was tested and was found to reduce $k_{i,ox}$ slightly (expt. 9). Again, it was found that TG_{II} activity was extended in the presence of DTT.

Comparing experiments 2 and 8 in Table 3-1, lowering the temperature had the effect of reducing both the apparent crosslinking and inactivation rate constants by similar amounts, giving apparent activation energies of 3.7 kcal/mol and 2.4 kcal/mol, respectively. Addition of 50mM DTT as an anti-oxidant had a similar relative effect at 21°C (expt. 8 vs. 10) and at 37°C (expt. 3 vs. 4).

In the presence of cells there is expected to be a limit to the amount of antioxidant that can be used without eliciting adverse cytotoxic effects. To test this hypothesis, cells were cultured in the presence of varying amounts of DTT as described in Section 3.2.1. As shown in Figure 3-8 concentrations in the millimolar range can be harmful to cells. Therefore, only a limited advantage can be gained by adding DTT to the pre-gel solution if cytotoxic effects are to be minimized. In practice losses in transglutaminase activity by inactivation can be overcome simply by adding excess enzyme. As will be shown in Section 5.4.5, addition of transglutaminase has no observable negative effect on cell growth ($\leq 3\mu\text{M}$ TG).

TG_{II} kinetics were strongly influenced by pH. For example, varying the pH from 7.5 (expt. 2) to 7.1 (expt. 5) at 37°C resulted in a 50% increase in the apparent crosslinking rate and a slight reduction in the apparent inactivation rate. At pH 6.0 (expt. 6) the apparent inactivation rate is reduced 3-fold from the rate at pH 7.5 (expt. 3) with similar apparent crosslinking rates. A large reduction in pH to 4.0 resulted in total loss of measurable activity (expt. 7). At 21°C, changing the pH from 7.5 (expt. 8) to 6.0 (expt.

11) resulted in a similar apparent crosslinking rate yet reduced the apparent inactivation rate by approximately 3-fold, similar to the effect measured at 37°C.

3.2.3 Discussion

Our finding that the initial rate of self-crosslinking is dependent on $[E]_t^{0.67}$ for the range of TG_{II} concentrations examined indicates that only a fraction of the total enzyme concentration is initially available for catalysis of the peptide substrate. The amount of enzyme available for catalysis is consistent with a model in which the enzyme binds to itself (Figure 3-5, Equation (3-7)). Evidence that this binding is followed by TG_{II}-catalyzed crosslinking that negatively affects the enzyme is provided by the proportionality of the time-dependent activity (Figure 3-7) as described by (3-11). Reports of TG_{II}-containing high molecular weight species formed by TG_{II} activity^{3, 4} might suggest a mechanism whereby successive crosslinks on a single TG_{II} molecule would additively attenuate activity either by inducing conformational changes or by sterically inhibiting access to the active site. Either of these effects could certainly depend on the particular molecule crosslinked to the enzyme.

The presence of PEG-bound substrates may effect self-crosslinking in two ways. The PEG chain alone might enhance the probability of TG-self-association through excluded volume effects. Also, if a PEG-bound substrate becomes covalently attached to a TG molecule thereby linking a PEG chain to the enzyme, subsequent TG / TG-PEG interactions may be disfavored, reducing the likelihood of self-association.

In vivo, self-crosslinking may play a regulatory role in two ways: localization and attenuation. Self-crosslinking would limit the distance TG_{II} could diffuse from the point of secretion, facilitating the role TG_{II} has been shown to play at and near the cell surface¹⁶. By this mechanism one might assume that TG_{II} must retain full activity after being crosslinked the cell surface or surrounding extracellular matrix, however an identical activity gradient could be maintained with total inactivation following self-crosslinking only requiring a proportionally higher rate of synthesis and secretion. It is yet uncertain what role proteolytic degradation¹⁷ might play in activity attenuation relative to covalent binding investigated here, non-covalent binding as has been seen with fibrinogen in the case of erythrocyte TG but not TG_{II}¹⁸, or by oxidation of the active site or surface moieties⁸.

Evidence of an oxidative inactivation mechanism separate from the crosslinking function under physiologic conditions is provided by the finding that significant uncrosslinked substrate remains at the observed completion of the reaction in the absence of an antioxidant, whereas in the presence of 50 mM DTT reactions eventually proceed to completion. The reaction time course in the presence of DTT are consistent with pseudo-second order inactivation mechanism implied by TG_{II} acting as an amine acceptor substrate (Figure 3-4, Scheme D, Equations (3-9) and (3-10)), If self-crosslinking were the sole mechanism for inactivation, conversion (c.f. Figure 3-7) would in all cases asymptotically approach unity. This finding is supported by reports of TG_{II} susceptibility to Cu²⁺-catalyzed oxidation⁸. Interestingly, it was found that the oxidation of free surface cysteines to cystine may be a route to inactivation, as oxidation of approximately 4

cysteine residues correlated to 100% loss of activity, reversible by addition of excess DTT⁸.

Support for inactivation by both self-crosslinking and oxidation can be found in the excellent fit of the data from Aeschlimann and Paulsson⁵ shown in Figure 3-9 where the final amount of self-labeling of TG_{II} by ³H-putrescine measured at 750nM TG_{II} was significantly greater than 6 times the amount measured at 125nM, as would be expected from stoichiometric radiolabeling. Although their data were taken at a slightly higher pH (8.3), the agreement with the rate constants measured here (Figure 3-7, caption) is quite good both in the effective time constant for reaction and the final relative level of radiolabeling.

The pH-dependence of TG_{II} self-crosslinking points to the possibility of an interesting control mechanism for the expression of TG_{II}. A relatively high self-reactivity at pH~7.5, would result in a negative control mechanism attenuating activity over time. This attenuation may also serve to insure that TG_{II} activity does not persist as it diffuses from the point of expression. A relatively low self-activity at slightly lower pH levels would allow the activity to persist. This may have implications for the role of transglutaminase in wound-healing processes. At the point of severe injury poor perfusion can lead to a drop in tissue pH to as low as pH 5.0 or less¹⁹. At pH levels below 6.7, irreversible cell damage can occur¹⁹ which could then lead to release of intracellular TG_{II}. Under these conditions, the blood clotting cascade would likely become mobilized, resulting in fibrin crosslinking by another transglutaminase, Factor XIII. The presence of elevated and sustained levels of TG_{II} activity may aid in tissue

stabilization. During the process of repair granulation tissue forms, characterized by rapid synthesis of connective tissue and angiogenesis. The pH of this environment is closer to 7.0²⁰, where we measured (pH7.1) an apparent activity 50% higher than at pH 7.5, yet with a similar inactivation rate necessary for spatial regulation.

3.3 Transglutaminase Activity With PEG-Bound Substrates

Modification of enzymes and other therapeutic proteins with PEG chains is a common approach to enhancing the half life of these molecules in the bloodstream²¹. Such modifications typically do not substantially alter protein activity, presumably because small substrates can readily diffuse to the active sites without hindrance from the PEG chains. The situation here is the inverse of the therapeutic one -- here, a small substrate is being modified with a large PEG chain -- and we were concerned that the swollen, randomly-coiled PEG chain might impair the substrate's ability to reach the enzyme's active site. We thus compared the enzyme activity of PEG-bound substrates to free substrate by measuring the coupling of a standard, easily-detected donor amine, monodansyl cadaverine (mdc), to PEG-glycine-glutamine-glycinamide (PEG-GQG_a). PEG-GQG_a was synthesized from the same nominally tetrafunctional PEG molecule described in Section 4.3. Kinetic experiments were performed by the method described in Appendix A5.

Based on the initial rate and the maximal mdc coupling achieved, an apparent rate constant of $1.2 \pm 0.4 \text{ mM}^{-1} \text{ min}^{-1}$ (mean \pm S.E. for a reaction profile) was calculated from the initial rate when enzyme inactivation (Section 3.2) was insignificant. This compares

well with a literature value for benzyloxycarbonyl-glycine-glycine-glutamine-glycine of $1.3 \text{ mM}^{-1} \text{ min}^{-1}$ for mdc incorporation under the same buffer conditions²². It is not entirely surprising that the activity of the enzyme is unaffected by the presence of the large PEG chain. PEG is highly mobile in aqueous solution and recent measurements using the surface force apparatus have demonstrated that PEG-tethered ligands can bind to receptors under conditions where the PEG chain stretches to its fully-extended length to bind²³.

TABLE 3-1

APPARENT RATE CONSTANTS FOR TG_{II}-MEDIATED INACTIVATION

Expt. #	Temp. (°C)	pH	μM TG _{II}	Antioxidant	$k_{i,app}(\text{min}^{-1})^a$
1	37	7.5	0.5	--	0.057
2	37	7.5	1.0	--	0.047
3	37	7.5	2.0	--	0.051
4	37	7.5	2.0	50mM DTT	0.021
5	37	7.1	1.0	--	0.043
6	37	6.0	2.0	--	0.017
7	37	4.0	1.0	--	no rxn.
8	21	7.5	1.0	--	0.038
9	21	7.5	1.0	10μM GSH	0.034
10	21	7.5	1.0	50mM DTT	0.019
11	21	6.0	1.0	--	0.012

^aApparent first order rates ($k_{i,app}$) were derived from a model where Figure 3-4, Scheme A solely describes the mechanism for TG_{II} inactivation. These values are useful for comparisons only and are not expected to represent rate constants for elementary reactions.

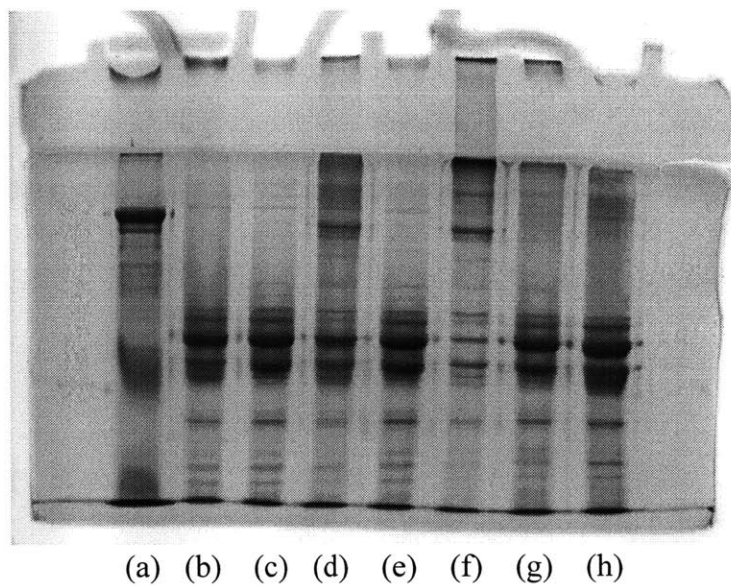


Figure 3-1. SDS-PAGE gel demonstrating tissue transglutaminase self-crosslinking at pH7.4. Lanes contain: weight markers (see Section 3.2.1) (a); aliquot directly from -70°C storage (b); 0mM calcium, 4 °C (c); 8mM calcium, 4 °C (d); 0mM calcium, 37 °C (e); 8mM calcium, 37 °C (f); 8mM calcium, 37 °C, 5mM monodansyl cadaverine (g); 1 week, 0mM calcium, 4 °C (h).

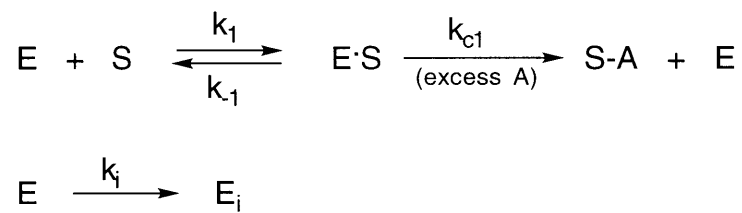


Figure 3-2. Transglutaminase (E) mediated crosslinking between a amine acceptor substrate (S) and amine donor substrate (A), including a transformation from the active (E) enzyme to an inactive state (E_i) through an apparent first-order process.

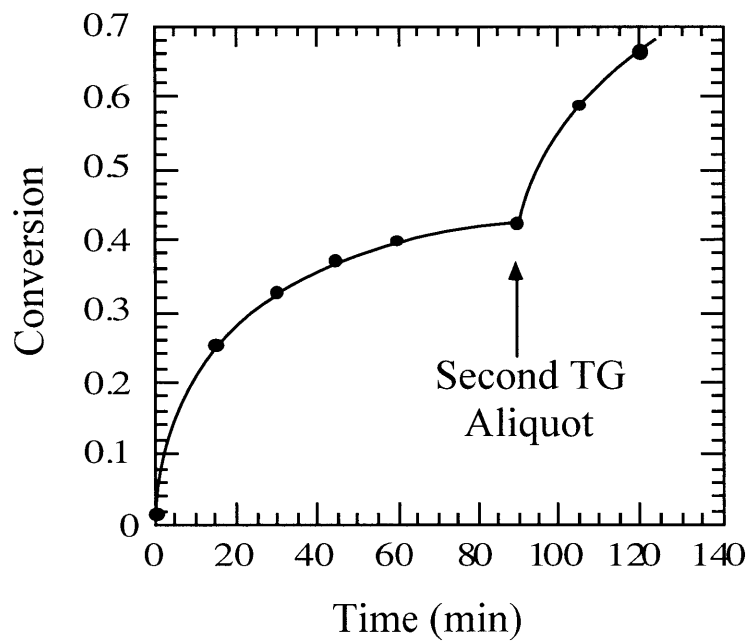
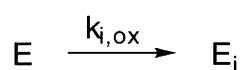
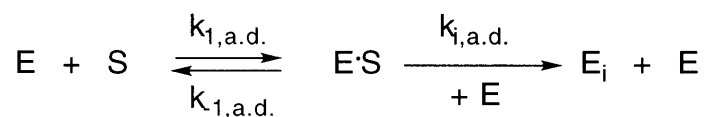


Figure 3-3. Demonstration of gradual loss of enzyme activity. Aliquots of enzyme were added at 0 minutes and 90 minutes. Conditions were as specified in Section 3-2.

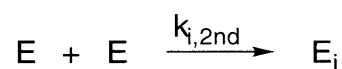
Scheme A



Scheme C



Scheme B



Scheme D

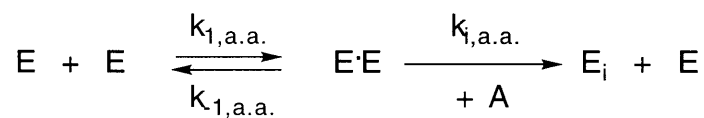


Figure 3-4. Possible TG_{II} inactivation processes. Scheme A describes a first-order process that may be driven by oxidation. Scheme B is a simple second-order process. Schemes C and D are more complex reactions where TG_{II} acts as an amine donor or an amine acceptor, respectively.

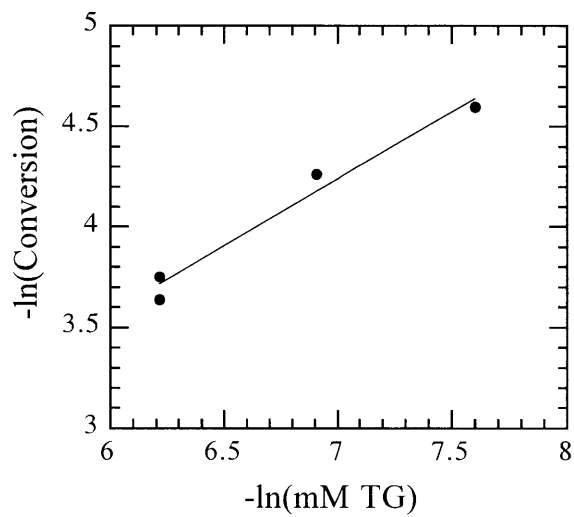


Figure 3-5. Initial rate as a function of initial enzyme concentration. A log-log plot gives the slope ($\phi=0.67$) as the reaction order with respect to $[E]_0$.

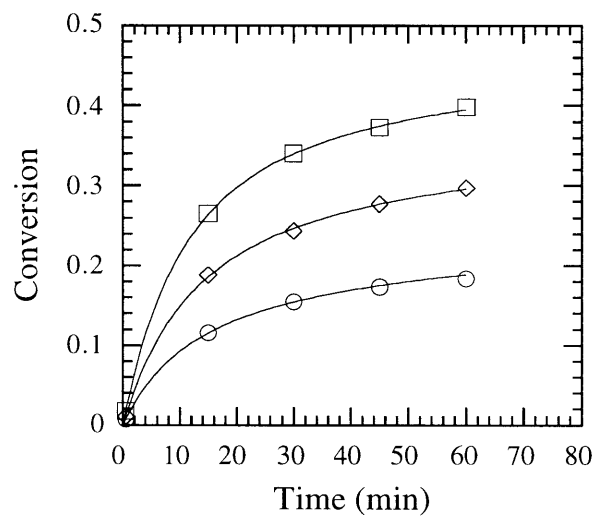


Figure 3-6. Comparison of data and model predictions where inactivation is presumed to be solely through self-crosslinking with TG acting as an amine acceptor (Figure 3-4, Scheme D). Best fit, as defined in Materials and Methods, gives $k_{i,a.d.} = 0.61 \text{ min}^{-1}$, 0.46 min^{-1} and 0.42 min^{-1} for $[E]_t = 0.50 \mu\text{M}$ (o), $1.00 \mu\text{M}$ (◊) and $2.00 \mu\text{M}$ (□), respectively.

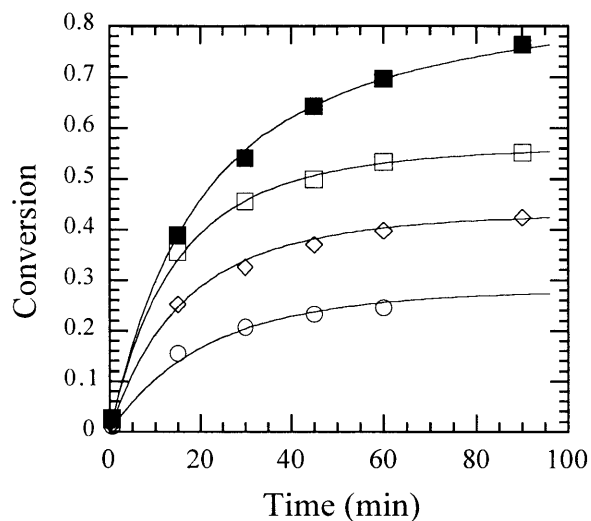


Figure 3-7. Comparison of data and model predictions where inactivation is presumed to occur by self-crosslinking with TG acting as an amine acceptor (Figure 3-4, Scheme D) as well as oxidation (Figure 3-4, Scheme A). All model curves were generated from the individual initial conditions (0.5 μ M TG / 0mM DTT (\circ), 1.00 μ M TG / 0mM DTT (\diamond), 2.00 μ M TG / 0mM DTT (\square) and 2.00 μ M TG / 50mM DTT (\blacksquare)) with (3-4), (3-10) and (3-11), using best fit (Materials and Methods) constants of $k_{i,a,d} = 0.16 \text{ min}^{-1}$, $K_{mi,a,d} = 0.42 \text{ }\mu\text{M}$, $k_{c1} = 5.5 \times 10^2 \text{ min}^{-1}$, $K_{m1} = 7 \text{ mM}$. For the case of 50mM DTT, $k_{i,ox}$ was assumed to be negligible, and set to zero, while for the three cases without DTT, the best fit was found to be $k_{i,ox} = 0.040 \text{ min}^{-1}$.

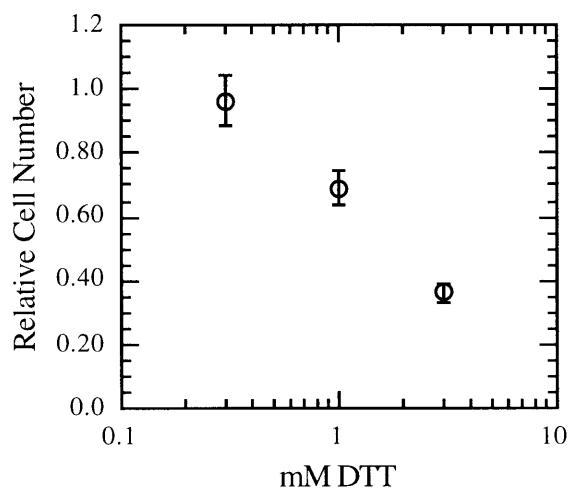


Figure 3-8. Effect of dithiothreitol (DTT) on cell number after 24 hours. Cell numbers are normalized to the 0 mM DTT control.

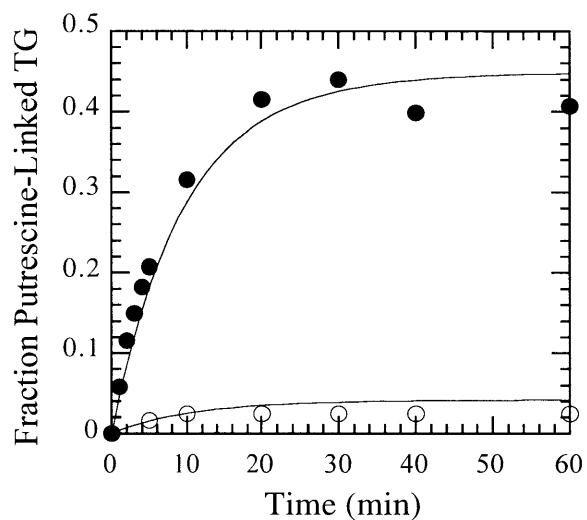


Figure 3-9. Previously published self-crosslinking data⁵ (points), compared with model predictions (lines) inclusive of measured rate constants (c.f. Figure 3-7 caption). Model prediction was based solely on initial conditions of 125 nM (o) and 750 nM (●) TG_{II} and 0 mM exogenous substrate. The ordinate was normalized to match that of Aeschlimann and Paulsson, therefore only relative values (125 nM vs. 750 nM) and time scales should be considered relevant.

3.4 References

1. Greenberg, C.S., Birckbichler, P.J. & Rice, R.H., *FASEB*, "Transglutaminases: multifunctional cross-linking enzymes that stabilize tissues," **5**: 3071-3077 (1991).
2. Raghunath, M., *et al.*, *J. Clin. Invest.*, "Cross-linking of the dermo-epidermal junction of skin regenerating from keratinocyte autografts - Anchoring fibrils are a target for tissue transglutaminase," **98**(5): 1174-1184 (1996).
3. Barsigian, C., Stern, A.M. & Martinez, J., *Journal of Biological Chemistry*, "Tissue (Type II) Transglutaminase Covalently Incorporates Itself, Fibrinogen, or Fibronectin into High Molecular Weight Complexes on the Extracellular Surface of Isolated Hepatocytes," **266**(33): 22501-22509 (1991).
4. Birckbichler, P.J., Orr, G.R., Carter, H.A. & M K Patterson, J., *Biochem. Biophys. Res. Commun.*, "Catalytic formation of epsilon-(gamma-glutaminy)lysine in guinea pig liver transglutaminase," **78**(1): 1-7 (1977).
5. Aeschlimann, D. & Paulsson, M., *J. Biol. Chem.*, "Cross-linking of laminin-nidogen complexes by tissue transglutaminase," **266**(23): 15308-15317 (1991).
6. Aeschlimann, D., Paulsson, M. & Mann, K., *J. Biol. Chem.*, "Identification of Gln726 in nidogen as the amine acceptor in transglutaminase-catalyzed cross-linking of laminin-nidogen complexes," **267**(16): 11316-11321 (1992).
7. Clarke, D.D., Mycek, M.J., Neidle, A. & Waelsch, H., *Arch. Biochem. Biophys.*, "The incorporation of amines into protein," **79**: 338-354 (1959).
8. Boothe, R.L. & Folk, J.E., *J. Biol. Chem.*, "A reversible, calcium-dependent, copper-catalyzed inactivation of guinea pig liver transglutaminase," **244**(2): 399-405 (1969).
9. Nakaoka, H., *et al.*, *Science*, "Gh: a GTP-binding protein with transglutaminase activity and receptor signaling function," **264**: 1593-1596 (1994).
10. Press, W.H., Flannery, B.P., Teukolsky, S.A. & Vetterling, W.T. *Numerical Recipes*, **1986**, Cambridge University Press, Cambridge.
11. Gorman, J.J. & Folk, J.E., *J. Biol. Chem.*, "Structural features of glutamine substrates for transglutaminases: role of extended interactions in the specificity of human plasma factor XIIIa and the guinea pig liver enzyme," **259**: 9007-9010 (1984).

12. Folk, J.E., *J. Biol. Chem.*, "Mechanism of action of guinea pig liver transglutaminase: VI. order of substrate addition," **244**(13): 3707-3713 (1969).
13. Chung, S.I., Shranger, R.I. & Folk, J.E., *J. Biol. Chem.*, "Mechanism of action of guinea pig liver transglutaminase: VII. Chemical and stereochemical aspects of substrate binding and catalysis," **245**(23): 6424-6435 (1970).
14. Chung, S.I. & Folk, J.E., *J. Biol. Chem.*, "Kinetic studies with transglutaminases: the human blood enzymes (activated coagulation factor XIII) and the guinea pig hair follicle enzyme," **247**(9): 2798-2807 (1972).
15. Michaelis, L. & Menton, M.L., *Biochem. Z.*, "Die kinetik der invertinwirkung," **49**: 339-369 (1913).
16. Barsigian, C., Fellin, F.M., Jain, A. & Martinez, J., *J. Biol. Chem.*, "Dissociation of fibrinogen and fibronectin binding from transglutaminase-mediated cross-linking at the hepatocyte surface," **263**(28): 14015-14022 (1988).
17. Zhang, J.W., Guttman, R.P. & Johnson, G.V.W., *J. Neurochem.*, "Tissue transglutaminase is an in situ substrate of calpain: regulation of activity," **71**(1): 240-247 (1998).
18. LeMosy, E.K., *et al.*, *J. Biol. Chem.*, "Visualization of purified fibronectin-transglutaminase complexes," **267**(11): 7880-7885 (1992).
19. Silver, I.A., *Phil. Trans. Soc. Lond. B.*, "Measurement of pH and ionic composition of pericellular sites," **271**: 261-272 (1975).
20. Jensen, J.A., Hunt, T.K., Scheuenstuhl, H. & Banda, M.J., *Lab. Invest.*, "Effect of lactate, pyruvate, and pH on secretion of angiogenesis and mitogenesis factors by macrophages," **54**(5): 574-578 (1986).
21. Harris, J.M. (ed) (1992) *Poly(ethylene glycol) Chemistry*. Topics in Applied Chemistry. Edited by Katritzky, A.R. & Sabongi, G.J., Plenum Press, New York
22. Gorman, J.J. & Folk, J.E., *J. Biol. Chem.*, "Structural features of glutamine substrates for human plasma factor XIIIa (activated blood coagulation factor XIII)," **255**(2): 419-427 (1980).
23. Wong, J.Y., Kuhl, T.L., Israelachvili, J.N., Mullah, N. & Zalipsky, S., *Science*, "Direct measure of a tethered ligand-receptor interaction potential," **in press**: (1997).

4 ENZYMATICALLY CROSSLINKED POLY(ETHYLENE GLYCOL)/POLYLYSINE GELS

4.1 Introduction

This preliminary study of enzymatically crosslinked poly(ethylene glycol) (PEG) hydrogels was designed as a survey of parameters that effect gel formation and properties of the resulting gels. Experiments on equilibrium gel swelling, protein partitioning, diffusion and cell compatibility were designed as assessments of how enzymatically crosslinked PEG gels might perform as cell encapsulants.

A relatively simple model system was devised to carry out this study, comprised of a synthetic PEG-bound amine acceptor substrate and a commercially available amine donor substrate as described below. More complex systems including amine acceptor substrates of higher activity (Section 5.3.1), PEG-linked amine donor substrates (Section 5.3.2), and substrates with collagenase-degradable linkages (Chapter 6) are explored in subsequent chapters.

4.2 Gel Precursor Design

The design of gel precursors was driven by the substrate specificity requirements of the crosslinking enzyme transglutaminase as discussed in Section 1.5.4. For this feasibility study, the simplest transglutaminase substrates were used. For the amine-acceptor substrate, absence of charge near the glutamine residue is necessary presumably due to a hydrophobic pocket at the active site¹. For this reason glutaminamide was used rather than glutamine. For the amine donor substrate, the requirements are less stringent.

Many primary amines are known to be substrates for transglutaminase at various levels of activity. The highest reaction rates are obtained for lysine when a hydrophobic amino acid immediately follows the lysine residue, reading N to C². This structure is reproduced in a well-known amine donor, monodansyl cadaverine³ (Appendix A5). To incorporate hydrophobic character into the amine donor substrate, a random copolymer of lysine and phenylalanine (poly(KF)) was used to insure a population of the preferred substrate. Poly(lysine) was also attempted in the hope that lysine lacking an adjacent hydrophobic residue would be sufficiently active, yet these failed to gel. We therefore compared gels made from various amounts of PEG-Q_a and poly(KF).

4.3 Materials and Methods

Materials. A polyfunctional precursor, nominally "Tetrahydroxy PEG" ("PEG-(OH)₄") was purchased from Polysciences. Poly(ethylene glycol) (PEG) standards were from Scientific Polymer Products (90.4k M_w, 1.03 M_w/M_n; 35.2k M_w, 1.04 M_w/M_n; 10.9k M_w, 1.18 M_w/M_n; 3.07k M_w, 1.06 M_w/M_n). Glutaminamide (Q_a) was purchased from Bachem. Tresyl-chloride was obtained from Aldrich. Triethylamine from Fisher was purified prior to use by distillation. Poly(lysine:phenylalanine)•HBr (Dp_{vis}=185; 54 mol% lysine; MW_{vis}=33.2kD), poly(lysine)•HBr(25.7kD, MW(LALLS)=25.0kD; Dp(vis)=123, Dp(LALLS)=120; Mw/Mn=1.20 by SEC-LALLS) and poly(lysine)•HBr(1kD, Dp(vis)=6) were purchased from Sigma. Phosphate buffered saline (PBS) (0.20g/L KCl, 0.20g/L KH₂PO₄, 8.00g/L NaCl, 1.15g/L Na₂HPO₄, 2.16g/L Na₂HPO₄•7H₂O, pH=7.1) was from Gibco. Monodansyl cadaverine was purchased from

Aldrich. Transglutaminase and the diffusion test proteins -- hen egg lysozyme, bovine erythrocyte carbonic anhydrase and bovine serum albumin -- were purchased from Sigma.

Transglutaminase Storage and Activity Assay. Enzyme aliquotting was performed in a 4°C cold room. Lyophilized transglutaminase was dissolved in a transglutaminase Storage Buffer⁴ of 10mM Tris-Acetate at pH=6.0 with 160mM KCl, 1mM EDTA and 2mM DTT. The aliquotted enzyme solution was stored at -70°C until use.

Transglutaminase activity was determined by the method of Folk and Chung⁴. Briefly, the incorporation of hydroxylamine into carbobenzyloxy-glutaminyglycine is measured by a colorimetric assay of the complex formed between the reaction product and acidic ferric chloride. The activity of the aliquotted enzyme was found to be 0.010 U/mL where one transglutaminase unit is defined by the amount necessary to form 1 mmol of hydroxamate per minute from N-a-benzyloxycarbonyl-glutamine-glycine and hydroxylamine at pH 6.0 at 37°C.

Transglutaminase Activity With PEG-bound Glutamine. To compare transglutaminase's activity towards peptidyl and PEG-bound glutamine residues, a standard transglutaminase activity assay based on the incorporation of monodansyl cadaverine (mdc) was carried out on PEG-glycine-glutamine-glycinamide (PEG-GQG_a). PEG-GQG_a was synthesized by tresyl-mediated coupling (described below) in a solvent of dimethylformamide with methylene chloride. The assay reaction was carried out at room temperature with 9.56mg/mL PEG-GQG_a and 1.64mg/mL mdc in 100mM Tris/chloride buffer containing 30mM NaCl, 1mM EDTA and 50mM CaCl₂. At various times during the reaction, aliquots were separated by gel permeation chromatography (c.f. next section) to quantify the amount of PEG-linked mdc versus unlinked mdc.

Gel Permeation Chromatography. Aqueous gel permeation chromatography (GPC) for analysis of PEG-OH and PEG-Q_a compounds was performed using two columns in series (TSK G4000PW and TSK G6000PW) with water/0.05% sodium azide as the mobile phase. Detection was by refractive index and light scattering. To calculate absolute molecular weights from light scattering data, the dn/dc of pure poly(ethylene oxide) was used.

Aqueous GPC for the transglutaminase activity assay was performed on a TSK G2000PW column with aqueous 0.05% sodium azide at 1.00mL/min using UV photodiode array (200nm - 350nm range) detection.

Aqueous GPC for analysis of gel leachates was performed on three GPC columns in series (2xTSKG4000PW and 1xTSKG3000PW). The mobile phase was 50mM Tris·HCl with 50mM Tris base at 1.50mL/min. Detection was at 266nm.

Organic GPC for PEG-OH and PEG-Q_a characterization was run on two columns in series (Phenomenex linear and 1000Å styrene-divinylbenzene) with chloroform at 1.00 mL/min at room temperature. Detection was by refractive index. For molecular weight determination, a calibration curve was generated using monodisperse linear PEG's.

PEG-OH and PEG-Q_a Characterization. The PEG precursor is described by the manufacturer as a predominately tetrafunctional reaction product of 10k PEG with bisphenol A diglycidyl ether (structure I of Figure 4-2, "PEG-OH"). The product contains a mixture of single 10k chains, double PEG chains (structure I of Figure 4-2) as well as molecules containing three or more chains. Based on UV spectral analysis the product was found to contain approximately one bisphenol unit per PEG chain. This could be explained either by some degree of stacking of bisphenol units (structure II of

Figure 4-2) due to aggregation during the synthesis process or by an incomplete synthesis reaction, resulting in molecules which terminate in bisphenol units (structure III of Figure 4-2). It is presumed that the synthesis reaction is run to completion and that structure II accounts for the concentration of bisphenol units in the product, implying that “PEG-OH” will have 2 hydroxyl groups for each PEG chain. The presumption of structure II is supported by evidence of branched species discussed below.

To determine the molecular weight distribution, PEG-OH was separated by both organic and aqueous gel permeation chromatography (GPC) under the conditions described above. Whereas PEG-Q_a in chloroform formed only unfilterable aggregates, PEG-Q_a was analyzed by aqueous GPC only. Using organic GPC, PEG-OH single chains (at 10.2K by linear PEG stds.) were baseline separated from double chains (at 22.3K by linear PEG stds.) and higher multiples, confirming the molecular weight of a single chain. It is possible that the presence of relatively stiff bisphenol A in the double PEG chain enlarges the PEG random coil somewhat, causing it to elute at a slightly higher molecular weight than twice the single chain molecular weight. Peak integration gives 68wt% single chains, 7.3wt% double chains and 25wt% of triplets or higher. Species beyond 50K were beyond the linear range of the organic column.

Aqueous GPC with light scattering and refractive index detection was used to better resolve the higher molecular weight species. The highest molecular weight species was found to be $7.6 \cdot 10^6$ g/mol by LS, equivalent to approximately 700 chains. By comparison with the molecular weight of this species based the elution volume of high molecular weight linear poly(ethylene oxide) standards ($1.0 \cdot 10^6$ g/mol), it was concluded

that high molecular weight PEG-OH has some degree of branching, possibly by bisphenol self-reaction shown in structure III.

Pre-gel Macromer Synthesis. A multifunctional glutaminy-PEG adduct, PEG-Q_a was synthesized by tresyl-mediated coupling. PEG-OH (40g) was dried by incubation at 4°C overnight in 300mL dry methylene chloride over molecular sieves. Just prior to use the PEG/methylene chloride solution was decanted from the sieves. The sieves were rinsed with two 25mL portions of dry methylene chloride to yield a total of 350mL of the PEG/methylene chloride solution. To this was added 2.64mL triethylamine with stirring. To initiate the tresylation, 2.0g tresyl chloride was added dropwise. The reaction flask was filled with dry argon and stirred for two hours. The resulting PEG-Tr was purified by successive reprecipitations from acidified methanol using decreasing amounts of acid (37% aq. HCl in MeOH: 1x 1.7 μL/mL, 1x 0.67 μL/mL, 2x 0.33 μL/mL, 2x pure MeOH). Residual amounts of methanol were removed *in vacuo*. Dry PEG-Tr was aliquotted into vials and stored at -70°C until use. Based on the manufacturers stated molecular weight of 18.5K for PEG-OH, tresylation as found to be 90% ± 2% based on sulfur elemental analysis [53.72%C, 8.61%H, 0.54%S; average of two samples].

For the PEG/Q_a coupling reaction, 2.15g of PEG-Tr was added to 19.6mL of a solution of 100mM Q_a•HCl and 200mM imidazolyl-acetate buffer at pH7.0. The coupling proceeded overnight at 4°C. Under these conditions in a separate experiment the apparent second order rate constant for the displacement of the tresyl group by Q_a was measured to be 0.13 M⁻¹min⁻¹ by monitoring the loss of primary amines of Q_a by the o-phthalaldehyde fluorometric assay for primary amines⁵. The solution was frozen and

dried by lyophilization. Purification was by successive reprecipitations from methanol. Residual amounts of methanol were removed *in vacuo*. The absence of residual uncoupled glutaminamine was verified by the o-phthaldialdehyde fluorometric assay for primary amines. Elemental analysis showed a substitution level of 0.126 ± 0.012 mmol Q_a per gram of polymer based on nitrogen elemental analysis [55.05%C, 8.83%H, 0.53%N; average of two samples]

PEG-OH and PEG- Q_a have identical molecular weight distributions (Figure 4-3), indicating that no detectable scission or crosslinking of PEG chains occurred during the synthesis process.

Network Formation. All gels were formed with 2.5 U/mL (2.3 μ M) transglutaminase and 6mM calcium chloride in a buffer of 50% transglutaminase Storage Buffer and 50% Reaction Buffer (100mM Tris-HCl, 1mM EDTA, pH8.3) at 37°C. The mixture of the enzyme plus the buffers has a pH of 7.5 at 37°C. Gels for the diffusion assay were made with 20wt% PEG- Q_a (25mM Q_a) and 5.0wt% poly(KF)•HBr (149mM Lys). For swelling measurements, gels were made with 20%/5%, 10%/5%, and 20%/2.5% PEG- Q_a /poly(KF)•HBr concentrations. Gel components were mixed at 4°C, then warmed to 37°C for gelation.

To measure the amount of unreacted PEG- Q_a and poly(KF), gels were cast in the bottom of a 12.0mm diameter glass vial and allowed to equilibrate in a series of three PBS wash solutions over a time span of 13 days (well beyond the observed equilibrium as well as the theoretical equilibrium based on analysis of measured diffusion behavior of several solutes). The wash solutions were analyzed by aqueous GPC with detection at 266nm.

Swelling Measurements. Experiments conducted in a uniaxial swelling mode. Gels were formed in the bottom of a 12.0mm diameter glass vial as described above and allowed to swell to equilibrium by addition of excess PBS on top of the formed gel. The swelling ratio, α , defined as the ratio of the swollen gel volume to the initial volume, is the ratio of the final (equilibrium) gel height to the initial gel height for the case of uniaxial swelling.

Diffusion Assay. A two half-cell diffusion apparatus was used to measure the diffusion constant of macromolecules in PEG-poly(KF) gels. The gel was formed and swollen in a 3/4 inch inner diameter stainless steel ferrule secured to a glass slide. After swelling, the gel was further incubated for 4 days in multiple volumes of PBS to remove trace unreacted polymers and enzyme. To assemble the apparatus, gel and ferrule were inverted onto 0.45 μ m Millipore PVDF (type HVLP04700) filter paper. The ferrule was then loaded into the washer housing and backed by another section of filter paper.

At the start of each experiment, the donor cell was filled with 3mL of a PBS solution of a single test protein (1-2 mg/mL), and the acceptor cell was filled with 3mL of pure PBS. The concentration of the acceptor cell was monitored over time by absorbance at 280nm. Experiments were conducted at 22 ± 1 °C.

For partition coefficient determination, a gel was cast in the bottom of a 12.0mm diameter glass vial, allowed to swell to an equilibrium height (12.5mm), and cleared of unreacted poly(KF) and PEG-Q_a by multiple PBS washes over four days. A mixture of the test proteins (2.0mg/mL BSA, 1.0 mg/mL carbonic anhydrase and 3.0mg/mL lysozyme in PBS) was added to the top of the gel, allowing the proteins to diffuse into the gel over 13 days. Samples of the protein solution above the gel were taken

periodically and separated by aqueous GPC with detection at 280nm to quantify the concentration of each protein individually. To compensate for the possibility of protein adsorption to the glass vial and protein degradation, a control vial containing the protein mixture but no gel was also monitored by aqueous GPC with detection at 280nm. According to mathematical analysis of the time required to reach equilibrium, using measured diffusion coefficients, all proteins were expected to be in equilibrium after 13 days. These predictions were supported by constancy of protein concentration in the supernatant by 13 days and thus partition coefficients were determined at the 13 day time point.

Cell Compatibility. All cell compatibility experiments were carried out with balb/c 3T3 cells in a culture media of high glucose Dulbecco's Modified Eagle Medium supplemented with 200mM L-glutamine, 10% calf serum and 1% penicillin / streptomycin to inhibit bacterial growth. All products were from Gibco.

For cell-contact experiments sub-confluent cultures were rinsed with phosphate buffered saline (PBS) prior to addition of test solutions. Test solutions consisted of PBS (control; n=3), gelation buffer (see *Network Formation* above; n=3), PEG/polyKF gel (see *Network Formation* above; n=2) and transglutaminase alone at gelation concentration (n=2). After one hour serum-containing media was added to each well. After 36 hours each well was assessed for attached cells and viability by tripan blue dye exclusion.

For experiments designed to assess the effect of transglutaminase on cell attachment and growth, cells were dispersed in Versine (0.2g/L EDTA in PBS, Gibco) and plated in 96-well plates with serum-free media (32 μ L) in the presence varying amounts of transglutaminase (8 μ L). After one hour, 160 μ L of serum-containing media was added to

each well. Cell numbers were counted at 1, 2 and 3 day time points. All experiments were done in triplicate.

For cell encapsulation experiments, cells were detached from culture dishes by trypsinization. Trypsinization was stopped by the addition of an equal volume of soybean trypsin inhibitor (0.25mg/mL, Gibco). Two microliters of cell suspension was added to 28 μ L of pre-gel solution (see *Network Formation* above). Two microliters of calcein AM (Molecular Probes) was added just prior to enzyme addition. Gelation was allowed to proceed for one hour at 37°C at which time fluorescent images were photographed to assess cell viability by calcein AM fluorescence.

4.4 Results and Discussion

The concentrations of precursors can potentially affect gel formation in several ways, but a key lower bound on each precursor concentration can be identified. Poly(KF) is assumed to act as a rigid crosslink point for the mobile PEG chains; thus, its concentration determines the average distance between crosslinks. The poly(KF) concentration must then be at least great enough that the average distance between crosslinks, $(C_{\text{poly(KF)}} * N_A)^{-1/3}$, is less than the fully extended length of the PEG chains (60 nm) in the PEG-Q_a precursor. To achieve network formation with the minimum structural functionality (greater than two) at an average crosslink, the concentration of PEG chains functionalized on each end with Q_a must be at least 3/2 the concentration of poly(KF). Effects of absolute and relative concentrations of each of the precursors are discussed below in the context of gelation results.

The concentrations of poly(KF), poly(K), and PEG-Q_a used to form gels in this study, and the resulting gel properties, are shown in Table 4-1 and gels will be referred to by the designations listed there. The average distances between crosslinks for the concentrations of poly(KF) shown in Table 4-1 -- 10 nm for 5wt% and 13 nm for 2.5wt% -- are comparable to the RMS end-to-end distance of the PEG chains (10 nm) or slightly greater. The concentrations of PEG-Q_a used were 6-12 fold greater than the minimum (lower bound) concentration and are well above the minimal overlap concentration (1.4wt%) for 10k PEG chains. All gels were formed with at least a six-fold stoichiometric excess of lysine:Q_a residues, corresponding to on average 8-17 PEG chains crosslinked to a single poly(KF) chain, assuming all Q_a residues and poly(KF) react. The concentration of enzyme was approximately three orders of magnitude lower than the concentration of poly(KF) in all cases.

20/5.0 mixtures formed clear colorless gels with significant viscosity increases within 30 minutes. The gelation time is thus comparable to the estimate, obtained above, based on negligible diffusion resistance of the enzyme during gel formation. Based on analysis of components washed from the gel, 90% of the initial poly(KF) and 91% of the initial PEG-Q_a was covalently linked in the gel. The majority of leached PEG material comprised single chains. Reducing either the poly(KF) or the PEG-Q_a by half (20/2.5 and 10/5.0 gels) also allowed formation of clear gels, but small amounts of opacity concentrated at the top of both types of the gel were observed. The 10/2.5 combination formed only a viscous, opaque solution. No evidence of gelation was observed for either poly(K) precursor, despite comparable concentrations of available lysines, confirming the structural specificity of the enzyme.

The presence of opacity most likely is indicative of microgels that did not become crosslinked into the bulk of the gel. Excess fluid added to the top of the 20/2.5 and 10/5 dispersed the opaque portion, indicating incomplete gel formation in the upper opaque region. The clear regions of all gels remained entirely intact over several weeks in water.

Several explanations are possible for the observed incomplete gel formation. A tendency towards phase separation may play a role. PEG solutions with high concentrations of salt are known to phase separate into PEG-rich and PEG-poor phases⁶. This phenomenon is typically observed for small (2-3k) PEG at salt concentrations an order of magnitude higher than those found in the present study, yet at longer chain lengths, this effect is enhanced. Another possibility is a reaction driven inhomogeneity. During the process of gel formation, it is possible that a slight density increase in crosslinked PEG's could cause the more fully crosslinked species to sink, increasing the likelihood that a continuous gel layer would form below the discontinuous microgel layer. In the case of the 20/2.5 gel, it is possible that a transglutaminase-catalyzed termination side-reaction may play a role. It has been shown that the rate of the competing hydrolysis reaction of PEG-glutamine \rightarrow PEG-glutamic acid is enhanced as the concentration of the lysine substrate is reduced^{7, 8}. This reduction of the number of crosslinkable moieties could lead to the observed incomplete reaction.

4.4.1 Equilibrium Swelling Behavior

Swelling behavior is an important parameter for many of the intended applications of the gels and was used to assess features of the resulting network structure. Gels were

swollen to equilibrium in cylindrical glass vials and exhibited swelling ratios in the range 1.5 - 2.1 (Table 4-2).

These swelling data can be used to estimate the efficiency of linking the both ends of a PEG- Q_a macromer into the gel under the different gelation conditions by modifying Flory's equilibrium swelling theory to account for the types of crosslinks in the PEG- Q_a /poly(KF) gels. Analysis of swelling data provides the number of elastically effective chains in the gel, and this number can be compared to the total number of macromer chains present in the gel. Elastically effective chains may arise from both chemical crosslinks and physical crosslinks (entanglements), and thus separate information on the relative numbers of physical and chemical crosslinks is needed to estimate of the fraction of free chain ends.

The important physical aspect of the gel to be captured in equilibrium swelling analysis is the stretching of Gaussian chains. We define a crosslink as a non-Gaussian, or stiff region that joins together two or more Gaussian chains. Due to the long persistence length of peptides in general and the expected rod-like structure of poly(KF) in ionic solutions^{9, 10}, it is most appropriate to define each poly(KF) molecule as a node or crosslink. The presumed network structure is depicted in Figure 4-1. The functionality, f , of any particular crosslink is then number of PEG chains attached to a particular poly(KF) molecule. The theoretical mean crosslink functionality is determined from the stoichiometry of the reaction solution; *e.g.*, a 20/5 gel would lead to a theoretical crosslink functionality of 17, or 17 PEG chains attached to each poly(KF) molecule. The crosslink functionality distribution of poly(KF) is not known *a priori*, however -- the theoretical value is a maximum which may not be reached, and we presume a distribution

of crosslink functionalities will exist in the gel. Following the original development of Flory, we derived an expression for the number of elastically effective chains in the gel, ν_e , as a function of f for the case of polydisperse network functionality, and defined a parameter Φ which represents the salient features of the network structure:

$$\Phi = \frac{\text{number of elastically effective chains}}{\text{number of macromer chains}} \quad (4-1)$$

Details of the derivation and data analysis are provided in Appendix B. Values of Φ from equation (B17) for various proportions of PEG to poly(KF) are given in Table 2 and can be compared to gain insight into the process of PEG-poly(KF) gel formation. Note that Φ can be greater than one, since physical entanglements lead to elastically effective chains. In an ideal gel it would be possible to quantify the number of dangling chain ends based on Miller-Macosko theory^{11, 12}, thus making Φ a measure of entanglements for the case of negligible chain loops. However in PEG-poly(KF) gels, the reactivity of each lysine is dependent on adjacent amino acid residues to an unknown degree, precluding the use of this type of probabilistic analysis.

Values of $\Phi(20/5)$ and $\Phi(10/5)$ are comparable and significantly lower than $\Phi(20/2.5)$. Thus, the poly(KF) concentration appears to exert a dominant effect. It is unlikely this effect arises from stoichiometric reaction considerations; lysine residues are present in excess relative to Q_a residues and free lysine concentrations change only slightly throughout the gelation reaction (17% for the 20/5 gel and 8.5% for the 10/5 gel).

Furthermore, since the extent of completion of the transglutaminase reaction is a function of lysine concentration, in the absence of diffusion limitations on transglutaminase (affirmed below), the proportion of dangling ends in the 20/5 should be slightly higher than in the 10/5 gel and $\Phi(20/5)$ should be slightly less than $\Phi(10/5)$. The opposite is observed -- $\Phi(20/5)$ is slightly greater than $\Phi(10/5)$.

It is probable that the concentration of physical entanglements contributes significantly to the differences in Φ . The average molecular weight between entanglements M_{en} , is 2200 in bulk PEG¹³, and is greater for PEG in solution. Gnanou and coworkers¹⁴ determined the fraction of physical entanglements in end-linked PEG gels with tetrafunctional crosslinks as a function of polymer volume fraction in the gel and reported a decreasing fraction of entanglements with decreasing polymer volume fraction and chain length. At a pre-gel polymer volume fraction of 0.32, Gnanou et al. reported that 30% of the chains were entangled for gels with 5.6k PEG chains; we expect a similar amount of overlap for 10k PEG at a volume fraction of 0.20. In the PEG/poly(KF) gels, it is expected that the localization of many chains at PEG-poly(KF) crosslinks (17-34) would increase entanglements over the case of the Gnanou study -- we expect more physical entanglements in gels with higher average PEG concentration *or* higher concentration of PEG at the poly(KF) crosslink.

This interpretation is consistent with the data. With half the number of poly(KF) molecules in the 20/2.5 gel as in the 20/5 gel, the mean crosslink functionality doubles from 17 to 34 -- effectively doubling the concentration of PEG chains in the vicinity of the crosslink and increasing the probability of entanglements. Likewise, $\Phi(20/5)$ is

somewhat greater than $\Phi(10/5)$ indicating that the bulk PEG concentration exerts a similar effect, but less profound.

In applications of these gels as cellular scaffolds, it may be desirable to reduce the swelling ratio as much as possible. The data in Table 2 imply a means of controlling swelling behavior of PEG-poly(KF) gels by variations in PEG- Q_a and poly(KF) concentrations, yet the formation of a microgel layer is indicative of lower limits of both constituents. Still, there are alternative means of achieving the effects of a higher degree of entanglements and higher crosslink densities. Fractionation of the PEG-OH starting material into a pool of higher molecular weight species could reduce the likelihood of microgel formation, allowing for lower concentrations of PEG- Q_a to be used. Reducing the molecular weight of the PEG chains would also tend to reduce the degree of swelling. Manipulation of the poly(KF) molecule could influence swelling effects as well. By increasing the amount of lysine in poly(KF) by either increasing the proportion of lysine or increase the molecular weight, a higher crosslink density could be achieved. Any of these manipulations may affect other gel properties in a positive or negative way.

4.4.2 Protein Partitioning and Diffusion

Diffusion of proteins in the gels is important both for gel formation, where restrictions on diffusion of the enzyme may impair gel formation, and for the function, since many cellular functions are governed by macromolecular nutrients and cytokines released by adjacent cells or transported from blood. Diffusion and partition coefficients were determined by a combination of steady state and transient flux measurements in a standard 2-cell diffusion chamber and by equilibrium measurements of partitioning. The

partition coefficients for the gel is defined as $K_{pg} = c_{gel} / c_{bulk}$. The apparent values of K_{pg} for lysozyme, carbonic anhydrase, and albumin are shown in Table 3 along with the physicochemical properties of the proteins. The small proteins exhibit comparable exclusion from the gel while albumin shows an apparent partitioning into the gel. Albumin has an isoelectric point (IE) of 4.7¹⁵ and is thus negatively charged at pH 7.1, which makes it attractive to the positively charged lysine residues of poly(KF) in the gel. Thus the apparent partition coefficient for albumin is the product of the true partition coefficient (due to excluded volume) and a binding term. Carbonic anhydrase is slightly acidic (IE=5.9¹⁶) yet appears to behave in a neutral fashion with respect to partitioning.

The steady-state flux across the gel, $N_{protein}$, is written in terms of the overall concentration difference between the bulk concentration in the donor chamber, $c_{1\infty}$, and that in the receiver chamber, $c_{2\infty}$, as

$$N_{protein} = (c_{1\infty} - c_{2\infty}) / R_{TOT}. \quad (4-2)$$

The overall resistance to mass transfer, R_{TOT} , is the sum of the diffusion resistance of the gel, the diffusion resistances of each supporting membrane (presumed identical), and the convection resistances of each stirred cell (presumed identical):

$$R_{TOT} = \frac{\delta_g}{K_{pg} D_g} + \frac{2\delta_m}{K_{pm} D_m} + \frac{2}{k_c}. \quad (4-3)$$

where δ_g and δ_m are the thicknesses of the gel sample and the PDVF support membrane, respectively, D_g and D_m are the diffusion coefficients in the gel and membrane, and k_c is the convective mass transfer coefficient.

The convective resistances are negligible in comparison to the diffusion resistances in this system, and we can thus write the resistance in the support membranes as a fraction of the total resistance as:

$$\frac{2\delta_m / (K_{pm} D_m)}{2\delta_m / (K_{pm} D_m) + \delta_g / (K_{pg} D_g)} = \frac{1}{1 + \left(\frac{\delta_g}{2\delta_m}\right) \left(\frac{K_{pm}}{K_g}\right) \left(\frac{D_m}{D_g}\right)} \quad (4-4)$$

For this experimental arrangement $\delta_g \approx 300\delta_m$ (i.e., gel = 3 mm and membrane = 0.01 mm), and the partition coefficients, which are governed by excluded volume effects, should be of comparable values for the membrane and gel. We also expect that the diffusion coefficients will be comparable in magnitude or that the gel diffusion coefficient will be less than that in the membrane due to the large, open pores in the membrane compared to the gel. Thus, the resistance of the support membranes is estimated to be <10% of the gel and can be neglected for our purposes here. These assumptions are supported by the values of the measured diffusion coefficients for small solutes in the gel, which are equivalent to those in free solution. Steady state flux measurements, achieved when $t \approx 0.5\delta_g^2 / D_g$, thus allow the product $K_g D_g$ to be determined¹⁷.

Independent values of the diffusion coefficients may be extracted from analysis of the transient regime. In the absence of binding to the matrix, the species balance for protein diffusion in the gel is

$$\frac{\partial c_g}{\partial t} = D_g \frac{\partial^2 c_g}{\partial x^2} \quad (4-5)$$

Under our experimental conditions, the initial concentration of protein in the gel is zero, $c_{1\infty} \gg c_{2\infty}$ and $c_{2\infty} \equiv 0$ throughout the experiment, and thus

$$\frac{Q_t}{\delta_m c_g} = \frac{D_g t}{\delta_g^2} - \frac{1}{6} - \frac{2}{\pi^2} \sum_1^{\infty} \frac{(-1)^n}{n^2} \exp(-D_g n^2 \pi^2 t / \delta_g^2) \quad (4-6)$$

where Q_t is the total amount of material which has passed through the gel at time t . As $t \rightarrow \infty$, this solution approaches a line which has an intercept on the t -axis given by

$$\tau_{lag} = \delta_g^2 / 6D_g \quad (4-7)$$

The diffusion coefficients for carbonic anhydrase and lysozyme were determined by both steady state and time lag analysis, and the two analyses led to values which were not statistically different from each other and comparable to the values for diffusion in free solution (Figure 4-4).

The apparent partition coefficient for albumin is greater than one and thus albumin binds to the gel, probably to the positively-charged poly(KF). While rapid, reversible

binding does not affect the steady-state flux, the binding sites act as a sink during transient diffusion and this results in a lower apparent value of the diffusion coefficient. For rapid, reversible binding, the transient species balance becomes

$$\frac{\partial c_g}{\partial t} = \frac{D_g}{1 + \frac{N_t K_d}{(K_d + c_g)^2}} \frac{\partial^2 c_g}{\partial x^2} \quad (4-8)$$

where N_t is the concentration of binding sites in the gel, c_g is the concentration of free (unbound) ligand in the aqueous phase in the gel, and the dissociation constant, K_d , relates the concentration of unoccupied binding sites, N , and the concentration of bound protein-site complexes, $N-p$, to the concentration of protein in free solution within the gel:

$$K_d = \frac{[N][c_g]}{[N - p]} \quad (4-9)$$

At very high protein concentrations, the diffusion coefficient approaches the true value, and at very low protein concentrations, the apparent diffusivity becomes $D_g / (1 + N_t / K_d)$. The concentration of poly(KF) in the gel is about 1 mM and the size of poly(KF) (~28 nm x 1-2nm, based on 1.5Å rise per residue in an alpha helix) suggests it can bind 1-2 albumin molecules (13 x 4 nm) each, along with the crosslinked PEG chains; thus $N_t \sim 1-2$ mM. An albumin concentration of ~0.01 mM was used in the partitioning experiments; i.e., $c_g \ll N_t$ and thus $N \sim N_t$. The total concentration in the gel, $c_{g,tot}$ was 3.9 times greater than that in free solution, c_∞ . Since $c_g \sim 0.5c_\infty$,

$N - p \cong 7c_g$ and $K_d \cong [N_t] / 7$. Under the experimental conditions used, $c_g \sim 0.01$ mM $\ll K_d$ and thus it follows $D_{g,apparent} = D_g / (1 + 7)$.

The apparent BSA diffusivity was calculated from the time-dependent solution and is a factor of 8 less than diffusion in free solution, which indicates that the true diffusivity of BSA in the gel is the same as that in free solution (Figure 4-4). PEG gels formed from 10k linear diacrylates show similar behavior with the BSA diffusion coefficient in the gel on the order of the value in free solution as calculated from protein release data¹⁸. PEG gels formed from the acrylated form of the same PEG precursor used in this study are also highly permeable to BSA¹⁹. However, PEG gels formed by radiation-crosslinking linear PEG to obtain a molecular weight between crosslinks (M_c) comparable to the size of the PEG macromer chains used here (10k) significantly inhibit diffusion of albumin compared to free solution²⁰. For radiation-crosslinked gels, which have a uniform gel structure comprising tetrafunctional crosslinks, $K_{pg} \sim 1$ whereas for the enzymatically crosslinked gels, $K_{pg} \sim 0.5$, suggesting that the gels possess different structures.

From this analysis, we can infer the diffusion characteristics of the enzyme in the gel, which we expect to be comparable to the diffusion behavior in free solution based on the rapidity of gel formation. The diffusion coefficient of transglutaminase in free solution is 0.68×10^{-6} cm²/sec at 20°C²¹, a value greater than that for BSA (0.576 cm²/sec at 20°C). Transglutaminase has a greater mass than BSA (77K vs. 67K) but is more spherical, resulting in a lower Stokes-Einstein radius for transglutaminase (32Å vs. BSA of 36Å). Thus, the gel should present negligible diffusional resistance to the enzyme during or after gel formation.

4.4.3 Cellular Interactions

The nature of cellular interactions is a key concern when designing a cell scaffold. Unfavorable cellular interactions can lead to cell death or an adverse immune response that may result in infiltration by cells of the immune system and/or fibrous capsule formation around the offending material. Therefore, the success of a tissue engineered construct is highly dependent on eliciting, at worst, only a mildly negative response.

The choice of poly(ethylene glycol) (PEG) as the polymer backbone was based in part on a favorable lack of cellular interactions by virtue of the non-protein adsorbing characteristics of PEG²². As other molecules have been added to this system to allow for crosslinking, it was necessary to explore the possibility of cytotoxicity of this gel system. This was done in two ways: culturing cells in contact with gel components and encapsulating cells by enzymatically crosslinked gel formation.

Cells encapsulated within an enzymatically crosslinked gel would only be exposed to certain components until they are diluted by free diffusion *in vivo*. Cell compatibility of gelation components (Section 4.3) were performed over a one hour time period as a possible relevant time scale for cell contact. Where cells were challenged with gelation buffer, transglutaminase with buffer and a gel formed directly on top of the cells, it was found that in all cases cells remained attached and viability was greater than 99%, identical to a phosphate buffered saline control.

To test the influence of transglutaminase on cell attachment and subsequent growth, cells were seeded on tissue culture polystyrene in the presence of varying amounts of transglutaminase. The results are shown in Figure 4-5. Cell growth over three

days was found to be similar to control for all concentrations tested, up to 3.0 μ M.

Attachment appeared to be positively influenced by the presence of transglutaminase. At 0.10 μ M and 0.30 μ M transglutaminase plating efficiencies were found to be similar to control, the 0.30 μ M case giving slightly higher cell numbers. When plated in the presence of 1.0 μ M or 3.0 μ M transglutaminase cell attachment is positively influenced at similar levels as compared to the control. This effect appears to be sigmoidal as no further enhancement is gained from increasing the transglutaminase concentration from 1.0 μ M to 3.0 μ M.

A test for cell compatibility of encapsulation within TG-crosslinked PEG gels was performed by suspending cells in a pre-gel solution prior to enzyme addition. After the gel had formed (1 hour), live cells were visualized on a fluorescent microscope, identified by a viable cell indicator, calcein AM. Many live cells could be seen throughout the gel, indicating live cells could be delivered and encapsulated within a PEG/poly(KF) gel.

This variety of tests indicate that the gel components and the process of gel formation are not expected to be acutely toxic to cells. To confirm this hypothesis, more extensive testing with a variety of cell types could be performed. As previously mentioned, potential immunogenicity will also play a role in the survival of a tissue engineered construct composed of a PEG/poly(KF) gel. *In vitro* as well as *in vivo* experiments should be performed to assess the degree of expected immunogenicity for human applications.

TABLE 4-1
GELATION BEHAVIOR OF MACROMERS

Initial [poly(x)] wt% (mM)	Initial [PEG-Qa] wt% (mM)	Designation %PEG/%KF	Gel Appearance	% Precursor Retained in Final Gel	
				PEG(Qa)	poly(KF)
<i>poly(KF), 33K</i>					
5 (1.4)	20 (12.5)	20/5	clear, colorless gel	91.....	90
5 (1.4)	10 (6.3)	10/5	clear gel with thin opaque layer on the top	86.....	60
2.5 (0.7)	20 (12.5)	20/2.5	clear gel with thin opaque layer on the top	84.....	31
2.5 (0.7)	10 (6.3)	10/2.5	no gel; viscous, opaque solution	-	-
<i>poly(K), 1K</i>					
5 (50)	20 (12.5)	-	no gel; clear solution	-	-
<i>poly(K), 25K</i>					
5 (2.0)	20 (12.5)	-	no gel; clear viscous solution	-	-

TABLE 4-2**SWELLING AND NETWORK BEHAVIOR OF PEG-POLY(KF) GELS**

Gel Composition	Swelling Ratio, α	entanglement ratio, Φ
20/5	2.1	1.2
20/2.5	1.5	2.5
10/5	1.8	0.93
10/2.5	-	-

TABLE 4-3

PROPERTIES OF PROTEINS USED IN DIFFUSION EXPERIMENTS

Property	Lysozyme	Carbonic Anhydrase	BSA
M_w (kilodaltons)	14.3	29	66
$D_{free\ solution}^{reference}$ ($\times 10^6$ cm ² /s)	1.1 ²³	1.0 ²⁴	0.58 ²⁵
$K_{pg,apparent} \pm$ S.E.	0.46 \pm 0.02	0.46 \pm 0.06	3.9 \pm 0.2
isoelectric point	11	5.9	4.7
$C_{1\infty}$ (mg/mL) \pm S.E.	0.850 \pm 0.004	1.808 \pm 0.009	2.06 \pm 0.02

PEG-(glutaminamide)



poly(Lys:Phe)



TG

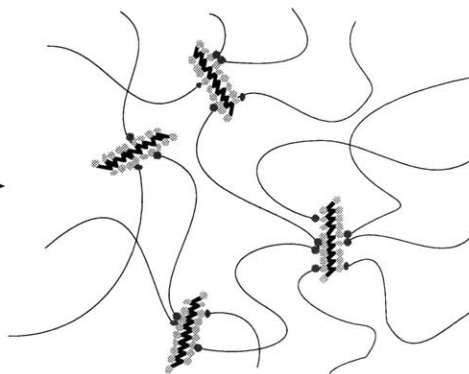
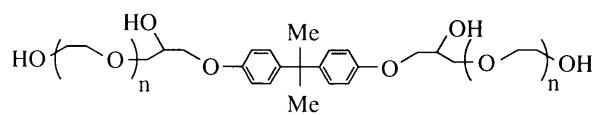
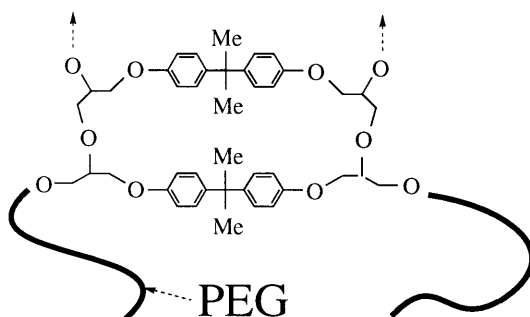


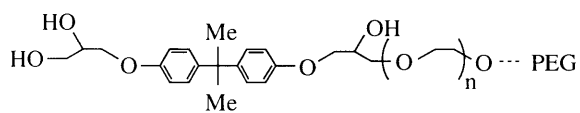
Figure 4-1. Transglutaminase (TG) crosslinking reaction with glutaminamide-functionalized PEG and poly(Lysine:Phenylalanine) to form a network. Each poly(KF) molecule is considered a crosslink node for the purposes of equilibrium swelling calculations.



I



II



III

Figure 4-2. Possible structured of nominally "Tetrahydroxy PEG" ("PEG-(OH)₄") from Polysciences.

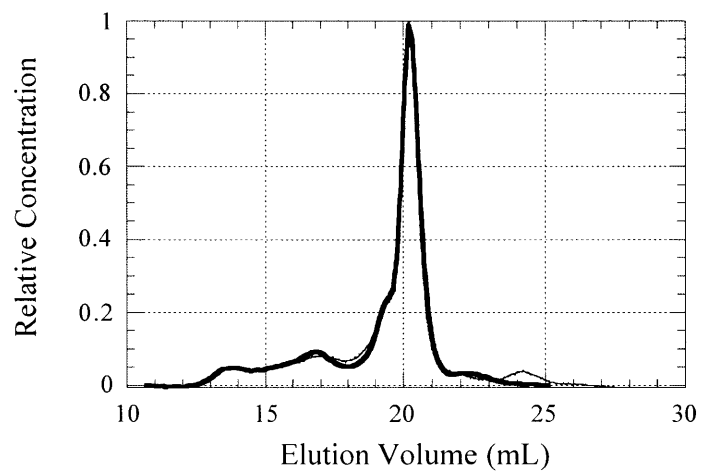


Figure 4-3. Gel permeation chromatogram for synthesis starting material (PEG-OH) (thick line) and pregel macromer (PEG-Q_a) (thin line).

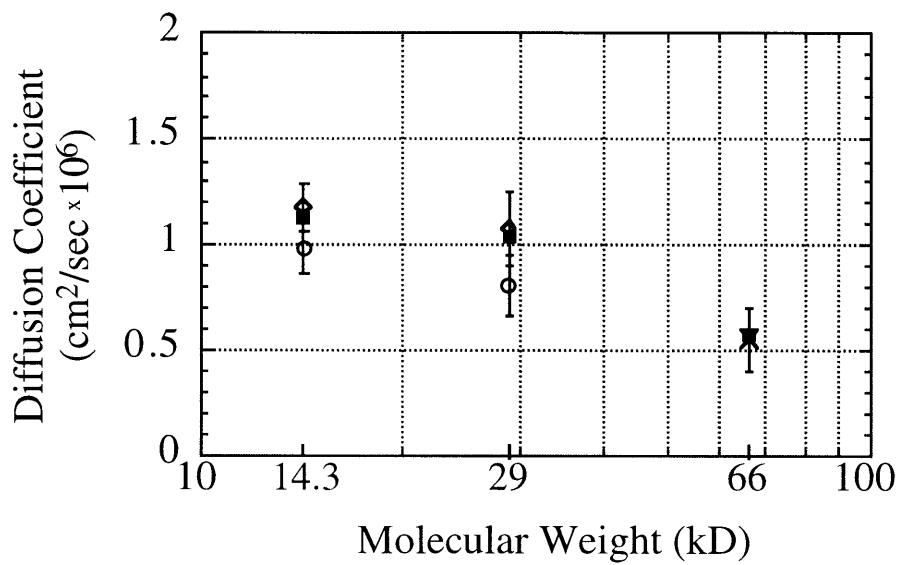


Figure 4-4. Diffusion coefficients for solutes of various molecular weights in 20/5 gel: Lysozyme (14.3kD), Carbonic Anhydrase (29kD) and Bovine Serum Albumin (66kD). Values shown include literature values for free diffusion (■) as well as measured values from steady-state (◇), time lag (o) and transient (×) analysis of equation (4-6).

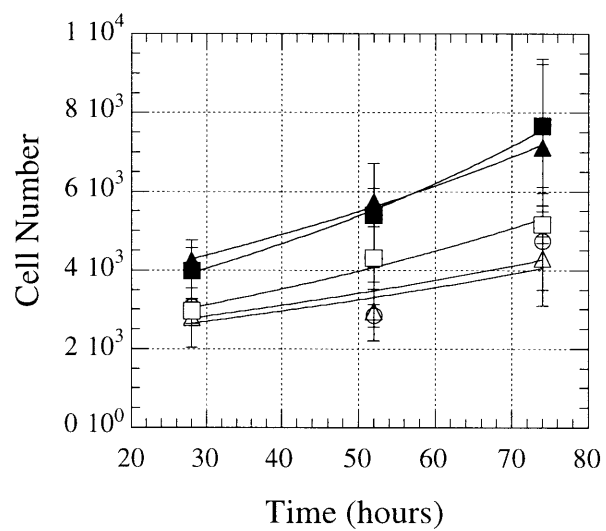


Figure 4-5. Effect of transglutaminase on cell attachment and growth. Data shown for 0 μM (○), 0.10 μM (△), 0.30 μM (□), 1.0 μM (▲) and 3.0 μM (■) transglutaminase.

4.5 References

1. Folk, J.E., *Adv. Enz.*, "Mechanism and basis for specificity of transglutaminase-catalyzed epsilon-(gamma-glutamyl) lysine bond formation," **54**: 1-56 (1983).
2. Schrode, J. & Folk, J.E., *J. Biol. Chem.*, "Stereochemical aspects of amine substrate attachment to acyl intermediates of transglutaminases: human blood plasma enzyme (activated coagulation factor XIII) and guinea pig liver enzyme," **254**(3): 653-661 (1979).
3. Lorand, L., *et al.*, *Biochem.*, "Specificity of guinea pig liver transglutaminase for amine substrates," **18**(9): 1756-1765 (1979).
4. Folk, J.E. & Chung, S.I., *Met. Enz.*, "Transglutaminases," **113**: 358-375 (1985).
5. S S Simons, J. & Johnson, D.F., *J. Org. Chem.*, "Reaction of o-phthaldialdehyde and thiols with primary amines: formation of 1-alkyl(and aryl)thio-2-alkylisoindoles," **43**(14): 2886-2891 (1978).
6. Kenkare, P.U. & Hall, C.K., *AIChE Journal*, "Modeling of Phase Separation in PEG-Salt Aqueous Two-Phase Systems," **42**(12): 3508-3522 (1996).
7. Folk, J.E., *J. Biol. Chem.*, "Mechanism of action of guinea pig liver transglutaminase: VI. order of substrate addition," **244**(13): 3707-3713 (1969).
8. Chung, S.I. & Folk, J.E., *J. Biol. Chem.*, "Kinetic studies with transglutaminases: the human blood enzymes (activated coagulation factor XIII) and the guinea pig hair follicle enzyme," **247**(9): 2798-2807 (1972).
9. Saito, H., Ohki, T., Kodama, M. & Nagata, C., *Biopolymers*, "Salt-Induced Conformational Change of Random Copolymers (Lys50,Typ50)_n and (Lys50Phe50)_n Studied by ¹H- and ¹³C- Nuclear Magnetic Resonances. Aggregation Behavior of Helical Segments," **18**: 1065-1072 (1979).
10. Arfmann, H.A., Labitzke, R. & Wagner, K.G., *Biopolymers*, "Nature of Amino Acid Side Chains and Alpha-Helix Stability," **14**: 1381-1393 (1975).
11. Miller, D.R. & Macosko, C.W., *Macromolecules*, "A New Derivation of Post Gel Properties of Network Polymers," **9**(2): 206-211 (1976).
12. Macosko, C.W. & Miller, D.R., *Macromolecules*, "A New Derivation of Average Molecular Weights of Nonlinear Polymers," **9**(2): 199-206 (1976).
13. Ferry, J.D. *Viscoelastic Properties of Polymers*, **1980**, John Wiley and Sons, New York.

14. Gnanou, Y., Hild, G. & Rempp, P., *Macromolecules*, "Molecular Structure and Elastic Behavior of Poly(ethylene oxide) Networks Swollen to Equilibrium," **20**(7): 1662-1671 (1987).
15. Fasman, G.D. (ed) (1976) *Handbook of Biochemistry and Molecular Biology*, 3rd Ed., CRC Press, Boca Raton, FL
16. Lindkog, S., *et al.* in *The Enzymes* (ed. Boyer, P.D.) 600 (Academic Press, New York, 1971).
17. Crank, J. *The Mathematics of Diffusion*, **1992**, Clarendon Press, Oxford.
18. West, J.L. & Hubbell, J.A., *Reactive Polymers*, "Photopolymerized hydrogel materials for drug delivery applications," **25**: 139-147 (1995).
19. Pathak, C.P., Sawhney, A.S. & Hubbell, J.A., *Journal of the American Chemical Society*, "Rapid Photopolymerization of Immunoprotective Gels in Contact with Cells and Tissue," **114**(21): 8311-8313 (1992).
20. Merrill, E.W., Dennison, K.A. & Sung, C., *Biomaterials*, "Partitioning and Diffusion of Solutes in Hydrogels of Poly(Ethylene Oxide)," **14**(15): 1117-1126 (1993).
21. Folk, J.E. & Cole, P.W., *J. of Biol. Chem.*, "Mechanism of action of guinea pig liver transglutaminase," **241**(23): 5518-5525 (1966).
22. Nagaoka, S., *et al.* in *Polymers as biomaterials* (eds. Shalaby, S.W., Hoffman, A.S., Ratner, B.D. & Horbett, T.A.) (Plenum Press, New York, 1985).
23. Sophianopoulos, A.J., Rhodes, C.K., Holcomb, D.N. & Holde, K.E., *Journal of Biological Chemistry*, "Physical Studies of Lysozyme," **237**(4): 1107-1112 (1962).
24. Reynaud, J., Rametta, G., Savary, J. & Derrien, Y., *Biochim. Biophys. Acta*, "Donnees Physiques sur les anhydrases carboniques X1 et Y," **77**: 521-523 (1963).
25. Foord, R., *et al.*, *Nature*, "Determination of Diffusion Coefficients of Haemocyanin at Low Concentration by Intensity Fluctuation Spectroscopy of Scattered Laser Light," **227**: 242-245 (1970).

5 KINETICS OF ENZYMATICALLY CROSSLINKED POLY(ETHYLENE GLYCOL) GEL FORMATION

5.1 Gelation Kinetic Theory

The time required for a gelling system to undergo the transformation from a liquid to a semi-solid state is a function of the criteria by which the gel point is defined as well as the rate of crosslink formation and the functionality of the crosslinking moieties. A useful convention defines the gel point as the transformation from viscous liquid to elastic gel. This definition provides an observable measure of gelation while at the same time implying a mathematical criteria for gel formation¹. Figure 5-1 illustrates the interplay of macromer functionality and crosslinking kinetics. It is readily apparent from the representation in Figure 5-1 that not all ends must be crosslinked in order to achieve gel formation. As the number of arms per molecule increases, the fraction of those arms that must become crosslinked in order to produce a gel decreases. Thus macromer structure sets the fractional conversion of end-groups that must be achieved to reach the gel point. The kinetics of crosslink formation determine the rate at which this critical conversion is approached.

Here the kinetics of gelation were explored by developing a predictive kinetic model then testing this model against observed gelation times. This model (Section 5.1.1-2) predicts key parameters that will affect gelation times such as the initial concentration of macromers, substrate kinetics and transglutaminase concentration.

Kinetics of PEG-polylysine gels were studied in the conditions used in Chapter 4, employing various concentrations of pre-gel macromers. Kinetics of PEG-PEG gels were studied with two prototypical amine acceptor substrates (see Section 5.3) of differing kinetics. PEG-PEG gelation kinetics were explored as a function of enzyme concentration.

5.1.1 Structural Criteria

A mathematical description of the critical point of gelation is constructed around the degree of branching found in the system at any given time. This is most naturally formulated via probabilistic arguments¹. The formulation starts with a number of necessary assumptions about certain aspects of the gel that would be extremely difficult to measure. We assume no loops (i.e. polymer unit connected to itself through a small number of chains) and no entanglements that would act as virtual crosslinks. Consider the present system of PEG-Gln_{nGln} and PEG-Lys_{nLys}, where n_{Gln} and n_{Lys} are the number average functionality of glutamines and lysines, respectively. The probability of any particular glutamine *residue* being covalently linked to a PEG-Lys_{nLys} molecule is given by the fractional conversion to ϵ -(γ -glutaminy1)-lysine for glutamine, X_{Gln} , assuming equal reactivity of all glutamine residues. To find the expected number of *additional* PEG-Gln_{nGln} molecules connected to this PEG-Lys_{nLys} molecule, the fractional conversion of lysine, X_{Lys} must be multiplied by the number of opportunities for branching, $(n_{Lys}-1)$. Therefore the expected number of PEG-Gln_{nGln} molecules connected to any particular glutamine residue via PEG-Lys_{nLys} is given by,

$$\alpha = X_{\text{Gln}} X_{\text{Lys}} (n_{\text{Lys}} - 1) = \frac{X_{\text{Gln}}^2 (n_{\text{Lys}} - 1)}{r_{\text{Gln/Lys}}} \quad (5-1)$$

where $r_{\text{Lys/Gln}}$ is defined as the ratio of lysine residues to glutamine residues initially present.

As the reaction proceeds, PEG molecules are linked together to form chains with varying amounts of branching. The value of α defined above can be found to assess the likelihood that a repeat unit (PEG-Gln--Lys-PEG-Lys--Gln-PEG) will be completed. The expected number (Φ) of PEG-Gln_{nGln} molecules connected via a PEG-Lys_{nLys} molecule to another PEG-Gln_{nGln} molecule is given by the product of α and the number of opportunities for branching, $(n_{\text{Lys}}-1)$, or,

$$\Phi = \alpha (n_{\text{Gln}} - 1) = \frac{X_{\text{Gln}}^2 (n_{\text{Lys}} - 1)(n_{\text{Gln}} - 1)}{r_{\text{Gln/Lys}}} \quad (5-2)$$

When Φ exceeds unity, infinite extension of network chains become possible. Thus the critical condition for gelation based on $\Phi_c = 1$ in terms of X_{Gln} can be expressed as,

$$X_{\text{Gln,c}} = \sqrt{\frac{r_{\text{Gln/Lys}}}{(n_{\text{Lys}} - 1)(n_{\text{Gln}} - 1)}} \quad (5-3)$$

Of course the above treatment is equally valid if the roles of glutamine and lysine are reversed. But this is only true of the structural requirements for gelation. When kinetics are considered to derive the time required to reach $X_{\text{Gln,c}}$, differences in concentrations of glutamines and lysines are significant.

5.1.2 Kinetic Criteria

In order to predict the time at which gelation will occur, it is necessary to define a relationship between $X_{\text{Gln,c}}$ and time through equations of the form, $dX_{\text{Gln,c}}/dt = f([\text{Lys}], [\text{Gln}], [\text{TG}], k_{\text{i..i}})$. In this way the approach to the gel point and rate of crosslink formation is governed by the underlying kinetics of transglutaminase activity (see Chapter 3).

Transglutaminase-mediated amide formation between an amine donor and an amine acceptor is known to follow a modified double-displacement mechanism²⁻⁴ as discussed in Section 1.5.3. The reaction occurs in two steps. First, transglutaminase reacts with the amine acceptor, forming a thioester bond at the active site with the release of ammonia. The subsequent protonation of ammonia makes this step essentially irreversible. In the second step, the amine donor displaces the amine acceptor from the enzyme, forming an amide bond.

The first catalytic step is often rate limiting⁴. Therefore the kinetics of crosslink formation can be written as (See Section 3.2.2.2),

$$\frac{d[\text{crosslink}]}{dt} = -\frac{d[\text{Gln}]}{dt} = \frac{k_{\text{cat}}[\text{TG}]_t[\text{Gln}]}{K_{\text{m,app}} + [\text{Gln}]} \quad (5-4)$$

where $[\text{TG}]_t$ is the total enzyme concentration. In the case where enzyme inactivation is negligible over the time scale of gelation (see Section 3.2.2.3), this integrates to,

$$t = \frac{X_{\text{Gln}} \left(\frac{[\text{Gln}]_0}{K_{\text{m,app}}} \right) - \ln(1 - X_{\text{Gln}})}{\frac{k_{\text{cat}}}{K_{\text{m,app}}} [\text{TG}]_t} \quad (5-5)$$

where $[\text{Gln}]_0$ is the initial concentration of amine acceptor. This equation defines the time required to reach a particular conversion given the initial amine acceptor substrate concentration, the amine acceptor substrate kinetic parameters and the concentration of transglutaminase. Conditions under which enzyme inactivation can be neglected include slightly acidic pH (~ 6.0) and large ($\sim 5.0\mu\text{M}$) TG concentrations. The former was chosen here to enable exploration of sub- $5.0\mu\text{M}$ TG concentrations.

Substitution of the structural gelation criteria into the kinetic equation yields and expression for the time to gelation (t_c):

$$t_c = \frac{\left(\frac{[\text{Gln}]_0}{K_{\text{m,app}}} \right) \sqrt{\frac{r_{\text{Gln/Lys}}}{(n_{\text{Lys}} - 1)(n_{\text{Gln}} - 1)}} - \ln \left(1 - \sqrt{\frac{r_{\text{Gln Lys}}}{(n_{\text{Lys}} - 1)(n_{\text{Gln}} - 1)}} \right)}{\frac{k_{\text{cat}}}{K_{\text{m,app}}} [\text{TG}]_t} \quad (5-6)$$

By inspection it can be seen that for substrates where $K_{m,app}$ deviates significantly from the initial concentration of glutamine residues, $[Gln]_0$, equation (5-6) may reduce to a simpler form.

5.2 Materials and Methods

PEG Characterization. Branched poly(ethylene glycol) (bPEG) of the structure shown in Figure 5-2, nominally 40kD and 8arms per molecule, was obtained from Shearwater polymers. By size exclusion chromatography with refractive index and light scattering detection, this bPEG was found to have a weight-average molecular weight of 38kD and a number average molecular weight of 33kD, giving a polydispersity of 1.16. By elemental analysis of sulfur following tresylation (see Section 2.2) the molecular weight per arm was calculated to be 4.4kD, implying a number-average of 7.76 arms per molecule. Based on the method of synthesis (anionic, core-first), it is presumed that much of the polydispersity is accounted for with the variation in the number of arms rather than the length of each arm.

Peptide Synthesis. Peptidyl transglutaminase substrates were synthesized on an automated peptide synthesizer as described in Appendix A2.

PEG-Peptide Coupling. Amine acceptor substrates were covalently linked to bPEG by tresyl chemistry, discussed in Section 2.2. Peptide G, H and I were coupled to bPEG at pH7.5, and room temperature where coupling via the sulfhydryl group of cysteine is favored.

Amine donor substrates were covalently linked to bPEG via tresyl chemistry (see Section 2.2) except for PEG-diamine (MW=3400) which was purchased from Shearwater Polymers. bPEG-amine was synthesized in methanol at 40°C in 2M ammonia. bPEG-OBEA (oxy-bis(ethyl amine)) was synthesized with 0.50M OBEA at pH8.3 and 4°C. bPEG-Lys-NH₂ was synthesized with 60mM Lys(ε-BOC)-NH₂ at pH 8.0 and 4°C. The derivative was purified by dialysis (10kD MWCO cassettes: Pierce) and lyophilized. The BOC protecting group was removed with trifluoroacetic acid containing 5% water and 2% ethanedithiol as scavengers. Trifluoroacetic acid was removed by rotoevaporation. The product was dissolved in water, purified by dialysis and lyophilized. bPEG-GCLKG was synthesized with 60mM GCLKG at pH7.5 and at room temperature (22°C). Coupling via the cysteine sulfhydryl was confirmed by the retention of free primary amines as detected by o-phthaldialdehyde (Appendix A7).

Characterization. Peptide-functionalized bPEG was characterized based on the ratio of peptide to PEG by ¹H-NMR. Calculations for number functionality were made based on characterization of the bPEG starting material described above. Covalent linkage via cysteine was verified by conservation of free primary amines as determined by the o-phthaldialdehyde method (Appendix A7).

Kinetic Measurements. Kinetic measurements were made for each amine acceptor peptide by monodansyl cadaverine coupling as described in Appendix A5. Kinetic experiments were conducted at 5.0μM TG, 37°C in 8mM CaCl₂, 80mM KCl 5mM Tris and 50mM 2-(N-morpholino)-ethane sulfonic acid (MES), pH6.0. Initial rate

experiments (amine acceptor concentration: 5.0mM, 2.5mM, 1.67mM and 1.25mM) were conducted such that no more than 10% of the substrate was depleted.

Gelation Time Measurements. In a typical experiment, 15 μ L-20 μ L of a solution containing 10mM of both PEG-linked substrates (acceptor and donor) in 100mM MES, pH6.0 was mixed with an equal volume of enzyme at the desired concentration in a microcentrifuge tube. These concentrations correspond to approximately 10 wt% PEG. The mixture was brought to 37°C in a constant temperature water bath. To initiate the crosslinking reaction, calcium was added to 8mM from a 300mM stock solution.

Due to the limited amount of macromers available small gel volumes (30 μ L-40 μ L) were employed. With these limited volumes the most reproducible assessment of gel formation was found to be by probing with a paper clip. Gelation was assessed by a combination of stirring and sweeping the solution up the sides of the microcentrifuge tube. The time at which the mixture seized to the paper clip was taken as the gel point. Gelation times were measured for transglutaminase concentrations of 2.0 μ M, 3.0 μ M and 5.0 μ M. All measurements were conducted in duplicate.

5.3 Transglutaminase Substrate Design

5.3.1 Amine Acceptors

Structure of the amine acceptor substrates is somewhat tightly regulated (for a detailed discussion see Section 1.5.4). Glutamine residues are known to be the best substrates, consistent with transglutaminase activity *in vivo*. In developing amine

acceptor substrates for use as viable crosslink substrates on poly(ethylene glycol) (PEG) macromers, small peptide substrates were designed based on known peptide substrate activity (Table 1-2).

Table 5-1 lists the amine substrates used in this work along with the measured kinetic constants associated with TG-mediated crosslinks of these substrates when covalently linked to PEG. In the case of Peptide B, covalently linking substrates to PEG was shown to have no significant effect on the kinetics of crosslinking as shown in Section 3.3.

Peptides A and B were used in the initial feasibility studies of enzymatically crosslinked PEG gels (see Chapter 4). Peptide A, glutaminamide, is the smallest known substrate for which transglutaminase has significant activity. The C-terminal of glutamine has been aminated to eliminate the negative charge of glutamine. Peptide B, with similar activity to Peptide A, was patterned after the well-known TG_{II} substrate ZQG (see Section 3.3 and Appendix A6).

Peptide C is a modification of Peptide B with the insertion of a leucine residue adjacent to and on the carboxyl-side of the active glutamine residue. Based on literature reports⁵ it was anticipated and confirmed that this configuration would give approximately an order of magnitude higher kinetics than without the leucine residue. Only a leucine addition was attempted, although other hydrophobic residues may have yielded similar or faster kinetics⁵.

Peptide D was an attempt to combine an amine acceptor substrate and an amine donor substrate on the same molecule. By the known geometry of the active site⁶ a

glutamine and lysine on the same peptide would not be able to crosslink. While Peptide D is an excellent amine acceptor substrate, it exhibited no measurable donor activity as measured by a standard assay (Appendix A6). Non-activity of the lysine residue may be explained by the secondary structure of Peptide D in solution. Only approximately 10% of the lysine residues were reactive towards o-phthaldialdehyde (Appendix A7), a fluorescent probe for primary amines. Therefore the lysyl amine may be shielded from solution, possibly neutralized by the glycyl carboxylate, although self-crosslinking is difficult to rule out experimentally and remains a possible explanation for non-reactivity.

The design of Peptides E-H was driven by a desire to incorporate collagenase-sensitive peptidyl sequences into the gel backbone (see Chapter 6). The first peptide synthesized in this sequence included a collagenase cleavage sequence, Gly-Pro-Leu-Gly-Ile-Ala, along with the sequence of Peptide C to make Gly-Pro-Leu-Gly-Ile-Ala-Gly-Gln-Leu-Gly. This peptide was cleavable by collagenase, but was not TG_{II}-active. This was somewhat surprising given the success of Peptide C, but was not inconsistent with the difficulties encountered with Peptide D. To overcome this difficulty it was surmised that inclusion of a charged residue close to the glutamine residue may favorably affect the accessibility by making the peptide more hydrophilic. With this in mind, Peptide F was synthesized with the amine acceptor sequence (Gly-Gln-His-Ser-Gly) inspired by published synthetic substrates^{7, 8} based on the sequence surrounding an active glutamine in N,N-dimethylcasein. Peptide F was found to possess activity both as a collagenase substrate and as a TG_{II} substrate (see Section 5.4). Peptide G is identical to Peptide F, but with a cysteine inserted to facilitate linkage to PEG (see Section 2.2).

Peptide H was designed as a collagenase-substrate-free control analog to Peptide G (see Chapter 6).

5.3.2 Amine Donors

Achieving high amine donor activity is most important in maintaining maximum substrate specificity relative to other chemical moieties that might be included for other purposes such as cell adhesion or proliferation (see Section 1.4). High amine donor activity is less important to gel formation than amine acceptor activity as the reaction of transglutaminase with the acceptor is generally limiting (see Chapter 3).

Structure of the amine donor substrates is far less regulated than for the amine acceptor substrates (for a detailed discussion see Section 1.5.4). The most significant requirement is lack of branching for at least four carbon units, as in the structure of lysine. *In vivo* lysine as well as other straight chain amines and polyamines are substrates for transglutaminase. In Chapter 4 it was shown that poly(lysine:phenylalanine) would act as an amine donor, while poly(lysine) was a poor substrate possibly due to excessive charge density.

A number of different amine donor substrates were tested as potential amine substrates. All species were measured for transglutaminase activity with the ZQG coupling assay described in Appendix A6. Their kinetic values are listed in Table 2-2. Although the kinetic values are useful for relative comparison of amine donor substrates, under gelation conditions, addition of the amine acceptor substrate is generally limiting. Therefore the relative kinetic rate constants predict how various amine donor substrates

might compete with one another or with natural substrates found *in vivo*. This is an important criteria for selection of amine acceptor substrate as gelation is to be carried out in contact with body fluids. Clearly, the substrate GCLKG will be most selectively incorporated into transglutaminase-mediated crosslinks.

5.4 Results and Discussion

Gelation times were measured in a variety of conditions to test the ability of equation (5-6) to predict gelation times. Gelation times were measured for PEG/poly(KF) gels explored in Chapter 4 by varying the relative amounts of the two components. Concentrations were chosen to replicate those used in Chapter 4: 20/5, 10/5 and 20/2.5 wt% PEG-Q_a / wt% poly(KF). Experiments with PEG/PEG gels focused on variations in enzyme concentrations. For the PEG/PEG gels two amine acceptor substrates with different kinetics were examined. PEG/PEG gels were formed with equal amine acceptor and donor concentrations over a range of enzyme concentrations: 2.0 μ M, 3.0 μ M and 5.0 μ M.

5.4.1 PEG/poly(KF) Gels

For the case of PEG/poly(KF) gels explored in Chapter 4 the PEG-Q_a macromers were largely difunctional with a number average functionality of 2.06 ($=n_{\text{Gln}}$). The poly(KF) molecules had a much higher functionality ($n_{\text{Lys}} = 100$). For reaction mixtures

comprising 20/5, 10/5 and 20/2.5 wt% PEG-Q_a / wt% poly(KF), $X_{\text{Gln,c}}$ (5-3) was found to be 0.23, 0.33 and 0.16, respectively.

Gels were formed at varying ratios of initial substrate concentrations as described in Section 4.2 but with 8.2 μ M TG. Gels of 20/2.5, 20/5 and 10/5 correspond to initial ratios of lysine to glutamine ($r_{\text{Lys/Gln}} \equiv C_{\text{K,o}}/C_{\text{Qa,o}}$) of 3, 6 and 12, respectively. Results are shown in Figure 5-3. The model capture the positive correlation with increasing $r_{\text{Lys/Gln}}$, however in all cases gelation times were somewhat longer than predicted by equation (5-6). This may be due to assumptions made in formulating this model. Equation (5-6) assumes no network imperfections such as loops that do not add to the network structure which would tend to lengthen measured gelation times. Also implicit in this model is an assumption of equal reactivity. However with such a large number of PEG ends per polyKF (33, 17 and 8 for 20/2.5, 20/5 and 10/5 gels, respectively) it is likely that steric effects will increase observed reaction times, especially for the 20/2.5 gel ($r_{\text{Lys/Gln}} = 3$). This may be manifested in a larger deviation from predictions for this gel.

5.4.2 PEG/PEG Gels

To test the correlation between equation (5-6) and gelation time measured by experiment, two PEG-peptide amine acceptor substrates, bPEG-[Peptide G]_{nG} and bPEG-[Peptide H]_{nH} of Table 2-1, and one bPEG-peptide amine donor substrate, bPEG-[Peptide I]_{nI} (Peptide I \equiv GCLKG of Table 2-2), were selected as model gel systems. For these particular polymers, n_G and n_H describe the number average functionality (n_{Gln}) for

the respective derivative. Similarly, $n_l = n_{Lys}$ for bPEG-[Peptide I] $_{n_l}$. Values for these parameters are summarized in Table 5-3 along with the calculated critical conversion, X_c , for each amine acceptor substrate based on equation (5-3).

To predict gelation times from equation (5-6) it was necessary to measure the kinetic parameters k_c and $K_{m,app}$ for each amine acceptor substrate. Initial rates at a constant enzyme concentration were measured at 37°C and pH6.0 by the method detailed in Appendix A5. Amine acceptor substrate concentrations were chosen to correspond to concentrations used in gelation experiments below. Values for k_{cat} and $K_{m,app}$ were regressed separately for each substrate, Peptide G and H, with equation (5-6) by minimizing the sum of the squares of the deviation from the measured data. Double reciprocal plots for substrate concentrations in the range to be used in gel formation are shown in Figure 5-4 and 5-5 for bPEG-[Peptide G] $_{n_G}$ and bPEG-[Peptide H] $_{n_H}$, respectively. Values for k_{cat} were found to be similar, but the value of $K_{m,app}$ for Peptide G was found to be somewhat less than for Peptide H, possibly to enhanced binding to the hydrophobic region absent in Peptide H. For peptide concentrations well below the measured K_m values, the relevant kinetic parameter becomes $k_{cat}/K_{m,app}$, for Peptide G and Peptide H, respectively.

For a given k_{cat} , and $K_{m,app}$, $r_{Gln/Lys}$ and $[Gln]_0$ equation (5-6) predicts gelation times as a function of $[TG]$. For simplicity, gels were formed at stoichiometric levels of amine acceptor and amine donor substrates, corresponding to a $r_{Gln/Lys}$ of unity. Gels were formed at $[Gln]_0 = 5\text{mM}$, chosen to insure generous overlap of polymer chains and thereby minimize the effect of self-termination.

Figures 5-6 and 5-7 show predicted and measured gelation times for the two macromer pairs examined. In both cases, the measured gelation rates come very close to theory. Spreads in measured gelation rates may be attributed to imperfect initial mixing or more likely due to difficulties in pin-pointing the gel point. As discussed in Section 4.3.2 and Appendix B, a number of counteracting deviations from the assumptions made in Section 5.3.1 may influence the correlation of equation (5-6) and experiment. Overlapping chains may cause virtual crosslinking, accelerating the observed gelation time. Crosslinks that do not add to the network structure such as loops would tend to delay the onset of gelation.

In contrast to the underprediction of this type of model for PEG/poly(KF) gels in Section 5.4.1, equation (5-6) consistently overpredicts the time to gelation. As noted in Section 5.4.1, steric hindrance around the poly(lysine) molecules may have violated the equal-reactivity assumption. In the case of PEG-PEG gels studied here, the substrates are more evenly distributed in space, perhaps validating the equal-reactivity assumption in this case. This would explain the opposite directions of the model-deviations for PEG/poly(lysine) and PEG/PEG gels.

TABLE 5-1
AMINE ACCEPTOR SUBSTRATES

Peptide	Composition	Measured kinetics ^a (mM ⁻¹ sec ⁻¹)
A	Gln-NH ₂	0.022
B	Gly-Gln-Gly	0.020
C	Gly-Gln-Leu-Gly	0.53
D	Gly-Gln-Leu-Lys-Gly	0.27
E	Gly-Pro-Leu-Gly-Ile-Ala-Gly-Gln-Leu-Gly	not detectable
F	Gly-Pro-Leu-Gly-Ile-Ala-Gly-Gln-His-Ser-Gly	0.75
G	Gly-Cys-Pro-Leu-Gly-Ile-Ala-Gly-Gln-His-Ser-Gly	0.78
H	Gly-Cys-Gly-Gln-His-Ser-Gly	0.59

^a Kinetic measurements, given as $k_{cat}/K_{m,app}$ were performed in 100mM Tris-Cl, pH7.4, 37°C on poly(ethylene glycol)-linked peptide substrates (~1mM) by methods detailed in Appendix A5.

TABLE 5-2
AMINE DONOR SUBSTRATES

Species	Structure	Measured kinetics ^a
PEG-diamine	PEG ^b -(NH ₂) ₂	0.090
bPEG-amine	bPEG-NH ₂	0.052
bPEG-OBEA	bPEG-NH ₂ CH ₂ CH ₂ OCH ₂ CH ₂ NH ₂	0.31
bPEG-Lysinamide	bPEG-NHCH(CH ₂ CH ₂ CH ₂ CH ₂ NH ₂)C(O)NH ₂	0.16
bPEG-[Peptide I]	bPEG-Cys(Gly)-Leu-Lys-Gly ^c	8.6

^a Kinetic measurements were performed in 100mM Tris-Cl, pH7.4, 37°C on poly(ethylene glycol)-linked peptide substrates by methods detailed in Appendix A6. Kinetic values in units of mM⁻¹ sec⁻¹.

^b PEG-(NH₂)₂ is aminated linear PEG (MW=3.4kD) from Shearwater Polymers.

^c Attachment via the cysteine sulfhydryl (of GCLKG) was confirmed by conservation of primary amine groups as compared to free peptide by o-phthaldialdehyde (see Appendix A7).

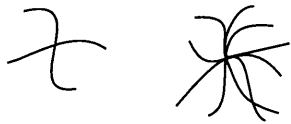
TABLE 5-3
SUBSTRATE-FUNCTIONALIZED PEG PROPERTIES

Species	Gram Polymer Per Millimole Peptide	Number of Functionalized Arms Per Molecule ^a	Critical Conversion (X_c) ^b
bPEG-[Peptide G] _{nG}	6.60	nG = 6.00	0.27
bPEG-[Peptide H] _{nH}	7.64	nH = 4.71	0.31
bPEG-[Peptide I] _{nI}	9.48	nI = 3.67	--

^a Number average value based on number average bPEG arm number (7.76) and coupling efficiency expressed as gram polymer per millimole peptide (by ¹H-NMR).

^b Conversion based on glutamine conversion with bPEG-[Peptide I]_{nI} at $r_{\text{Gln/Lys}} = 1$ by equation 5-3.

Macromer Structure



Enzyme Kinetics



Conversion at Gel Point

Conversion = $f(\text{time})$

Crosslinks

Time

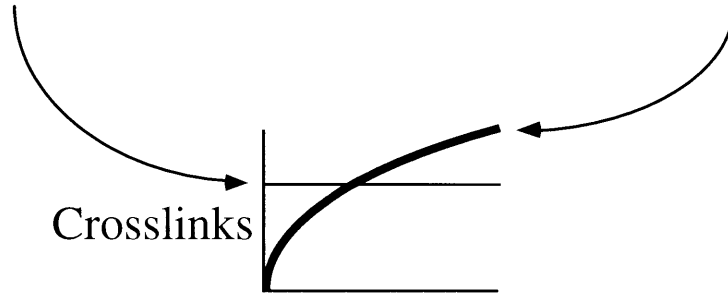


Figure 5-1. Determinants of gelation time.

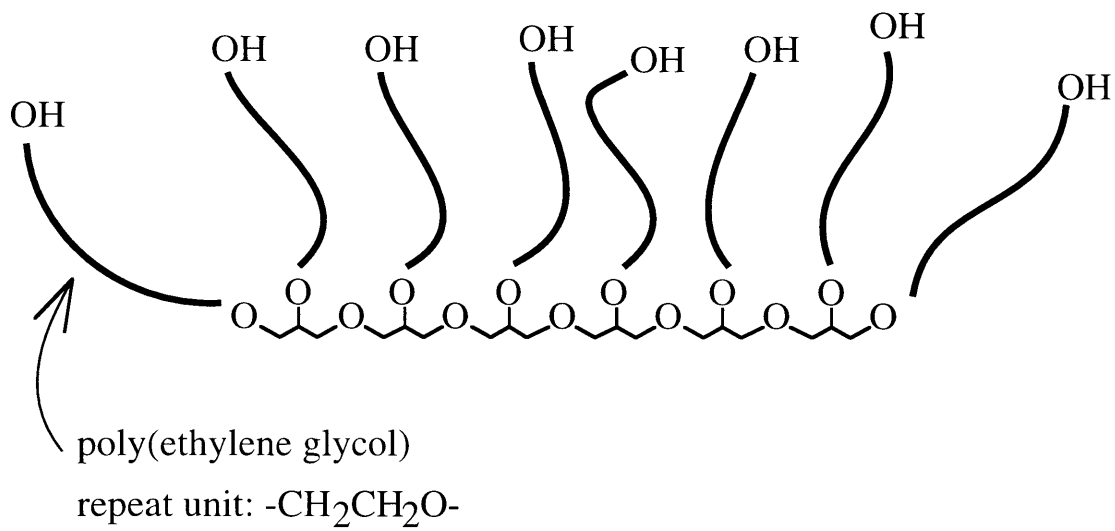


Figure 5-2. Nominal structure of branched poly(ethylene glycol) (bPEG). Polymer properties are discussed in Section 5.1.

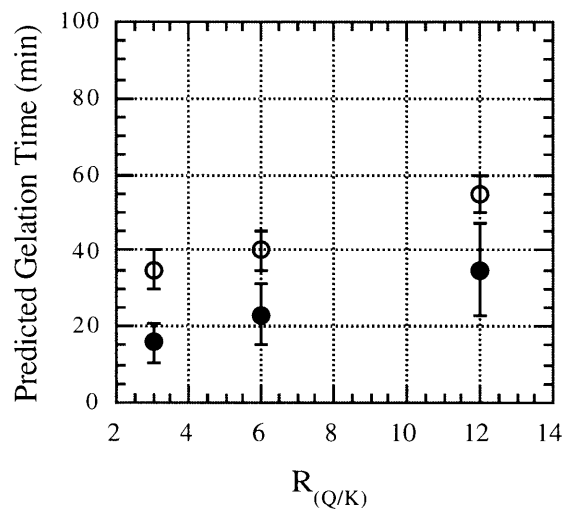


Figure 5-3. Predicted (●) and experimentally measured (○) time required to reach the gel point following enzyme addition as a function of the ratio of the initial concentration of the glutamyl substrate to lysyl substrate.

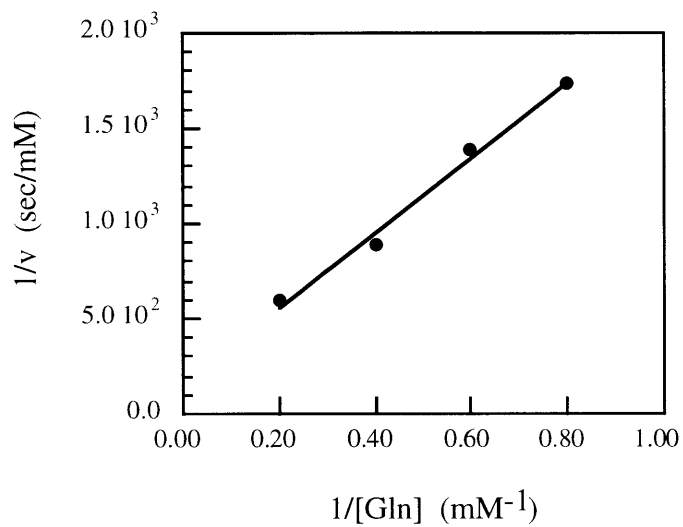


Figure 5-4. Double reciprocal plot for bPEG-[Peptide G]_{nG}. Chi-squared minimization fit (line) to data (points) of equation 5-4 yields $K_{m,app} = 7.6 \text{ mM}$; $k_{cat} = 0.86 \text{ sec}^{-1} \text{ mM}^{-1}$.

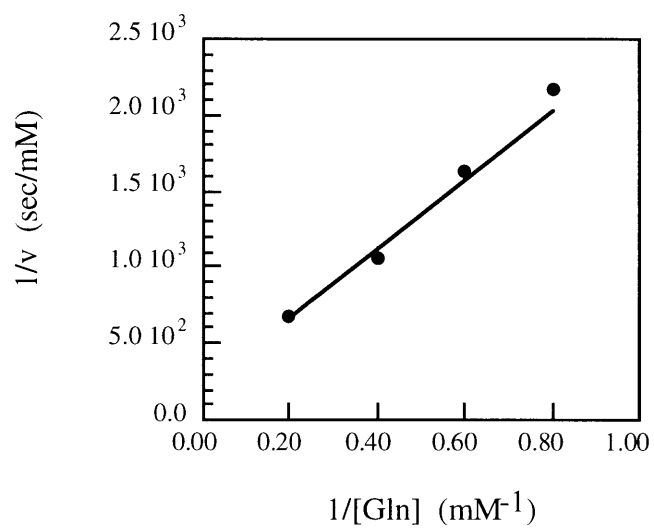


Figure 5-5. Double reciprocal plot for bPEG-[Peptide H]_{nH}. Chi-squared minimization fit (line) to data (points) of equation 5-4 yields $K_{m,app} = 11 \text{ mM}$; $k_{cat} = 0.95 \text{ sec}^{-1} \text{ mM}^{-1}$.

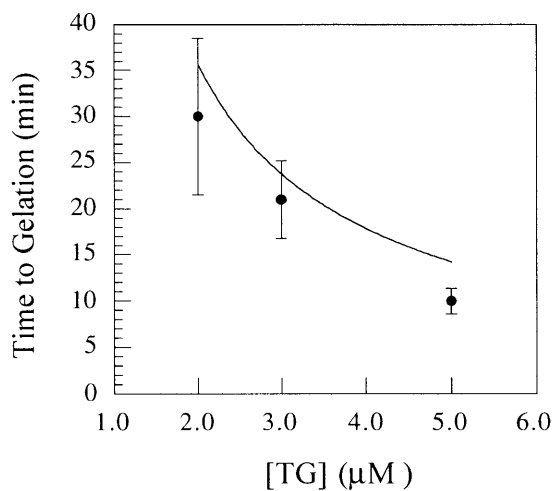


Figure 5-6. Time to gelation for bPEG-[Peptide G]_{nG} / bPEG-[Peptide I]_{nI} gel. Points (n=2) and standard deviation represent measured gelation times as compared to model predictions (line) based on macromer structure and substrate kinetics (see text).

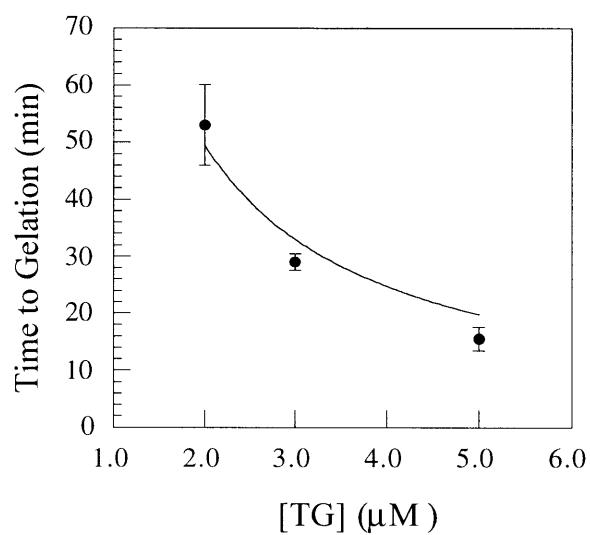


Figure 5-7. Time to gelation for bPEG-[Peptide H]_{nH} / bPEG-[Peptide I]_{nI} gel. Points (n=2) and standard deviation represent measured gelation times as compared to model predictions (line) based on macromer structure and substrate kinetics (see text).

5.5 References

1. Flory, P. *Principles of Polymer Chemistry*, **1953**, Cornell University Press, Ithaca, NY.
2. Folk, J.E., *J. Biol. Chem.*, "Mechanism of action of guinea pig liver transglutaminase: VI. order of substrate addition," **244**(13): 3707-3713 (1969).
3. Chung, S.I., Shranger, R.I. & Folk, J.E., *J. Biol. Chem.*, "Mechanism of action of guinea pig liver transglutaminase: VII. Chemical and stereochemical aspects of substrate binding and catalysis," **245**(23): 6424-6435 (1970).
4. Chung, S.I. & Folk, J.E., *J. Biol. Chem.*, "Kinetic studies with transglutaminases: the human blood enzymes (activated coagulation factor XIII) and the guinea pig hair follicle enzyme," **247**(9): 2798-2807 (1972).
5. Gross, M., Whetzel, N.K. & Folk, J.E., *J. Biol. Chem.*, "The extended active site of guinea pig liver transglutaminase," **250**(12): 4648-4655 (1975).
6. Folk, J.E., *Adv. Enz.*, "Mechanism and basis for specificity of transglutaminase-catalyzed epsilon-(gamma-glutamyl) lysine bond formation," **54**: 1-56 (1983).
7. Gorman, J.J., *J. Biol. Chem.*, "Structural features of glutamine substrates for transglutaminases: specificities of human plasma factor XIIIa and the guinea pig liver enzyme toward synthetic peptides," **256**: 2712-2715 (1981).
8. Gorman, J.J. & Folk, J.E., *J. Biol. Chem.*, "Structural features of glutamine substrates for transglutaminases: role of extended interactions in the specificity of human plasma factor XIIIa and the guinea pig liver enzyme," **259**: 9007-9010 (1984).

6 ENZYMATICALLY DEGRADABLE POLY(ETHYLENE GLYCOL) GELS

6.1 Background

A degradable gel may be advantageous in applications where the cell scaffold is to be temporary. Such a case might be found in skin¹ or articular cartilage regeneration² where it is hoped that cells will remodel the defect by secreting and organizing new extracellular matrix.

There are at least two methods of incorporating degradation sites into synthetic cell scaffolds: with hydrolytically or enzymatically cleavable moieties. Poly -lactides and -glycolides are common examples of the former, either by use of the polymer itself or by incorporating short segments into other polymers such as PEG³. However hydrolytically sensitive units such as lactides cleave at a set rate based at body temperature and pH which can be much more rapid than expected (hours versus days) due to the presence of esterase activity *in vivo*. Enzymatically cleavable sites offer dual advantage of slowing the rate of degradation and allowing cellular secretion of enzymes to control the rate of enzymolysis.

6.2 Design

We have incorporated a collagenase-susceptible site into the transglutaminase amine acceptor peptide between the point of PEG attachment and the active glutamine

residue. A series of dual-activity (TG and collagenase) peptides (Peptides E, F and G of Table 2-1) were designed based on published sequences of synthetic collagenase substrates⁴ as discussed in Section 5.3.1. By incorporation of a collagenase-susceptible linkage into the network structure, this process of scaffold dissolution will be governed by cellular secretion of collagenase, mimicking the natural turnover of extracellular matrix.

In this study sequential TG-mediated crosslinking and collagenase-mediated cleavage were studied both in the soluble form and in the gel state. It was demonstrated in both cases that collagenase could act on the intended substrates even after they had been covalently modified by transglutaminase-mediated crosslinking.

6.3 Materials and Methods

PEG Macromers. All PEG compounds used in this study are described in Section 5.2. bPEG refers to the 8arm, 40kD branched poly(ethylene glycol). Peptide substrate kinetics and sequences are listed in Tables 5-1 and 5-2.

Collagenase. The collagenase used here (purified from *Clostridium Histolyticum*: Worthington Biochemical Corporation) contains two collagenase fractions⁵: A (105kD) and B (57.4kD). Lyophilized collagenase was dissolved in phosphate buffered saline (Gibco, Ca/Mg-free) with 1mM EDTA at pH7.1. Aliquots of 100 μ L at 2.0 U/ μ L and 0.20 U/ μ L were stored at -70°C until use. One unit is defined by the amount of collagenase required to liberate one micromole of L-leucine equivalents from collagen in

five hours at 37°C and pH 7.5⁶. Bacterial collagenase used here cuts between at the leucine-glycine bond⁷ of Peptides E, F and G (Table 2-1), whereas human collagenase cleaves at the glycine-isoleucine bond of these peptides.

Collagenase was used at 0.2U/μL in 50mM tricine at pH 7.1 with 10mM CaCl₂ at 37°C for soluble peptide experiments. For gel dissolution experiments, 2.0U/μL collagenase was added to an equal volume of gel along with 1.5 volumes of water.

Collagenase/TG Substrates. Peptides E, F and G were tested for transglutaminase activity by the method detailed in Appendix A5 as discussed in Section 5.3.1. These peptides were also tested for collagenase activity in 50mM tricine pH7.5, 0.2M sodium chloride, 10mM calcium chloride and 0.20U/μL collagenase. Cleavage was monitored by reversed phase high performance liquid chromatography on an analytical C18 column with a mobile phase of 18% acetonitrile, 82% water and 0.1% trifluoroacetic acid at 0.8mL/min. Detection was at 215nm.

Soluble Crosslinking Followed by Collagenase Cleavage. Crosslinking of Peptide G to monodansyl cadaverine (mdc) was monitored by methods in Appendix A5. The resulting solution of Peptide G/mdc conjugate was exposed to collagenase as described above. This reaction was also monitored by size exclusion chromatography methods described in Appendix A5.

Collagenase Gel Dissolution. Gels (20μL) were formed in 1.0M Tris, pH7.1 at 20 wt% PEG with PEG-diamine (Table 2-2) for both bPEG-[Peptide G] and bPEG-[Peptide H] as a collagenase-stable control. Collagenase (20μL of 2.0U/μL), water (30μL) and a

solution of 1% dextran blue (5 μ L) was added to the top of the gel to visualize the otherwise invisible interface. Gels were incubated for 24 hours at 37°C and then assessed for collagenase stability.

Cell Attachment and Growth. Balb/c 3T3 cells were maintained in a culture media of high glucose Dulbecco's Modified Eagle Medium supplemented with 200mM L-glutamine, 10% calf serum and 1% penicillin / streptomycin to inhibit bacterial growth (all products from Gibco). Gels were formed in duplicate in 96-well plates by the method described in Section 5.2. Cells were seeded (15,000 cells/well) in serum-containing cell culture media (above) on top of gels four hours after gelation was initiated. The same number of cells were seeded into other wells (tissue culture plastic) for comparison. Pictures were taken at 1 day and 3 days to assess attachment and growth.

6.4 Results

In Section 5.3.1 a number of collagenase-sensitive peptides were described. These peptides were designed such that a collagenase-cleavable region was flanked by a TG-substrate and a site for PEG attachment. Therefore a TG-crosslinked PEG gel employing these peptides would be dissolved by collagenase activity. For use as temporary crosslinks, it is crucial that collagenase be able to recognize and cleave these peptides after the peptide has been covalently modified by transglutaminase during crosslink formation. To demonstrate that collagenase sequence did not depend on the presence of a free glutamine residue, collagenase-mediated cleavage was monitored *after*

transglutaminase-mediated crosslinking. The crosslinking reaction was performed on bPEG-[Peptide G] with monodansyl cadaverine as the amine donor under conditions described in Appendix A5. This soluble crosslinking reaction was monitored to enable quantification of the products. This demonstrated that Peptide G was transglutaminase-active. This product was then exposed to collagenase and monitored for enzymolysis by the same size exclusion chromatography described in Appendix A5. Transglutaminase coupling followed by collagenase-mediated cleavage is illustrated in Figure 6-1. This two step process models the desired crosslinking and subsequent chain cleavage desired in temporary cell scaffolds.

Gels formed from bPEG-[Peptide G] macromers via TG-mediated crosslinking were also susceptible to collagenase degradation. Conversely, collagenase did not degrade a gel that lacked the collagenase cleavage sequence, formed with bPEG-[Peptide H]. Additionally, gels containing bPEG-[Peptide G] were found to be stable to a collagenase-free control solution. The observed selective dissolution of Peptide G-containing gels is further evidence that the collagenase substrate remains active even when crosslinked into a gel network.

It is anticipated that cells encapsulated within these gels will secrete collagenase as they attempt to remodel their surroundings. Providing collagenase-susceptible cleavage sites on the hydrogel backbone creates a somewhat biomimetic gel in that encapsulated cells will be able to cleave the hydrogel network as they lay down native extracellular matrix. This effect could be modulated if a particular cell type was found to degrade the gel faster or slower than desired. Gel dissolution could easily be retarded by

employing a kinetically slower substrate. The rate of dissolution could be enhanced by improving the substrate kinetics or by linking multiple cleavage sites. Some advantage might also be gained by incorporating both rapid hydrolytically cleavable sites with collagenase-cleavable sites.

6.5 Cellular Interactions

As cells are to be encapsulated within these PEG gels, it is of interest to establish how cells might react to contact with these materials. To investigate cellular interactions with these gels, cells were seed on surfaced of pre-formed gels. Gels used in Section 5.4.2 (bPEG-[Peptide G]/bPEG-[Peptide I] and bPEG-[Peptide H]/bPEG-[Peptide I]) were used as a model. Peptide G has a collagenase-cleavable site located between the point of bPEG attachment and the TG substrate. Peptides H and I are not substrates for collagenase. This may be significant as balb/c 3T3 cells are known to synthesize and secrete transglutaminase⁸.

Cells were seeded on gels containing Peptides G and I, gels containing Peptides H and I, and tissue culture polystyrene as a control. Cells were examined with phase-contrast optical microscopy after 1 day and 3 days to assess cell attachment and growth. Results are shown in Figure 6-2. Cells were not visibly spread on either PEG gel at day 1, although the observed morphology is not inconsistent with observed behavior on other PEG gels. At day 3 there is a clear difference between the gel containing Peptides G and I, and the gel containing Peptides H and I. This difference may be due to a higher total mass fraction of peptide presentation in the G/I combination based on the respective

peptide formula weights of Peptide G (FW=1096D), Peptide H (FW=644D) and Peptide I (FW=477D). This may allow a greater degree of serum protein adsorption, enabling greater cell attachment. The observed difference may also be due to the function of Peptide G as a collagenase substrate. Cells may be burrowing into the surface of the gel to some degree, releasing PEG-peptide products that might have some effect on cell behavior.

It is encouraging that cells are able to proliferate, at least on the G/I Peptide combination. Incorporation of specific adhesion sites would likely enhance cell adhesion for both peptide-substrate combinations used here. Examination of encapsulated cell behavior may also give further insight as to how cells might perform when encapsulated within an enzymatically crosslinked PEG gel.

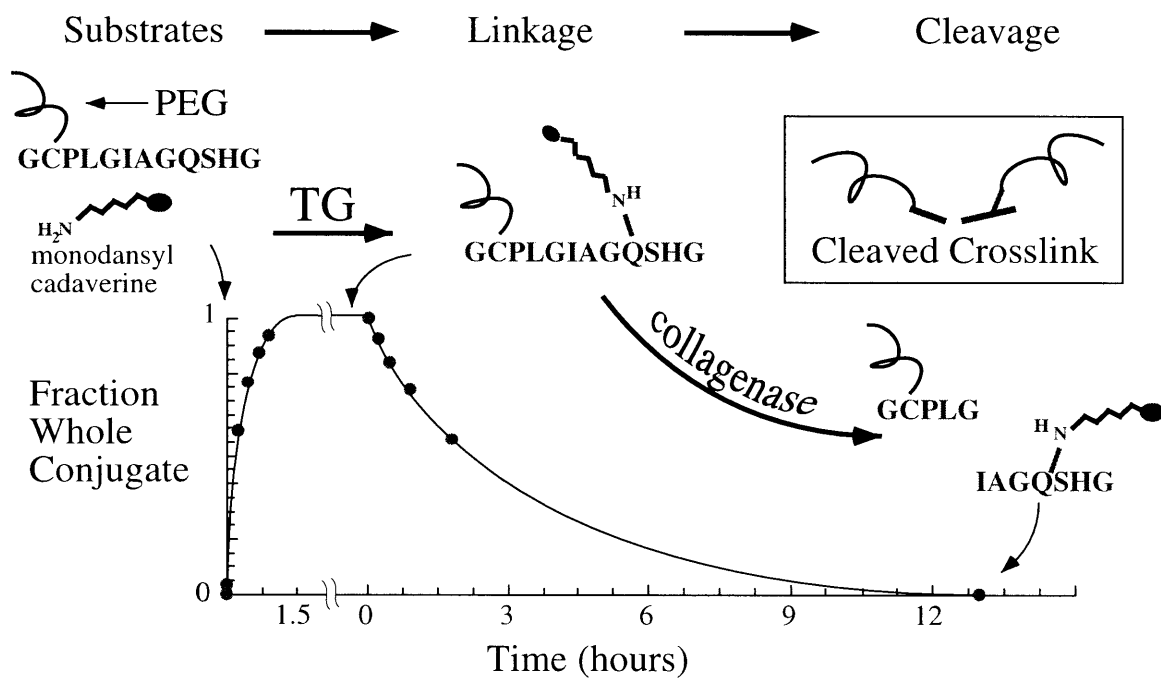


Figure 6-1. Demonstration of transglutaminase-mediated crosslinking followed by collagenase-mediated cleavage of PEG-bound peptide. In gel formation both substrates are attached to bPEG as shown in the inset.

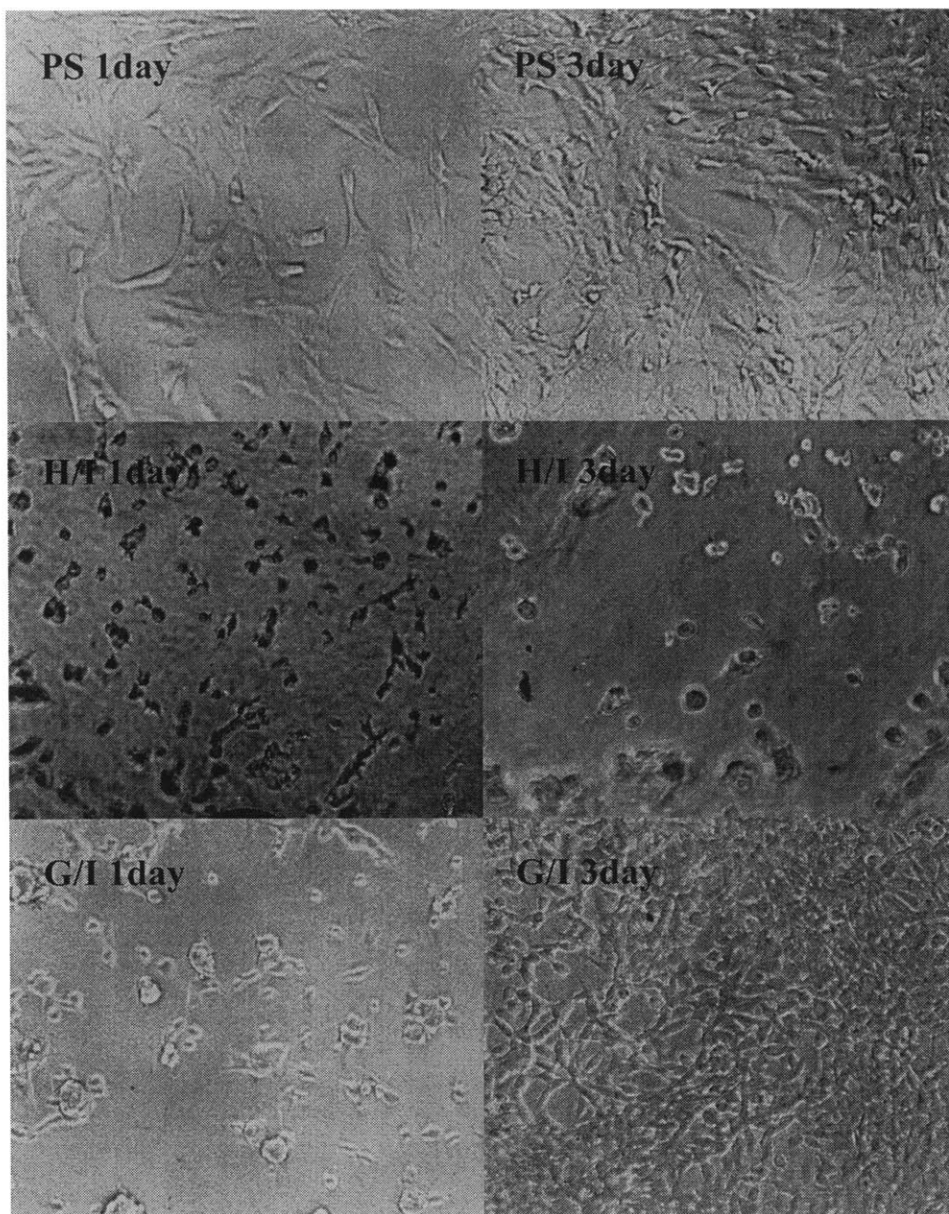


Figure 6-2. Balb/c 3T3 cells seeded on gels of bPEG-[Peptide G] / bPEG-[Peptide I] (G/I) and bPEG-[Peptide H]/bPEG-[Peptide I] (H/I). Same number of cells seeded on tissue culture polystyrene (PS) for reference. Images taken 1 day and 3 days after seeding.

6.5 References

1. Pachence, J.M. & Kohn, J. in *Principles of tissue engineering* (eds. Lanza, R., Langer, R. & Chick, W.) (R G Landes, Austin TX, 1997).
2. Brittberg, M., *et al.*, *New Engl. J. Med.*, "Treatment of deep cartilage defects in the knee with autologous chondrocyte transplantation," **331**(15): 889-895 (1994).
3. Han, D.K. & Hubbell, J.A., *Macromol.*, "Lactide-based poly(ethylene glycol) polymer networks for scaffolds in tissue engineering," **29**(15): 5233-5235 (1996).
4. Netzel-Arnett, S., Fields, G., Birkedal-Hansen, H. & Wart, H.E.V., *J. Biol. Chem.*, "Sequence specificities of human fibroblast and neutrophil collagenases," **266**(11): 6747-6755 (1991).
5. Harper, E., Seifter, S. & Hospelhorn, V., *Biochem. Biophys. Res. Comm.*, "Evidence for subunits in bacterial collagenase," **18**: 627 (1965).
6. Mandl, I., MacLennan, J., Howes, E., DeBellis, R. & Sohler, A., *J. Clin. Invest.*, "Isolation and characterization of proteinase and collagenase from *cl. histolyticum*," **32**: 1323 (1953).
7. Soberano, M. & Shoellmann, G., *Biochim. Biophys. Acta*, "Specificity of bacterial collagenase: studies with peptides newly synthesized using the solid-phase method," **271**: 133 (1972).
8. Gentile, V., Thomazy, V., Piacentini, M., Fesus, L. & Davies, P.J.A., *J. Cell Biol.*, "Expression of tissue transglutaminase in balb-c 3T3 fibroblasts - effects on cellular morphology and adhesion," **119**(2): 463-474 (1992).

7 ALTERNATIVE CROSSLINKING METHODS

7.1 Overview

There are certainly many ways to form crosslinks in an *in vivo* setting, some of which have been mentioned in Section 1.4. In the developmental stage of this thesis a number of different crosslinking chemistries were explored as viable candidates.

Ultimately, transglutaminase-mediated crosslinking was chosen to be implemented based a combination of a number of criteria, including biocompatibility, ease of synthesis, kinetic control and substrate specificity (see Section 1.4).

This chapter is included as a survey of alternative crosslinking procedures both as a historical perspective on the development of enzymatically crosslinked hydrogels and as a reference to those who may wish to pursue similar technologies.

7.2 Ionic Association: Alginate-Poly(Ethylene Glycol) Copolymers

Alginate is a natural polysaccharide isolated from brown algae. It is a linear copolymer of β -D-mannuronic acid (M) and α -L-guluronic acid (G) with extended repeats of each residue. Extended G regions are known to form interchain chelates with divalent cations, especially calcium¹. Interchain association of water-soluble polymer chains causes alginate solutions to gel.

Alginate gels continue to be used for cell encapsulation² despite issues associated with immunogenicity³ that are likely due to residual impurities⁴. Immunogenicity can

result in fibrous encapsulation of the implanted gel or device that will severely limit transport of essential biological molecules⁵.

To minimize possible adverse biological effects of alginate, a gel system was designed employing alginate only as a crosslinker and PEG as the water-soluble polymer that would bridge the crosslinks. The goal was then to attach short alginate segments to PEG chains to produce a more biocompatible gel. Short alginate segments from partially digested alginate were to be used in preliminary experiments. Concurrently synthetic poly guluronic acid, the portion of alginate responsible for gelation, was to be synthesized from an activated guluronate (Figure 7-1) to be polymerized in a trichloroacetimidate-mediated reaction⁶. This chemistry was chosen to insure 1,2-cis linkages essential for calcium chelation. Synthetic poly guluronic acid would maximize the strength of the crosslink while also maximizing the ratio of PEG to poly guluronic acid. However before this strategy could be advanced other crosslinking methods came to light that promised to be far less synthetically intensive.

7.3 Hydrophobic Association: β -Amyloid-Terminated PEG

Hydrophobic peptides were also explored as potential moieties for crosslinking through self-association. In particular a segment of synthetic β -amyloid (LMVGGVVIA)⁷ was available⁸. By attaching this hydrophobic oligopeptide to PEG ends it was reasoned that self-association would drive gelation.

The β -amyloid fragment was coupled to both ends of a linear PEG (MW=3.4kD) from the ditresylate (Shearwater Polymers) (see Section 2.2). A solution of PEG-(LMVGGVVIA)₂ in hexafluoroisopropanol was injected into water to induce aggregation. The resulting solution became somewhat cloudy, but gelation was not observed. It is likely that self-association of the peptide oligomer resulted in gels of only very small dimensions. Images taken by transmission electron microscopy were consistent with this hypothesis (Figure 7-2). It is not unsurprising that gels were difficult to form as PEG chains linked to other amyloid fragments have shown altered aggregation properties as compared to their non-PEG-linked form⁹.

7.4 Disulfide Bond Formation: Cysteine-Terminated PEG

The use of disulfide bonds as PEG crosslinks came about serendipitously during the development of alternative methods in ionic-bond-mediated crosslinking (see Section 6.1). A molecular configuration in which a sulfhydryl and a primary amine are separated by two methylene units was identified as a particular strong candidate for tetradentate (two-molecule) chelating of multivalent cations^{10, 11}. This sulfhydryl/amine configuration is present in the structure of cysteine, a naturally occurring amino acid, simplifying the synthesis and offering the possibility of acceptable biocompatibility. The envisioned design involved functionalizing multi-arm PEG with cysteine via the carboxylic group. Gelation could then be induced in a PEG-cysteine containing cell suspension by the addition of cations

A number of candidate cations were screened for cell toxicity in balb/c 3T3 cultures, maintained in a culture media of high glucose Dulbecco's Modified Eagle Medium supplemented with 200mM L-glutamine, 10% calf serum and 1% penicillin/streptomycin to inhibit bacterial growth (all products from Gibco). Cells were seeded in triplicate in the presence of 1mM or 10mM candidate cation or with no additional cations (control). Cell numbers were counted after 72 hours. These concentrations (1.0mM-10mM) were thought to be a useful range for gelation as 10mM in PEG-ends, requiring 5mM ions, would correspond to a 5% PEG gel (at 5kD/arm). Cell numbers were compared with control conditions (Figure 7-3). In all cases the presence of these cations at 1mM or greater had a negative effect on the cell number after 3 days. The smallest effect was observed in the case of 1.0mM Fe(III) Therefore iron(III) was chosen as the best ion candidate.

Aminated PEG of the same 'nominally tetrafunctional' structure as was used in Section 4.2 (Polysciences) was used here as a starting material. L-cysteine (N-BOC,S-trityl-L-cysteine, Bachem) was attached to aminated PEG in methylene chloride with 1,3-dicyclohexyl-carbodiimide (Aldrich) and 4-dimethylaminopyridine (Aldrich) as a catalyst. The product was deprotected in 2.5% ethanedithiol (Aldrich) and 5% water in trifluoroacetic acid (J.T. Baker).

Gels were formed by the addition of ferric chloride (FeCl_3) to a solution of 15% PEG-Cys₄. Stoichiometric amounts (15mM) of FeCl_3 were required for gel formation. Attempts to form gels at PEG concentrations less than approximately 10% formed only viscous solutions, suggesting insufficient overlap of PEG chains.

The method of gel formation for PEG-Cys₄ appeared to be through disulfide bond formation rather than simple cross-chelation of Fe(III) ions. This is based on the observation that upon FeCl₃ the PEG-Cys₄ solution would turn blue in less than a minute indicating chelation of the iron atom. However within one to two minutes this color would subside, possibly reflecting the release of iron from the cysteine complex. This release was not accompanied by dissolution of the gel. It is now hypothesized that a transition from Fe(III) to Fe(II) induced reduction of two cysteines to a cystine, covalently linking the PEG chains.

As the amount of iron required for gelation exceed the toxic levels approximated by Figure 7-3, this method was set aside in favor of the enzymatic crosslinking approach. Further work with different chelator/ion combinations may yield a more biocompatible gel that is ionically crosslinked or similarly stabilized via disulfide bonds.

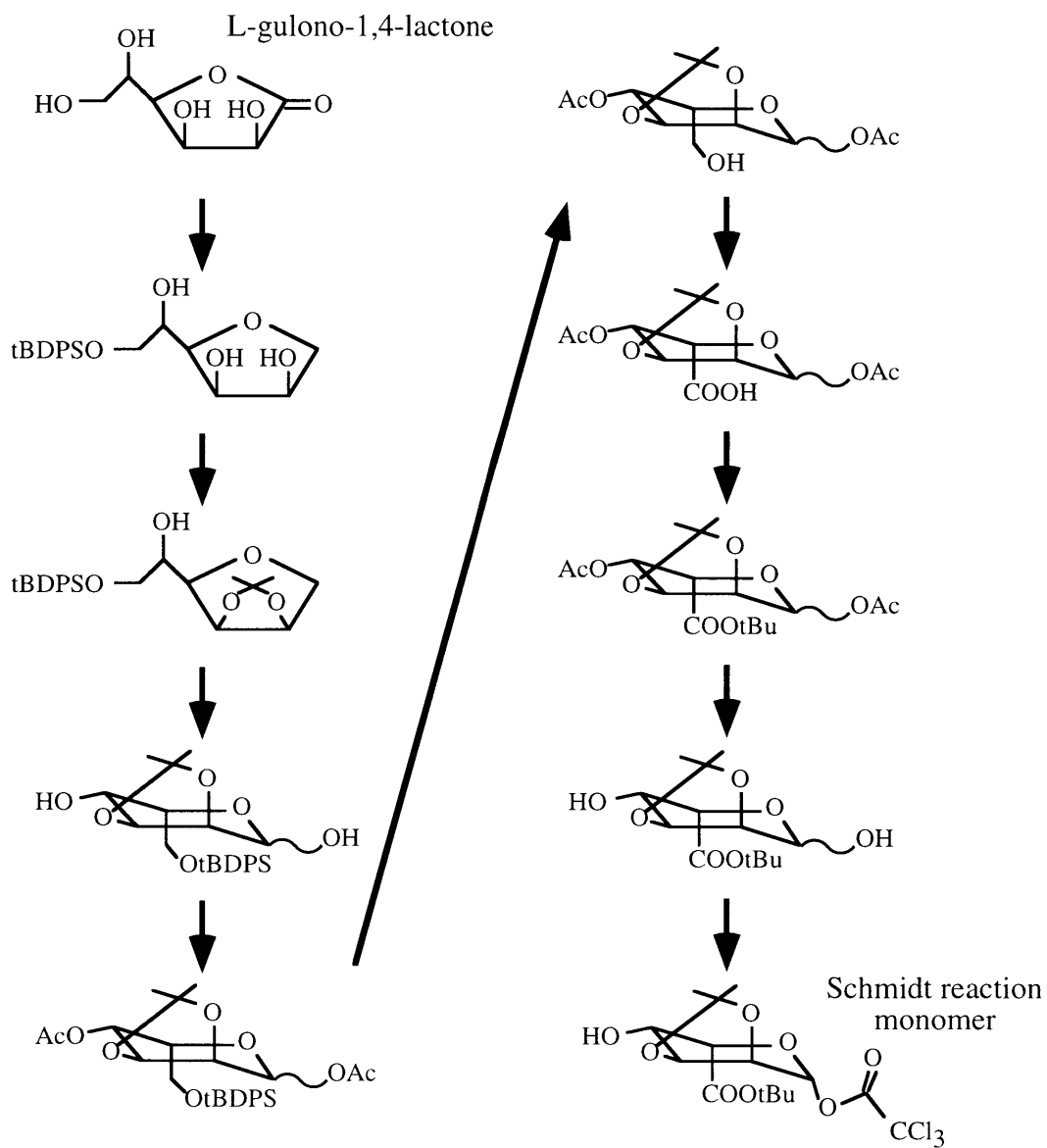


Figure 7-1. Synthesis scheme for monomer to be polymerized via Schmidt reaction into poly guluronic acid.

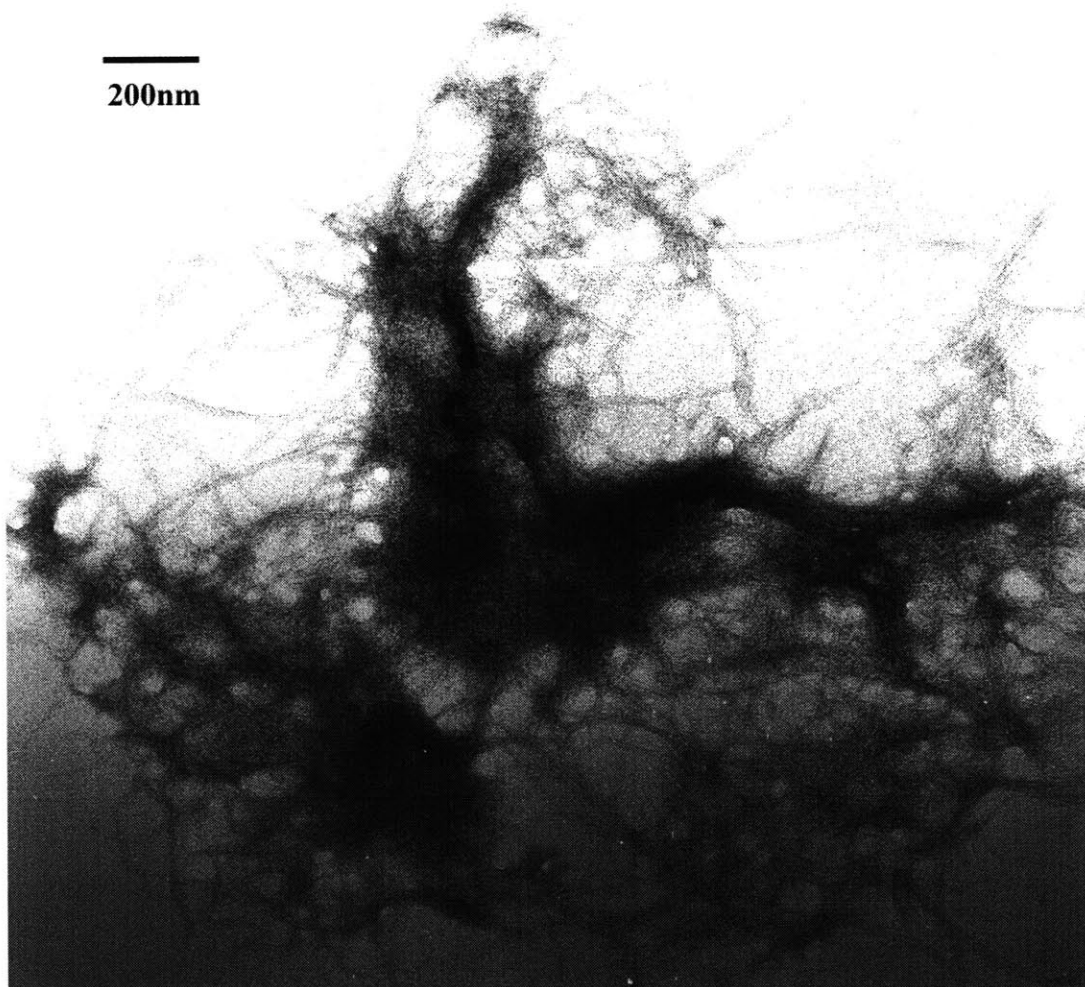


Figure 7-2. Transmission electron micrograph of PEG-(LMVGGVVIA)₂ aggregates.

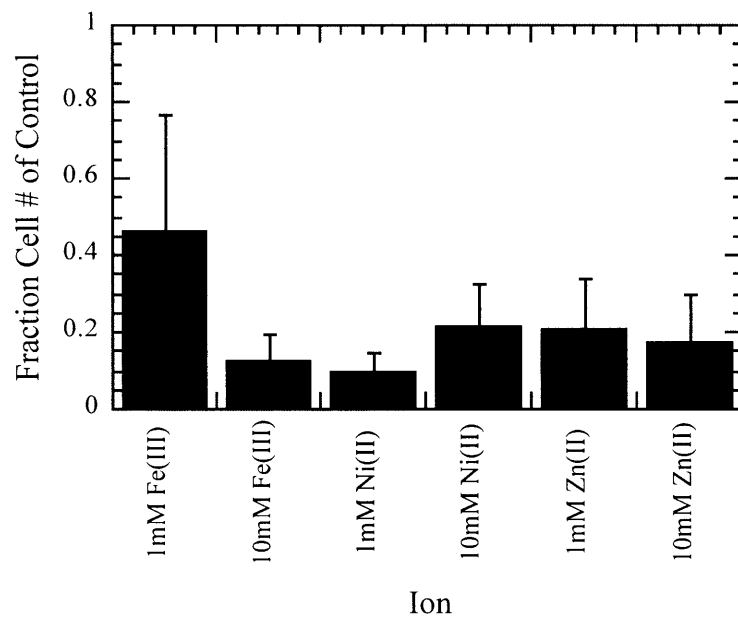


Figure 7-3. Cell toxicity experiments. Cell numbers 72 hours after plating are presented relative to control (no additional cation addition beyond media levels).

7.5 References

1. Grant, G.T., *FEBS Lett.*, "Biological interactions between polysaccharides and divalent cations: the egg-box model," **32**(1): 195-198 (1973).
2. Freed, L.E. & Vunjak-Novakovic, G., *Adv. Drug Del. Rev.*, "Culture of organized cell communities," **30**(1-2): 15-30 (1998).
3. Clayton, H.A., James, R.F.L. & London, N.J.M., *Acta Diabetol.*, "Islet microencapsulation: a review," **58**: 181-189 (1993).
4. Zimmermann, U., *Electrophor.*, "Production of mitogen-contamination free alginates with variable ratios of mannuronic acid to guluronic acid by free flow electrophoresis," **1992**(13): 269-274 (1992).
5. Otterlei, M., *J. Immunother.*, "Induction of cytokine production from human monocytes stimulated with alginate," **10**: 286-291 (1991).
6. Schmidt, R.R. & Michel, J., *Tett. Lett.*, "Direct O-glycosyl trichloroacetimidate formation. Nucleophilicity of the anomeric oxygen atom," **25**(8): 821-824 (1984).
7. Halverson, K., Fraser, P.E., Kirschner, D.A. & P T Lansbury, J., *Biochem.*, "Molecular Determinants of amyloid deposition on alzheimer's disease: conformational studies of synthetic beta-protein fragments," **29**: 2639-2644 (1990).
8. "A synthetic beta amyloid fragment was a gift of P T Lansbury of the Center for Neurologic Diseases, Brigham and Womens Hospital, Boston MA," :
9. Burkoth, T.S., *et al.*, *J. Am. Chem. Soc.*, "C-terminal PEG blocks the irreversible step in beta-amyloid(10-35) fibrillogenesis," **120**(30): 7655-7656 (1998).
10. Porter, L.J., Perrin, D.D. & Hay, R.W., *J. Chme. Soc. (A)*, "The interaction of cysteine methyl ester with metal ions. Part I. Nature of the complex species," : 118-126 (1969).
11. May, P.M., Linder, P.W. & Williams, D.R., *J. C. S. Dalton*, "Computer simulation of metal-ion equilibria in biofluids: models for the low-molecular-weight complex distribution of calcium(II), magnesium(II), manganese(II), iron(III), copper(II), zinc(II), and lead(II) ions in human blood plasma," : 588-595 (1977).

8 CONCLUSIONS

8.1 Summary

This work has focused on engineering the gelation process in a polymer system designed for cell encapsulation or other *in vivo* applications. Gelation is achieved by crosslinking an aqueous solution of a multi-functional form of poly(ethylene glycol) (PEG), creating a continuous network that contains greater than 90% water. PEG is in many ways an ideal biopolymer because of its hydrophilicity, low protein-binding and non-immunogenicity. Following an initial screening of potential crosslinking chemistries, enzymatic crosslinking was identified as the optimal strategy for this system based on kinetic control, crosslink substrate specificity, biocompatibility and ease of synthesis.

Enzymatic crosslinking is achieved by the action of a well-studied biological enzyme, transglutaminase (TG). TG is a family of enzymes that catalyze the formation of an amide linkage between the γ -carboxamide group of certain peptidyl glutamine residues and primary amines such as lysine. These calcium-dependent enzymes are ubiquitous throughout the body, forming crosslinks in skin, liver and blood clots. This system could be adapted to human therapeutic use by employing a human derived or recombinant TG, however for this study a commercially available TG was used for simplicity.

This work on enzymatically crosslinked PEG gels was constructed around a strong core development of the requisite technologies. An extended study of tresyl-

mediated synthesis was undertaken to insure maximal conversions for peptide-functionalized PEG conjugates. Additionally the crosslinking enzyme, transglutaminase, was extensively characterized to develop a fundamental understanding of the factors affecting kinetics and stability of this biological crosslinker.

The enzymatic crosslinking process was developed systematically by identifying the necessary design parameters to effectively control kinetics and enzyme specificity. The kinetics of TG-mediated crosslinking are most strongly controlled by the structure of the amine acceptor (glutamine) substrate. A number of TG-active peptidyl amine acceptor substrates were identified that varied in size and crosslinking kinetics. Amine donor substrates play a lesser role in crosslinking kinetics, yet still must be able to compete effectively for other biological amines that might be present in an *in vivo* application. A commercially available one-to-one copolymer of lysine and phenylalanine was the first multifunctional amine donor substrate to be used. Other various PEG-linked amine donor substrates were ultimately identified, with one peptidyl (5 amino acid) substrate exhibiting significantly faster kinetics than others examined.

Gel studies fell naturally into two categories: those with gels formed from PEG-linked amine acceptor substrates and poly(lysine:phenylalanine) (PEG/poly(KF) gels) and gels where both substrates were PEG-linked (PEG/PEG gels). Studies on PEG/poly(KF) gels focused on structural properties as determined by diffusional and swelling characteristics as well as early kinetic models and cellular compatibility. PEG/PEG gel studies focused on amine substrate development, extension of kinetic models as well as the implementation of degradable PEG/PEG gels.

PEG/PEG gels were engineered to be degradable in a biological milieu. This was achieved by the incorporation of collagenase-cleavable peptide moieties between the TG-active glutamine residue and the site of PEG attachment. This method of incorporation of degradation sites susceptible to enzymolysis is thought to be superior to degradation by hydrolysis because the latter strategy is complicated by the presence of esterases *in vivo*.

Preliminary cell culture work indicates that the gel components and gelation process is not acutely toxic to cells. This was not unexpected based on the benign biological interactions characteristic of PEG and ubiquitous presence of transglutaminase in nearly all tissues in the body.

8.2 Future Work

Enzymatically crosslinked PEG gels were designed as an enabling technology for tissue engineering. The gel developed here is a platform on which may be built any number of cell scaffolds tailored to specific applications. The ultimate cell scaffold is envisioned as a multi-functionalized gel, with the ability to influence cells to perform (attach, migrate, divide and differentiate) as appropriate for a particular tissue site. To achieve this goal the gel as it has been described here must be functionalized with bioactive moieties that can illicit the desired function. Addition of these types of functionalities might be incorporated through macromers containing both crosslinkable moieties as well as the function of interest (Figure 8-1).

The ability to engineer cellular manipulation through biomaterials is predicated on a deep understanding cell biology and cell function. The work presented here included a

number of preliminary experiments indicating that encapsulating 3T3 fibroblasts in enzymatically crosslinked PEG hydrogels would not be harmful to cells. This work must be expanded to relevant cell types, possibly cartilage cells (chondrocytes) or liver cells (hepatocytes). Extended cell culture must also be demonstrated. Ultimately, knowledge gained from *in vitro* experiments must be applied to the development of *in vivo* methods in the appropriate animal model.

Articular cartilage regeneration may be a useful model in which to demonstrate the application of enzymatically crosslinked PEG hydrogels. This topic has been the focus of much recent research¹. Articular cartilage is an attractive model by virtue of the fact that native tissue is two-dimensional, a geometry easily serviceable for nutrient delivery in an *in vitro/ex vivo* system. Additionally the metabolic requirements for chondrocytes is relatively low, a necessity in the avascular environment of the chondrocyte.

PEG gels may find wider applicability with use in conjunction with other biomaterials. The materials properties of PEG hydrogels might limit their use to soft tissue application. Therefore enzymatically crosslinked PEG hydrogels might be used in conjunction with an open-mesh structural polymer such as polylactide-co-glycolide (PLG) formulations. In this type of biomaterial composite, the PEG hydrogel would address the need of the cell on a molecular level (nm- μ m) while the PLG polymer would provide for structural integrity on larger length scales (μ m-mm).

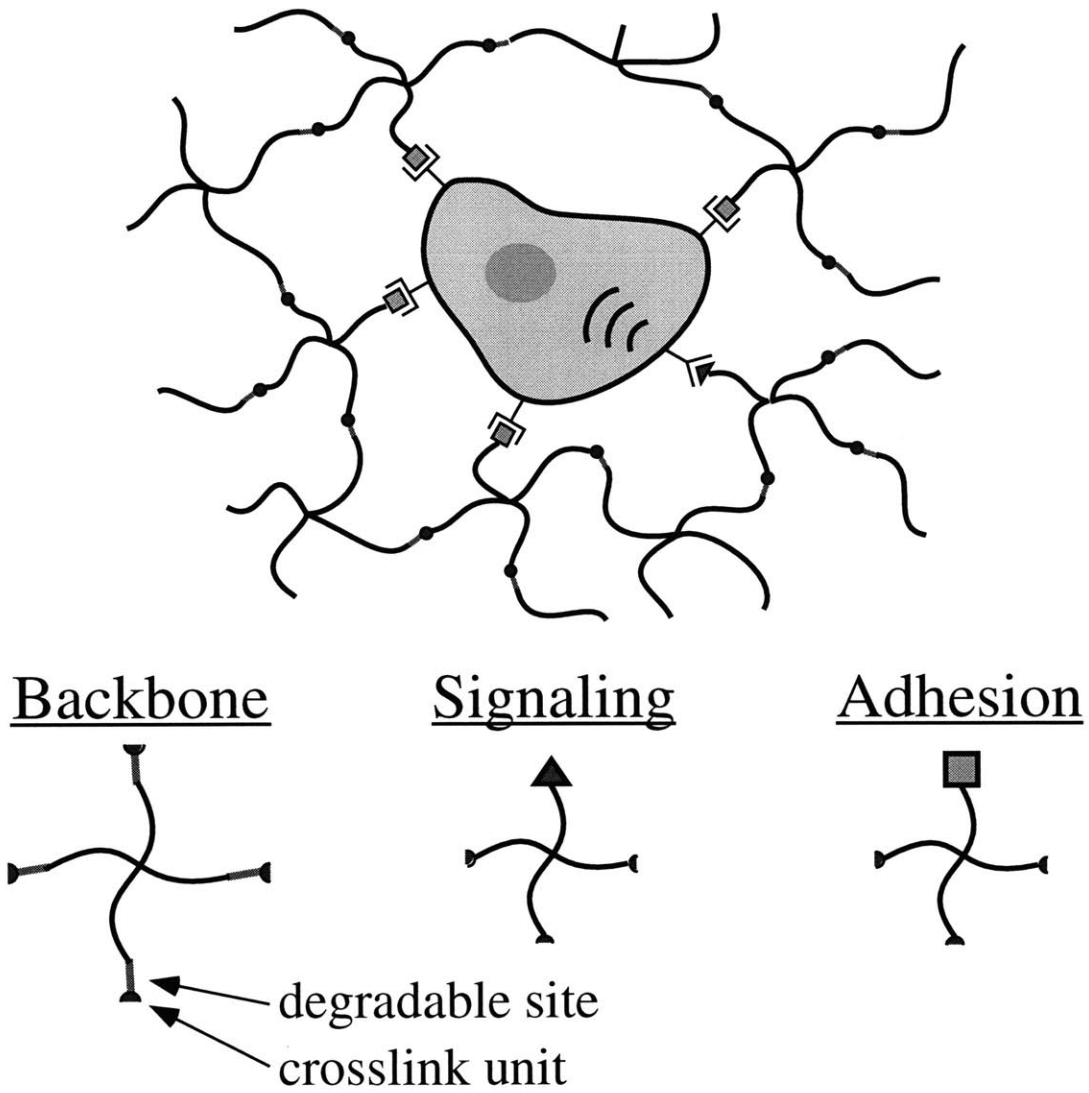


Figure 8-1. Modular model for enzymatically crosslinked hydrogels for tissue engineering.

8.3 References

1. Brittberg, M., *et al.*, *New Engl. J. Med.*, "Treatment of deep cartilage defects in the knee with autologous chondrocyte transplantation," **331**(15): 889-895 (1994).

APPENDIX A: PROTOCOLS

A1 Poly(Ethylene Glycol) Tresylation

A1.1 Background

The following procedure is general for converting hydroxyl groups to a trifluoroethanesulfonyl functionality¹. Further details are given in Section 2.2.

In general it is easiest to scale a tresylation to an integral number of tresyl chloride ampules (1g or 5g), as unused amounts should not be stored for later use unless extraordinary efforts are made to keep tresyl chloride dry and oxygen-free.

A1.2 Materials

- Hydroxyl-terminated poly(ethylene glycol)
- 2x (relative to PEG ends) molar amount of tresyl chloride (2,2,2-trifluoroethanesulfonyl chloride) (Aldrich).
- 10% molar excess (relative to TrCl) of freshly distilled triethylamine
- 4Å molecular sieves
- Dry methylene chloride (stored over molecular sieves)
- Distillation apparatus
- Argon source

A1.3 Procedure

Day Before

0. Calculate amount of all materials needed.
1. Distill triethylamine - discard first and last 10% of distillation.
2. Add about 1g 4A molecular sieves per 10mL triethylamine.
3. Seal well and store at 4°C.
4. In sealable flask (about 10mL flask volume per gram of PEG to be used), add 1g 4Å molecular sieves per 1g PEG to be used.
5. Rinse with an equal volume (approx.) of methylene chloride (MeCl_2) to remove residual sieve 'dust'.
6. Add pre-calculated amount of PEG.
7. Add about 5mL dry MeCl_2 per gram of PEG.
8. Swish until dissolved.
9. Store at 4°C overnight.

Day of Tressylation

1. Decant PEG solution into reaction flask that will accept rubber septum.
2. Wash sieves with small amount of dry MeCl_2 , adding wash to reaction flask.
3. Add stir bar and set stirring.
4. Add pre-distilled triethylamine.
5. Dropwise, slowly add TrCl .

6. Flush with Argon and seal, or maintain slow stream of Argon through reaction flask.
7. Leave stirring for 2 hours.
8. Reduce on a rotovap with a liquid nitrogen trap.
9. To a 500mL centrifuge bottle with 200mL anhydrous methanol (dry MeOH) with 400 μ L concentrated HCl (37%), add reaction contents.
10. Wash reaction flask with a portion of dry MeOH and add to centrifuge bottle.
11. Bring total solvent volume to about 400mL with MeOH.
12. Chill with liquid nitrogen to precipitate PEG.
13. Spin to settle PEG.
14. Pour off supernatant.
15. Redissolve in about 400ml dry MeOH.
16. Reprecipitate, spin, dispose of supernatant.
17. Redissolve in a minimum of dry MeOH.
18. Transfer to multiple 5mL vials or other appropriate small aliquots.
19. Freeze in -70 $^{\circ}$ C freezer.
20. Lyophilize to constant weight with liquid nitrogen trap.
21. Store PEG-Tr in -70 $^{\circ}$ C freezer.

A2 Peptide Synthesis

A2.1 Background

Peptide synthesis techniques have been well documented in the literature². Currently, two general step-wise synthesis strategies are widely used for multi-amino acid (>2-3) syntheses. These two techniques are classified according to the method by which protection of the α -amino group is held independent of the protection of side chain moieties during the synthesis steps as shown in Figure A1. The first method, t-BOC (N-tert-butoxycarbonyl), relies on two levels of acid lability. The t-BOC group (protecting the α -amine) is cleavable under relatively weakly acidic conditions and the side chain groups are designed to be less acid labile, requiring treatment with strong acids such as hydrofluoric acid. An alternative method, Fmoc (N-9-Fluorenylmethoxycarbonyl), employs both protecting groups which are base labile and those which are acid labile, a so-called *orthogonal* protection scheme. The Fmoc group (protecting the α -amine) is cleavable under basic conditions, while the side chain protecting groups require exposure to acid. Here, the Fmoc synthesis has been employed both due to the obvious safety advantages of avoiding HF as well as the reduced side reactions that can be accumulated with successive acid exposure in the t-BOC method.

A2.2 Procedure

All peptides used here were synthesized on a Rainin PS2000 Peptide Synthesizer by standard Fmoc methods in dimethylformamide (DMF). Reagents for the peptide

synthesizer were purchased from Rainin. Peptide resin (Wang) and all Fmoc-amino acids were purchased from American Peptide (Fmoc-Glycine, Fmoc-Proline, Fmoc-Leucine, Fmoc-Isoleucine, Fmoc-Alanine, Fmoc-Cysteine(trityl), Fmoc-Serine(t-butyl) and Fmoc-Histidine(trityl) with the exception of Fmoc-Glutamine(4-methyltrityl) from Bachem. Redistilled piperidine from Aldrich was used at a concentration of 20% (v/v) in DMF as the Fmoc deprotectant.

Peptides used in this study were synthesized in a 0.5mmole batches with Glycine-Wang resin from American Peptide. Synthesis proceeded from the carboxyl-terminal of the peptide to the N-terminal. The synthesis started with the C-terminal N-protected amino acid attached to the resin (Wang-glycine). In the first step of each cycle the N-terminal Fmoc was removed with 20% (v/v) piperidine in DMF. For the addition of each amino acid, the resin was exposed to 1.5mmole of Fmoc amino acid and 1.5mmole HTBU (2-(1H-Benzotriazol-1-yl)-1,1,3,3-tetramethyluronium hexafluorophosphate) (Peptide Technologies) in approximately 20mL of 0.40M N-methylmorpholine in DMF (Peptide Technologies). This cycle of Fmoc deprotection and amino acid addition was repeated for each residue. In the final cycle an Fmoc group was removed from the N-terminal residue.

The peptide was cleaved from the resin and deprotected with aliquots (100mL total) of 2.5% ethanedithiol (Aldrich) and 5% water in trifluoroacetic acid (TFA) (J.T. Baker), added over the course of one hour. Excess TFA was removed by rotary evaporation. The peptide was precipitated by pouring into diethyl ether. The precipitate was isolated by centrifugation, redissolved in a minimum of TFA and

reprecipitated three times. The final product was washed with diethyl ether. Residual amounts of ether was removed *in vacuo*. Purity was confirmed by reverse phase high performance chromatography, often on a C-18 analytical column with a gradient from 0.1% trifluoroacetic acid in water to 0.1% trifluoroacetic acid in acetonitrile.

A3 Transglutaminase Storage

Handling and process procedures using transglutaminase must be designed to maintain maximal activity. Loss of transglutaminase activity is largely dependent on exposure to calcium³. Upon exposure to calcium transglutaminase partitions into high molecular weight aggregates that cannot be dispersed even in boiling sodium dodecylsulfate³ (Section 3.2). Transglutaminase is protected and kept in the catalytic ‘off’ state by storage in small amounts, typically 1mM, of ethylenediaminetetraacetic acid (EDTA), a divalent ion chelator with a particularly strong affinity for calcium.

In the absence of calcium, the enzyme is largely stable to temperature and moderate pH changes around neutral. To insure maximal activity, all manipulations prior to use were performed in a 4°C cold room. The pH of the storage solution (7.1-7.4) depended on the particular application, buffered by phosphate (as calcium and magnesium-free PBS, 1x or 0.5x) or 10mM Tris HCl with 160mM potassium chloride. Although Tris possesses a primary amine, steric hindrance prevents involvement in transglutaminase-mediated reactions⁴. Tris is the most common buffer used in published work on transglutaminase activity.

Transglutaminase (Guinea Pig Liver Transglutaminase) was purchased from Sigma in lyophilized form, generally in the 2.0U size where the international unit for transglutaminase is defined by the assay described in Appendix A4. The transglutaminase powder is dissolved in the appropriate amount of storage buffer based

on the assay given for each lot. Transglutaminase is stored in aliquots of 20 μ L usually at a concentration of 0.2U/20 μ L or 0.1U/20 μ L. Once aliquotted, the enzyme is stored at -70°C until use.

A4 Colorimetric Transglutaminase Activity Assay

There exist a number of activity assays for transglutaminases, as detailed in Section 2.3.2. The colorimetric assay by quantification of hydroxylamine incorporation into an amine acceptor⁵, benzyloxycarbonyl-L-glutaminy-glyine (ZQG), remains the easiest to implement and is readily scaleable to a large number of simultaneous measurements with the use of microtiter plates. In fact this assay defines one ‘unit’ of transglutaminase as the amount required to produce one micromole of γ -glutaminy-hydroxylamine from ZQG per minute at 37°C and pH6.0. The assay could certainly be run under different conditions, keeping in mind issues of self-reactivity (see Section 3.4.1). Quantification of activity is by absorbance from a complex between the catalytically formed hydroxylamide and iron III under acidic conditions.

A4.1 Materials

- Tris-acetic acid buffer pH6.0, 1M in Tris
- ZQG (Benzyloxycarbonyl-L-glutaminy-glyine) (Sigma)
- 0.4M and 5M sodium hydroxide
- 2M Hydroxylamine hydrochloride (Aldrich)
- 0.1M Calcium chloride
- 0.02M EDTA (ethylenediaminetetraacetic acid)
- 5% (w/v) ferric chloride in 0.1M hydrochloric acid
- 15% (w/v) trichloroacetic acid in water

- 2.5M hydrochloric acid

A4.2 Procedure

A 0.2M ZQG (FW=337.5) reagent was made by dissolving ZQG in a minimum amount of 0.4M sodium hydroxide, then adjusting to the final volume at pH 6.0 with 2.5M HCl and water.

A ferric chloride reagent was prepared by mixing equal parts 5% (w/v) ferric chloride in 0.1M hydrochloric acid, 15% (w/v) trichloroacetic acid in water and 2.5M hydrochloric acid.

Just prior to the assay, 1.0mL of Tris-acetate buffer was mixed with 0.75mL of ZQG solution, 0.25mL calcium chloride solution, 0.25mL hydroxylamine solution and 0.25mL EDTA solution. This solution was brought to a final volume of 4.0mL and pH 6.0 with 5M NaOH and water. For each assay a portion of this mixture is warmed to 37°C. A solution of unknown enzyme concentration is added to initiate the reaction, typically 1:4 enzyme solution to assay solution. At 10 minutes the reaction is stopped by the addition of an equal volume of the ferric chloride solution. Activity is measured at 525nm where the product gives $\epsilon = 340 \text{ M}^{-1} \text{ cm}^{-1}$.

A5 SEC PEG/Monodansyl Cadaverine Assay

In measuring the activity of PEG-bound substrates, it is useful to exploit the size differences of the PEG-bound and non-bound substrates. With size exclusion chromatographic techniques, the amount of PEG-bound chromophores and non-bound chromophores can be quantified throughout the progress of a TG-mediated reaction.

For quantification of the kinetics of PEG-bound amine acceptors, a small chromophore, monodansyl cadaverine (A247) is used as the amine donor. As the reaction progresses, the monodansyl cadaverine will migrate from a peak at long elution times (small molecules) to the PEG-peptide peak at short elution times.

A5.1 Materials

- Monodansyl cadaverine (Aldrich)
- Tris base or MES (2-[N-morpholino]-ethanesulfonic acid) (Sigma)
- Amine acceptor substrate (unknown to be measured)
- Potassium phosphate, mono- and di-basic
- Calcium chloride
- Trifluoroacetic acid
- TSK G4000PW size exclusion column
- HPLC with UV/vis detection

A5.3 Procedure

A stock solution was made with 10mM calcium chloride, 10mM monodansyl cadaverine and 100mM of the appropriate buffer: MES for pH6.0 and Tris for pH>7. This solution was stored in 0.1mL aliquots at -70°C until use.

For each assay a known weight of the glutamine substrate (≤ 2 mM in glutamine) was dissolved in 80 μ L of the monodansyl cadaverine stock solution and brought to the appropriate temperature in a constant temperature water bath. At time zero, a 20 μ L aliquot of enzyme was added to the solution and vortexed. At each time point, an aliquot of reaction solution was injected onto a TSK G4000PW size exclusion HPLC column with a mobile phase of 2.0mM monobasic potassium phosphate with 5.0ppm TFA running at 4.0mL/min. Baseline separation of the glutamine substrate, mdc and the substrate-mdc conjugate is achieved due to minor hydrophobic interactions between mdc and the column resin. Quantification was by integration of absorbance at 247nm.

A6 SEC PEG/Z-Glutaminylglycine Assay

In general it is more difficult to directly measure the kinetics of amine donor substrates because steps previous to the addition of the amine donor substrates are generally rate limiting (see Sections 1.5.3 and 1.5.4). To measure the kinetics of amine substrates it is necessary to employ conditions where the enzyme is saturated with the first substrate, the amine acceptor. For this assay, benzyloxycarbonyl-glutaminyl-glycine (ZQG, $K_m = 7\text{mM}^6$) was used as the amine acceptor under saturating conditions.

This assay is based on the same quantitation principle as the SEC/monodansyl cadaverine assay in Appendix A5. Here, the amine acceptor substrate is a small molecule and the amine donor substrate is attached to PEG. The amine acceptor substrate used here, benzyloxycarbonyl-glutaminyl-glycine (ZQG), is also used in the colorimetric transglutaminase activity assay of Appendix A4.

A6.1 Materials

- Benzyloxycarbonyl-glutaminyl-glycine (ZQG) (Sigma)
- Tris base or MES (2-[N-morpholino]-ethanesulfonic acid) (Sigma)
- Amine donor substrate (unknown to be measured)
- Potassium phosphate, mono- and di-basic
- Calcium chloride
- TSK G4000PW size exclusion column
- HPLC with UV/vis detection

A6.2 Procedure

A stock solution was made with 10mM calcium chloride, 50mM ZQG and 100mM of the appropriate buffer: MES for pH6.0 and Tris for pH>7. This solution was stored in 0.1mL aliquots at -70°C until use.

For each assay a known weight of the amine donor substrate (≤ 2 mM in amine) was dissolved in 80 μ L of the ZQG stock solution and brought to the appropriate temperature in a constant temperature water bath. At time zero, a 20 μ L aliquot of enzyme was added to the solution and vortexed. At each time point, an aliquot of reaction solution was injected onto a TSK G4000PW size exclusion HPLC column with a mobile phase of 1.5mM monobasic potassium phosphate and 0.5mM dibasic potassium phosphate running at 4.0mL/min. Baseline separation of the glutamine substrate, ZQG and the substrate-ZQG conjugate was achieved due to minor hydrophobic interactions between ZQG and the column resin. Quantification was by integration of absorbance at 258nm.

A7 O-phthaldialdehyde Primary Amine Assay

The o-phthaldialdehyde fluorescent assay is a facile method of determining concentrations of primary amines to micromolar concentrations⁷. O-phthaldialdehyde undergoes a primary reaction with a sulfhydryl group (non-fluorescent) which then undergoes a cyclization reaction with primary amines to yield a fluorescent compound. A more sensitive alternative for primary amine detection is fluorescamine⁸, a synthetic analog of ninhydrin. This procedure tends to be more cumbersome since fluorescamine solutions must be prepared fresh prior to use.

A7.1 Materials

- O-phthaldialdehyde reagent (Sigma)
- Primary amine sample (unknown to be measured)

A7.2 Procedure

In a typical measurement, 2.0mL of o-phthaldialdehyde reagent is placed in a 3.0mL fluorometer cell and a background fluorescence reading is recorded (typically EX345, EM430). The fluorometer is kept in continuous measurement mode. An aliquot of the unknown sample (~0.1-2mM in amines), typically 5-100 μ L, is added to the 2.0 mL of solution and mixed by repeated pipetting. Continuous measurement is maintained until the fluorescence goes through a maximum. The measurement is taken as the difference between the maximum and the initial background reading. For increased accuracy,

multiple dilutions of unknown and standard are taken and their least squared slopes are compared.

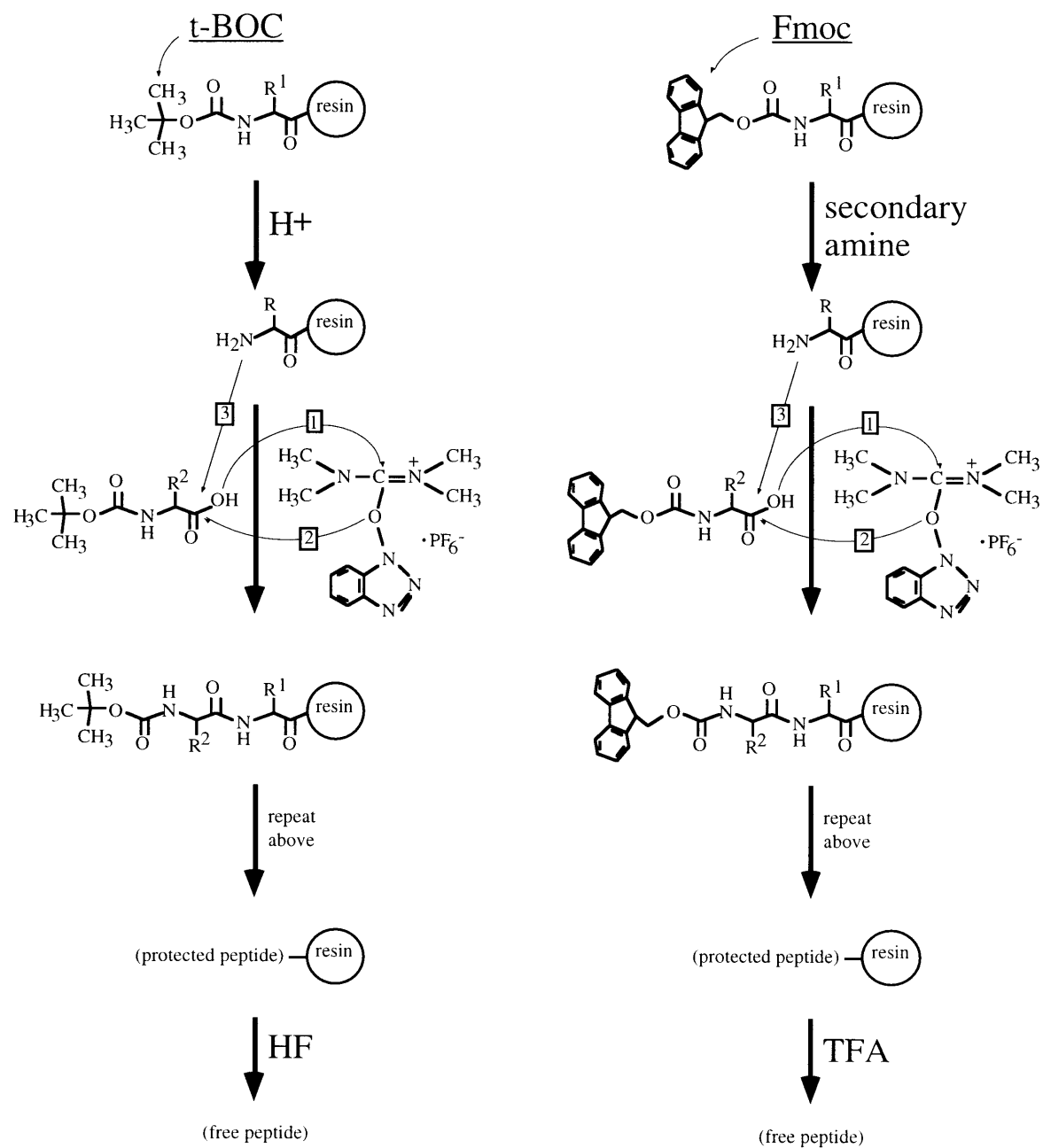


Figure A1. Peptide synthesis scheme for t-BOC and Fmoc procedures.

A8 References

1. Nilsson, K. & Mosbach, K., *Meth. Enzymol.*, "Immobilization of ligands with organic sulfonyl chlorides," **104**: 56-69 (1984).
2. Bodansky, M. *Principles of peptide synthesis*, **1993**, Springer-Verlag, Berlin.
3. Birckbichler, P.J., Orr, G.R., Carter, H.A. & M K Patterson, J., *Biochem. Biophys. Res. Commun.*, "Catalytic formation of epsilon-(gamma-glutaminy)lysine in guinea pig liver transglutaminase," **78**(1): 1-7 (1977).
4. Clarke, D.D., Mycek, M.J., Neidle, A. & Waelsch, H., *Arch. Biochem. Biophys.*, "The incorporation of amines into protein," **79**: 338-354 (1959).
5. Folk, J.E. & Chung, S.I., *Met. Enz.*, "Transglutaminases," **113**: 358-375 (1985).
6. Folk, J.E. & Chung, S.I., *Adv. Enz.*, "Molecular and catalytic properties of transglutaminases," **38**: 109-191 (1973).
7. S S Simons, J. & Johnson, D.F., *J. Org. Chem.*, "Reaction of o-phthaldialdehyde and thiols with primary amines: formation of 1-alkyl(and aryl)thio-2-alkylisoindoles," **43**(14): 2886-2891 (1978).
8. Udenfriend, S., *et al.*, *Science*, "Fluorescamine: a reagent for assay of amino acids, peptides, proteins, and primary amines in the picomole range," : 871-872 (1972).

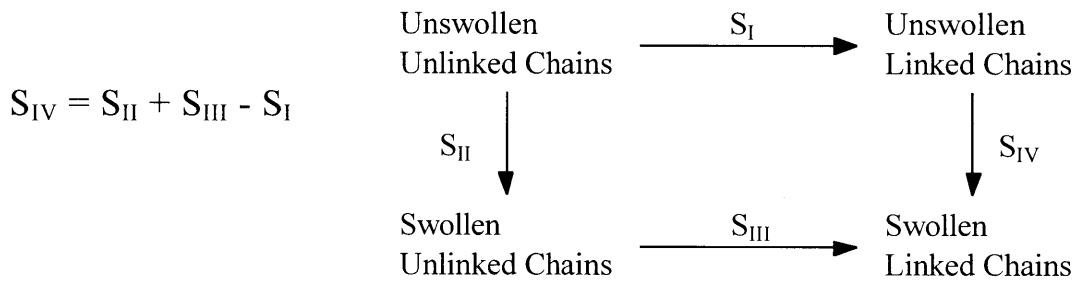
APPENDIX B: PEG/POLYLYSINE GEL STRUCTURE PREDICTIONS

B1 Thermodynamic Predictions

Equilibrium swelling data can be used to estimate the number of effective chains in the PEG-poly(KF) network. The number of effective chains may differ from the actual number of chains due to entanglements, loops and dangling ends. The actual number of chains can be calculated from the chain molecular weight distribution and compared with the calculated number of effective network chains to assess the degree of entanglements versus loops and dangling ends.

To proceed with such calculations, the number functionality of each crosslink must be known. In a two component gel such as PEG-poly(KF) the question arises as to where to define the crosslink. Realizing that the important physical aspect of the gel to be captured in our analysis is the stretching of Gaussian chains, it is necessary to define a 'crosslink' as a non-Gaussian, or stiff region that joins together two or more Gaussian chains. As mentioned in the discussion, it is most appropriate to define each poly(KF) molecule as a node or 'crosslink,' as in Figure 4-1. Thus the functionality of any particular crosslink will be the number of PEG chains attached to that particular poly(KF) molecule. The stoichiometry determines the mean crosslink functionality. For example a gel of 20wt% PEG-Q_a and 5.0wt% poly(KF)·HBr gives a mean crosslink functionality of 17, or 17 PEG chains attached to each poly(KF) molecule if all chains are

linked into the network. However, it is not initially obvious how the phenomenon of equilibrium swelling will depend on the distribution of crosslink functionalities. Because the crosslink functionality distribution of poly(KF) is not known *a priori*, the treatment of equilibrium swelling must be reformulated with consideration for a distribution of crosslink functionalities for poly(KF). To do this we can follow the method of Flory's original derivation for equilibrium swelling of multifunctional crosslinks¹. The total entropy of the swelling process can be described in three steps:



To describe this process appropriately, it is necessary to describe each PEG- Q_a as consisting of two PEG chains attached at the ends as shown in Figure 4-1, because the moiety joining the two chains can itself become covalently linked to poly(KF). Also note that it is probable that a single chain will be involved in crosslinks of different functionalities at each end. Therefore, it is best to define a variable, $e_{PEG,f}$, to denote the number of effective chain ends of a given functionality, f .

The first process, S_I , describes the entropy of joining all chains into the network. To form a network, all chain ends must be localized with the volume of their respective crosslinks. Ignoring, for the moment, that PEG chains are joined into pairs, the

probability of the first poly(KF) molecule in a crosslink of degree f being co-localized in a volume of a crosslink, dV , with f PEG ends is given by,

$$\varepsilon_{PEG,f} (\varepsilon_{PEG,f} - 1) (\varepsilon_{PEG,f} - 2) \cdots (\varepsilon_{PEG,f} - f + 1) (\delta V / V_o)^f \quad (B1)$$

The probability of the second crosslink forming is then,

$$(\varepsilon_{PEG,f} - f) (\varepsilon_{PEG,f} - f - 1) \cdots (\varepsilon_{PEG,f} - 2f + 1) (\delta V / V_o)^f, \quad (B2)$$

as so on. The total probability of forming all ($\varepsilon_{PEG,f}/f$) crosslinks of degree f is the product of all these factors, or:

$$\Omega_{1,f} = \varepsilon_{PEG,f}! \prod_{i=1}^{\varepsilon_{PEG,f}/f} [\delta V / V_o]^f = \varepsilon_{PEG,f}! (\delta V / V_o)^{\varepsilon_{PEG,f}} \quad (B3)$$

Until this point the PEG chains have been considered to be singlets. To account for the presence of doublets and higher multiples, the probability of joining the chains into the distribution of PEG multiplets found in PEG-Q_a can similarly be constructed as

$$\Omega_{1,join} = \left[(1)^{f_1 v_{PEG}} \right] \left[(f_2 v_{PEG} / 4)! \left(2 \partial V / V_o \right)^{f_2 v_{PEG} / 4} \right] \cdots \left[g(f_i v_{PEG}) \left(\partial V / V_o \right)^{\frac{f_i v_{PEG} (i-1)}{2i}} \right]$$

$$\Omega_{I,join} = \left(\frac{\partial V}{V_0} \right)^{\kappa_{PEG}} \prod_i g_i(f_i v_{PEG}) \quad \text{with} \quad \kappa = \sum_i \frac{f_i(i-1)}{2i} \quad (\text{B4})$$

where f_i is the weight fraction of PEG-Q_a molecules with i PEG chains. The factor κ can vary from $\kappa=0$ for the case of solely single chains to $\kappa=1/2$ at the limit of very large multiplets.

Taking into account that the PEG-poly(KF) system has a distribution of crosslink functionalities, the total probability of forming all network crosslinks is given by the product of the probabilities for each f divided by the probability of pairing chains into PEG-Q_a molecules. But we must also take into account that each poly(KF) molecules was randomly assigned a value of f by multiplying by the possible permutations. The total probability then becomes,

$$\Omega_I = \frac{v_{poly(KF),e}!}{\prod_{f=2}^{D_p} v_{poly(KF),e,f}!} \left(\frac{\prod_{f=2}^{D_p} \Omega_{I,f}}{\Omega_{I,join}} \right) = \frac{v_{poly(KF),e}! \prod_{f=2}^{D_p} \left[\left(\frac{\epsilon_{PEG,f}!}{v_{poly(KF),e,f}!} \right) \left(\frac{\delta V}{V_0} \right)^{\epsilon_{PEG,f}} \right]}{\left(\frac{\partial V}{V_0} \right)^{\kappa_{PEG}} \prod_i g_i(f_i v_{PEG})} \quad (\text{B5})$$

where D_p is the number of lysines per poly(KF) molecule and $n_{poly(KF),e}$ is the number of effective poly(KF) chains. Employing Stirling's approximation (for n large,

$\ln(n!) = n \ln(n) - n$), S_1 is given by:

$$S_I = k \ln \Omega_I$$

$$S_I = k \left[v_{poly(KF),e} \ln \left(\frac{v_{poly(KF),e}}{e} \right) - \kappa v_{PEG} \ln \left(\frac{\partial V}{V_o} \right) - \sum_i \ln(g_i(f_i v_{PEG})) \right. \\ \left. + \sum_{f=2}^{D_p} \left[\varepsilon_{PEG,f} \ln \left[\frac{\varepsilon_{PEG,f} \delta V}{V_o e} \right] - v_{poly(KF),e,f} \ln \left(\frac{v_{poly(KF),e,f}}{e} \right) \right] \right] \quad (B6)$$

For the second mixing step, using the subscript (0) to denote the unswollen state, the entropy can be expressed as

$$S_{II} = -k \left[n_{solv} \ln v_{solv} - n_{solv,0} \ln v_{solv,0} + v_{PEG} \ln \left(\frac{v_{PEG}}{v_{PEG,0}} \right) + v_{poly(KF)} \ln \left(\frac{v_{poly(KF)}}{v_{poly(KF),0}} \right) \right] \quad (B7)$$

where u_i , n_i and n_1 are volume fractions, number of polymer molecules and the number of solvent molecules, respectively. This can be re-expressed in terms of the swelling ratio, α , as

$$S_{II} = -k \left[n_{solv} \ln v_{solv} - n_{solv,0} \ln v_{solv,0} - (v_{PEG} + v_{poly(KF)}) \ln \alpha \right] \quad \text{where } \alpha = V/V_o \quad (B8)$$

Values for n_{PEG} and $n_{poly(KF)}$ can be calculated from

$$v_i = \frac{w_i N_A}{\beta_i M_i} \quad (B9)$$

where w_i is the weight of species i in the network, N_A is Avogadro's number, and M_i is the molecular weight of species i . The parameter b_{PEG} is the number average number of PEG chains per PEG-Q_a molecule, while $b_{poly(KF)}$ has a value of unity.

The third step of interlinking the diluted chains of step 2 is achieved in two steps: stretching followed by linking in a process similar to step 1. The elastic component is identical to Flory's except that in the PEG-poly(KF) system the gel is swollen uniaxially as described in the Section 4.2, yielding:

$$S_{III,el} = k \frac{\epsilon_{PEG}}{2} \left[\ln \alpha - \frac{(\alpha^2 - 1)}{2} \right] \quad (B10)$$

The stretching component development is identical to step 1 above. The result differs only in that the volume is V instead of V_0 .

$$S_{III,stretch} = k \left\{ v_{poly(KF),e} \ln \left(\frac{v_{poly(KF),e}}{e} \right) - \kappa v_{PEG} \ln \left(\frac{\partial V}{V} \right) - \sum_i \ln(g_i(f_i v_{PEG})) \right. \\ \left. + \sum_{f=2}^{D_p} \left[\epsilon_{PEG,f} \ln \left[\frac{\epsilon_{PEG,f} \delta V}{V e} \right] - v_{poly(KF),e,f} \ln \left(\frac{v_{poly(KF),e,f}}{e} \right) \right] \right\} \quad (B11)$$

Summing Equations (B6, B8, B10 and B11) gives:

$$S_{IV} = -k \left[n_{solv} \ln v_{solv} - n_{solv,0} \ln v_{solv,0} - \left((1-\kappa)v_{PEG} + v_{poly(KF)} \right) \ln \alpha + \epsilon_{PEG} (\alpha^2 - 1)/4 \right] \quad (B12)$$

Having derived an expression for the entropy of swelling, we can now focus on the condition where the PEG-poly(KF) gel has swollen to equilibrium. At the condition of equilibrium swelling,

$$N_A \left(\frac{\partial \Delta F_{swell}}{\partial n_{solv}} \right)_{T,P} = 0 \quad (B13)$$

where,

$$DF_{swell} = DH_{mix} - TDS_{mix} - TDS_{elastic} = \chi_{solv,PEG} v_{PEG} n_{solv} + \chi_{solv,poly(KF)} v_{poly(KF)} n_{solv} - TS_{IV} \quad (B14)$$

Using the following relations:

$$\left(\frac{\partial \alpha}{\partial n_{solv}} \right)_{T,P} = \frac{v_{solv,0}}{n_{solv,0}}, \quad \left(\frac{\partial v_{solv}}{\partial n_{solv}} \right)_{T,P} = \frac{v_{solv}}{n_{solv}} - \frac{v_{solv}^2}{n_{solv}}, \quad v_{solv} = 1 - \frac{v_{PEG,0} + v_{poly(KF),0}}{\alpha}, \quad (B15)$$

evaluation of (5) gives

$$N_A kT \left[\begin{aligned} & \ln \left[1 - \frac{v_{PEG,0} + v_{poly(KF),0}}{\alpha} \right] \\ & + \frac{1}{\alpha} (v_{PEG,0} + v_{poly(KF),0}) \left(1 + \frac{\chi_{solv,PEG} v_{PEG,0} + \chi_{solv,poly(KF)} v_{poly(KF),0}}{\alpha} \right) \\ & + \frac{v_{solv,0}}{n_{solv,0}} \left(\frac{\alpha \varepsilon_{PEG}}{2} - \frac{v_{PEG}(1-\kappa) + v_{poly(KF)}}{\alpha} \right) \end{aligned} \right] = 0$$

or,

$$\begin{aligned} \varepsilon_{PEG} / N_A &= \frac{2}{\alpha^2} \left\{ \frac{v_{PEG}(1-\kappa) + v_{poly(KF)}}{N_A} - \frac{n_{solv,0}}{N_A v_{solv,0}} \left[\alpha \ln \left(1 - \frac{v_{PEG,0} + v_{poly(KF),0}}{\alpha} \right) \right. \right. \\ & \left. \left. + (v_{PEG,0} + v_{poly(KF),0}) \left(1 + \frac{\chi_{solv,PEG} v_{PEG,0} + \chi_{solv,poly(KF)} v_{poly(KF),0}}{\alpha} \right) \right] \right\} \end{aligned} \quad (B16)$$

where $c_{solv,PEG}$ is taken as 0.45² and $c_{solv,poly(KF)} = 0.47$ (assumed to be bounded by the value for poly(lysine), $c_{water,poly(KF)} = 0.43$ ³ and the theoretical maximum $c = 0.5$).

The number of ends participating in effective crosslinks, e_{PEG} can be used to calculate a net entanglement ratio, F:

$$\Phi = \frac{\varepsilon_{PEG}/2}{\beta_{PEG} v_{PEG}} \quad (B17)$$

Values of F can be used to assess the degree of entanglements versus loops and dangling chain ends. Entanglements will increase F above unity while chain loops and chains

attached at only one end will tend to decrease F below unity. Therefore F gives a measure of the balance of the two effects.

To calculate F from Equation (B17) it is first necessary to calculate k of Equation (B4) and b_{PEG} of Equation (B9) which are dependent on the molecular weight distribution of PEG-Q_a. Contributions from single chain and double chain species were taken directly from organic GPC peak integrations ($f_1=0.679, f_2=0.073$). The weight fractions for species of 3 chains and higher were calculated from aqueous GPC light scattering/refractive index data. For the distribution of PEG-Q_a in Figure 4-2, $k=0.13$ and $b_{PEG}=1.4$.

In interpreting the values for F of different PEG/poly(KF) proportions, it is instructive to examine the sensitivity of the F to perturbations in the various parameters and variables in Equation (B16). A straightforward means of doing this is by evaluating $\partial\Phi/\partial m_i$ for every parameter and variable, m_i . This was done by varying a single m_i by 0.1% while holding every other $m_{j\neq i}$ constant and performing the following calculation:

$$\left(\frac{\partial\Phi}{\partial m_i}\right)_{m_{j\neq i}} \cong \frac{\left(\Phi\right)_{m_i+\Delta m_i, m_{j\neq i}} - \left(\Phi\right)_{m_i, m_{j\neq i}}}{\Delta m_i} \quad \text{where } \Delta m_i = 0.001 \cdot m_i \quad (\text{B18})$$

It is also useful to define a factor, h as

$$\eta(i) = m_i(\partial\Phi/\partial m_i) \quad (\text{B19})$$

The factor $h(i)$ is then a measure of the fractional change that would result in F for a given fractional change in m_i . For example, $h(i)=-2$ would mean that a 1% increase in m_i would cause a 2% decrease in F if $(\partial^2\Phi/\partial m_i^2) = 0$. Through this sensitivity analysis, it was found that a ($h(a)_{20/5 \text{ gel}}=-4.8$) and c ($h(c_{solv,PEG})_{20/5 \text{ gel}}=-4.0$) had the largest influence on F for all gels. The next largest influence was from r_2 ($h(r_2)_{20/5 \text{ gel}}=-1.7$). This suggests that the uncertainty in values for F are largely a function of the uncertainty in a and $c_{solv,PEG}$. The precision of the measurement of a predicts an uncertainty of 1.7%. A survey of literature values for $c_{solv,PEG}$ reveals that reported values^{2, 4-6} vary in a range of 0.43 to 0.45, the value of 0.45 giving the best agreement with SANS data⁷. This range could be taken as twice the uncertainty in $c_{solv,PEG}$ (2.2%). Using these values for the uncertainties in a and $c_{solv,PEG}$ and the values for $h(a)$ and $h(c_{solv,PEG})$ for the 20/5, 10/5 and 20/2.5 gels, uncertainties in F were calculated to be 12%, 9.4% and 28% respectively.

B2 References

1. Flory, P.J., *Journal of Chemical Physics*, "Statistical Mechanics of Swelling of Network Structures," **18**(1): 108-111 (1950).
2. Rogers, J.A. & Tam, T., *Canadian Journal of Pharmaceutical Sciences*, "Solution Behavior of Poly-Ethylene Glycols in Water Using Vapor Pressure Osmometry," **12**: 65 (1977).
3. Daniel, E. & Alexandrowicz, Z., *Biopolymers*, "Sedimentation and Diffusion of Polyelectrolytes. Part II. Experimental Studies with Poly-L-Lysine Hydrohalides," **1**: 473-495 (1963).
4. Merrill, E.W., Dennison, K.A. & Sung, C., *Biomaterials*, "Partitioning and Diffusion of Solutes in Hydrogels of Poly(Ethylene Oxide)," **14**(15): 1117-1126 (1993).
5. Edmond, E. & Ogston, A.G., *Biochemical Journal*, "An approach to the study of phase separation in ternary aqueous systems," **109**: 569 (1968).
6. Brandrup, J. & Immergut, E.H. (eds) (1989) *Polymer Handbook*, 3rd Ed., John Wiley and Sons, New York
7. Cabane, B. & Duplessix, R., *Journal of Physics (Paris)*, **43**: 1529 (1982).

APPENDIX C: RATE CONSTANT FITTING ALGORITHM

C1 Background

The following FORTRAN 77 algorithm was used to iteratively fit rate constants to a set of differential equations by coupling a χ -squared minimization routine with a step-wise differential equation solver, both extracted from Numerical Recipes¹. A fourth-order Runge-Kutta routine was used to generate data for conversion as a function of time from a set of guessed rate constants. This generated data was then compared with measured data to calculate a new set of more accurate rate constants, used as the 'guess' in the next iteration. A Levenberg-Marquardt (LM) chi-squared minimization routine generated this new guess. The same Runge-Kutta routine was used within the LM routine as well to calculate the necessary partial derivatives ($\partial\chi/\partial k_i$) for each rate constant, k_i . This process was repeated iteratively until χ was approximately minimized ($\chi_{n+1}/\chi_n < 0.0001\%$).

The following program is configured for fitting to a tresyl chloride coupling model (see Section 2.2.3), but could be easily reconfigured to fit any arbitrary set of differential equations to a set of measured data by changing the differential equations near the end of the program.

C2 FORTRAN Code

```
PROGRAM MODEL
IMPLICIT REAL*8 (A-H,O-Z)
INTEGER MA,IA(3),NDATA,NX(78),NY
REAL*8 Y(78),SIG(78),A(3),ALPHA(3,3),COVAR(3,3)
REAL*8 CHISQ,Z(3,193)
```

- c file name for data to be fit: DATA>DAT
- c number of y variables: NY
- c number of rate constants (parameters): MA

```
OPEN (1,FILE='DATA.DAT')
NDATA=36
NY=3
MA=3
WRITE (6,*) "READING DATA"
DO 2 I=1,NY
DO 1 II=0,(NDATA/NY-1)*NY,NY
READ(1,*) NX(I+II),Y(I+II),SIG(I+II)
WRITE (6,*) I+II
1 CONTINUE
2 CONTINUE
DO 3 I=1,NDATA
WRITE (6,*) NX(I),Y(I),SIG(I)
3 CONTINUE

ALAMDA=-1D0

CHISQ=1D0

DO 5 I=1,MA
DO 4 J=1,MA
ALPHA(I,J)=0.D0
COVAR(I,J)=0.D0
4 CONTINUE
A(I)=0.D0
IA(I)=0
5 CONTINUE
```

- c rate constants: $a(x)$
- c set a particular rate constant $a(x)$ as fixed: $ia(x)=0$
- c allow fitting of particular rate constant $a(x)$: $ia(x)=1$

```

A(1)=0.004782D0*3D2
IA(1)=1
A(2)=13.1D0
IA(2)=1
A(3)=0.5D0
IA(3)=0
99  CHIOLD=CHISQ
WRITE (6,*) "I'M CALLING MRQMIN",ALAMDA
CALL MRQMIN(NX,Y,SIG,NDATA,A,IA,MA,COVAR,ALPHA,
*CHISQ,ALAMDA,NY)
WRITE(6,*)CHISQ,A(1),A(2),A(3)
WRITE (6,*) ABS((CHIOLD-CHISQ)/CHIOLD)
IF (ABS((CHIOLD-CHISQ)/CHIOLD).GT.1D-6) THEN
  WRITE (6,*) "REP 1"
  GOTO 99
ENDIF
IF (CHIOLD.EQ.CHISQ) THEN
  WRITE (6,*) "REP 2"
  GOTO 99
ENDIF
WRITE (6,*) "CONSTANTS:"
WRITE (6,*) A(1)/3D2,A(2)
WRITE (6,*) "CHISQ:",CHISQ
WRITE (6,*) "STDEVS:"
WRITE (6,*) (COVAR(1,1)**0.5D0)/3D2,(COVAR(2,2)**0.5D0)
PKA=9.1D0
AMINE=10.D0**(8D0-PKA)/(1D0+10.D0**(8D0-PKA))*Y(3)
WRITE (6,*) "ALPHA:",A(2)*AMINE/(1D0+A(2)*AMINE)
WRITE (6,*) "FINAL MRQMIN CALL"
CALL MRQMIN(NX,Y,SIG,NDATA,A,IA,MA,COVAR,ALPHA,
*CHISQ,ALAMDA,NY)
8888  ALAMDA=0.D0
WRITE (6,*) "FINAL MRQMIN CALL"
CALL MRQMIN(NX,Y,SIG,NDATA,A,IA,MA,COVAR,ALPHA,
*CHISQ,ALAMDA,NY)
WRITE (6,*) "CONSTANTS:"
WRITE (6,*) A(1)/3D2,A(2)
WRITE (6,*) "CHISQ:",CHISQ
WRITE (6,*) "STDEVS:"
WRITE (6,*) (COVAR(1,1)**0.5D0)/3D2,(COVAR(2,2)**0.5D0)
PKA=9.1D0
AMINE=10.D0**(8D0-PKA)/(1D0+10.D0**(8D0-PKA))*Y(3)
WRITE (6,*) "ALPHA:",A(2)*AMINE/(1D0+A(2)*AMINE)

```

```

OPEN(200,FILE='C:\LP77\COUPLE.OUT')
CALL SOLVE_BY_RK (A,Z)
DO 6 I=1,193
    WRITE (200,7) (I-1),Z(1,I),Z(2,I),Z(3,I)
6  CONTINUE
CLOSE(200)

CLOSE (1)
STOP
7  FORMAT(1X,11(E20.10,','))
END

SUBROUTINE FUNCS(NX,NII,A,YCALC,DYNA,NA,NP)
IMPLICIT REAL*8 (A-H,O-Z)
REAL*8 Y(3,193),DY(3,193),A(3),SK(3),DK(3),DYNA(3),ITOT
INTEGER NX,NP
YCALC=0.D0
ITOT=192D0/960D0
INUM=0
NI=NII

DO 199 I=1,NA
    SK(I)=A(I)
    DK(I)=A(I)
199 CONTINUE

DO 299 I=1,NI,NP
    IF(I.GT.NP)THEN
        INUM=INUM+1
    ENDIF
299 CONTINUE

IF(NI.GT.NP)THEN
    NI=NI-INUM*NP
ENDIF

ISTEP=(NX*ITOT)+1
DO 399 I=1,NA
    CALL SOLVE_BY_RK(SK,Y)

    YCALC=Y(NI,ISTEP)

```

```

DK(I)=0.99D0*SK(I)
  CALL SOLVE_BY_RK(DK,DY)
DYCALC=DY(NI,ISTEP)

DYNA(I)=(YCALC-DYCALC)/(0.01D0*SK(I))

DK(I)=SK(I)

```

399 CONTINUE

```

RETURN
END

```

```

SUBROUTINE COVSRT(COVAR,MA,IA,MFIT)
IMPLICIT REAL*8 (A-H,O-Z)
INTEGER MA,MFIT,IA(3)
REAL*8 COVAR(3,3)
INTEGER I,J,K
REAL*8 SWAP
DO 12 I=MFIT+1,MA
  DO 11 J=1,I
    COVAR(I,J)=0.D0
    COVAR(J,I)=0.D0
11  CONTINUE
12  CONTINUE
    K=MFIT
    DO 15 J=MA,1,-1
      IF(IA(J).NE.0)THEN
        DO 13 I=1,MA
          SWAP=COVAR(I,K)
          COVAR(I,K)=COVAR(I,J)
          COVAR(I,J)=SWAP
13  CONTINUE
          DO 14 I=1,MA
            SWAP=COVAR(K,I)
            COVAR(K,I)=COVAR(J,I)
            COVAR(J,I)=SWAP
14  CONTINUE
            K=K-1
          ENDIF
15  CONTINUE
RETURN

```

END

C (C) COPR. 1986-92 NUMERICAL RECIPES SOFTWARE -X3#71JN>#('2150.

```
SUBROUTINE GAUSSJ(A,N,B,M)
IMPLICIT REAL*8 (A-H,O-Z)
INTEGER M,N,NMAX
REAL*8 A(3,3),B(3,3)
PARAMETER (NMAX=50)
INTEGER I,ICOL,IROW,J,K,L,LL,INDXC(3),INDXR(3),IPIV(3)
REAL*8 BIG,DUM,PIVINV
DO 16 J=1,N
  IPIV(J)=0
16  CONTINUE
DO 26 I=1,N
  BIG=0.D0
  DO 18 J=1,N
    IF(IPIV(J).NE.1)THEN
      DO 17 K=1,N
        IF (IPIV(K).EQ.0) THEN
          IF (ABS(A(J,K)).GE.BIG)THEN
            BIG=ABS(A(J,K))
            IROW=J
            ICOL=K
          ENDIF
        ELSE IF (IPIV(K).GT.1) THEN
          PAUSE 'SINGULAR MATRIX IN GAUSSJ1'
        ENDIF
      CONTINUE
    ENDIF
  CONTINUE
  IPIV(ICOL)=IPIV(ICOL)+1
  IF (IROW.NE.ICOL) THEN
    DO 19 L=1,N
      DUM=A(IROW,L)
      A(IROW,L)=A(ICOL,L)
      A(ICOL,L)=DUM
    CONTINUE
  DO 20 L=1,M
    DUM=B(IROW,L)
    B(IROW,L)=B(ICOL,L)
    B(ICOL,L)=DUM
  CONTINUE
20  CONTINUE
ENDIF
```

```

INDXR(I)=IROW
INDXC(I)=ICOL

IF (A(ICOL,ICOL).EQ.0.D0) PAUSE 'SINGULAR MATRIX IN GAUSSJ2'

PIVINV=1.D0/A(ICOL,ICOL)
A(ICOL,ICOL)=1.D0
DO 21 L=1,N
  A(ICOL,L)=A(ICOL,L)*PIVINV
21  CONTINUE
DO 22 L=1,M
  B(ICOL,L)=B(ICOL,L)*PIVINV
22  CONTINUE
DO 25 LL=1,N
  IF(LL.NE.ICOL)THEN
    DUM=A(LL,ICOL)
    A(LL,ICOL)=0.D0
    DO 23 L=1,N
      A(LL,L)=A(LL,L)-A(ICOL,L)*DUM
23    CONTINUE
    DO 24 L=1,M
      B(LL,L)=B(LL,L)-B(ICOL,L)*DUM
24    CONTINUE
  ENDIF
25  CONTINUE
26  CONTINUE
DO 28 L=N,1,-1
  IF(INDXR(L).NE.INDXC(L))THEN
    DO 27 K=1,N
      DUM=A(K,INDXR(L))
      A(K,INDXR(L))=A(K,INDXC(L))
      A(K,INDXC(L))=DUM
27    CONTINUE
  ENDIF
28  CONTINUE
RETURN
END
C (C) COPR. 1986-92 NUMERICAL RECIPES SOFTWARE -X3#71JN>#('2150.

```

```

SUBROUTINE
MRQCOF(NX,Y,SIG,NDATA,A,IA,MA,ALPHA,BETA,CHISQ,NP)
  IMPLICIT REAL*8 (A-H,O-Z)

```

```

    INTEGER MA, NDATA, IA(3), MMAX, NX(78), NP
    REAL*8 CHISQ, A(3), ALPHA(3,3), BETA(3), SIG(78),
    *Y(78)
    PARAMETER (MMAX=3)
    INTEGER MFIT, I, J, K, L, M
    REAL*8 DY, SIG2I, WT, YMOD, DYDA(78)
    MFIT=0
    DO 30 J=1, MA
        IF (IA(J).NE.0) MFIT=MFIT+1
30    CONTINUE
    DO 32 J=1, MFIT
        DO 31 K=1, J
            ALPHA(J,K)=0.D0
31    CONTINUE
        BETA(J)=0.D0
32    CONTINUE
    CHISQ=0.D0
    DO 35 I=1, NDATA

        CALL FUNCS(NX(I), I, A, YMOD, DYDA, MA, NP)

        SIG2I=1.D0/(SIG(I)*SIG(I))
        DY=Y(I)-YMOD
        J=0
        DO 34 L=1, MA
            IF(IA(L).NE.0) THEN
                J=J+1
                WT=DYDA(L)*SIG2I
                K=0
                DO 33 M=1, L
                    IF(IA(M).NE.0) THEN
                        K=K+1
                        ALPHA(J,K)=ALPHA(J,K)+WT*DYDA(M)
                    ENDIF
33                CONTINUE
                BETA(J)=BETA(J)+DY*WT
            ENDIF
34        CONTINUE

        CHISQ=CHISQ+DY*DY*SIG2I
35    CONTINUE
    DO 37 J=2, MFIT
        DO 36 K=1, J-1

```



```

        ALPHA(K,J)=ALPHA(J,K)
36  CONTINUE
37  CONTINUE
    RETURN
    END
C (C) COPR. 1986-92 NUMERICAL RECIPES SOFTWARE -X3#71JN>#('2150.

```

```

    SUBROUTINE MRQMIN(NX,Y,SIG,NDATA,A,IA,MA,COVAR,ALPHA,
*CHISQ,ALAMDA,NP)
    IMPLICIT REAL*8 (A-H,O-Z)
    INTEGER MA,NDATA,MMAX,IA(3)
    REAL*8 ALAMDA,CHISQ,A(3),ALPHA(3,3),COVAR(3,3),
*SIG(78),Y(78)
    PARAMETER (MMAX=3)
CU  USES COVSRT,GAUSSJ,MRQCOF
    INTEGER J,K,L,M,MFIT,NX(78),NP
    REAL*8 OCHISQ,ATRY(MMAX),BETA(3),DA(3)
    SAVE OCHISQ,ATRY,BETA,DA,MFIT
    NEG=0

    IF(ALAMDA.LT.0)THEN
        MFIT=0
        DO 40 J=1,MA
            IF (IA(J).NE.0) MFIT=MFIT+1
40    CONTINUE

c
c    step size for new guess goes as 1/alamda
c

        ALAMDA=1D2
        WRITE (6,*)"I'M CALLING MARQCOF - INITIALIZATION"
        CALL MRQCOF(NX,Y,SIG,NDATA,A,IA,MA,ALPHA,BETA,CHISQ,NP)
        OCHISQ=CHISQ
        DO 41 J=1,MA
            ATRY(J)=A(J)
41    CONTINUE
    ENDIF
    J=0
    DO 43 L=1,MA
        IF(IA(L).NE.0) THEN

```

```

J=J+1
K=0
DO 42 M=1,MA
  IF(IA(M).NE.0) THEN
    K=K+1
    COVAR(J,K)=ALPHA(J,K)
  ENDIF
42  CONTINUE
    COVAR(J,J)=ALPHA(J,J)*(1.D0+ALAMDA)
    DA(J)=BETA(J)
  ENDIF
43  CONTINUE
CALL GAUSSJ(COVAR,MFIT,DA,1)
IF(ALAMDA.EQ.0.D0)THEN
  CALL COVSRT(COVAR,MA,IA,MFIT)
  RETURN
ENDIF
J=0
DO 44 L=1,MA
  IF(IA(L).NE.0) THEN
    J=J+1
    ATRY(L)=A(L)+DA(J)
    IF (ATRY(L).LT.0D0) THEN
      ATRY(L)=ATRY(L)/10.D0
    ENDIF
  ENDIF
44  CONTINUE
  WRITE (6,*) ATRY
  WRITE(6,*)"I'M CALLING MARQCOF"
CALL MRQCOF(NX,Y,SIG,NDATA,ATRY,IA,MA,COVAR,DA,CHISQ,NP)
IF(CHISQ.LT.OCHISQ)THEN
  DO 555 II=1,MA
    IF (ATRY(II).LT.0D0) THEN
      NEG=1
    WRITE (6,*) "NEG"
    ENDIF
555  CONTINUE
    IF (NEG.EQ.0) THEN
      ALAMDA=0.25D0*ALAMDA
      OCHISQ=CHISQ
      J=0
      DO 46 L=1,MA
        IF(IA(L).NE.0) THEN

```

```

    J=J+1
    K=0
    DO 45 M=1,MA
        IF(IA(M).NE.0) THEN
            K=K+1
            ALPHA(J,K)=COVAR(J,K)
        ENDIF
45    CONTINUE
    BETA(J)=DA(J)
    A(L)=ATRY(L)
        IF (ATRY(L).LT.0D0) THEN
            ATRY(L)=ATRY(L)/10.D0
        ENDIF
    ENDIF
46    CONTINUE
    ELSE
        ALAMDA=8D0*ALAMDA
        CHISQ=OCHISQ
    ENDIF
ELSE
    ALAMDA=8.0D0*ALAMDA
    CHISQ=OCHISQ
ENDIF
RETURN
END

```

```

SUBROUTINE SOLVE_BY_RK (SK,P)
IMPLICIT REAL*8 (A-H,O-Z)

```

```

REAL*8 YSTART(4),SK(3),Y(4,193),P(3,193),PH(3)

```

```

NUM_YVAR = 4
NPOINTS = 193

```

```

XSTART = 0.D0
XSTOP = 193.D0
YSTART(1) = 0.04D0
YSTART(2) = 0.0D0
YSTART(3) = 0.1D0
YSTART(4) = 0.0D0

```

```

PH(1)=7.5D0

```

PH(2)=8.0D0
PH(3)=8.5D0

DO 51 J=1,3

CALL RUNGE_KUTTA(SK,NUM_YVAR,NPOINTS,XSTART,XSTOP,
* YSTART,Y,PH(J))

DO 50 I=1,193
P(J,I) = (YSTART(3)-Y(3,I))/YSTART(1)
50 CONTINUE

C WRITE (6,*) Y(2,193)/(YSTART(3)-Y(3,193)),PH(J)

51 CONTINUE

RETURN
END

SUBROUTINE DERIVS(SK,X,Y,DYDX,PH)
IMPLICIT REAL*8 (A-H,O-Z)
PARAMETER (NUM_YMAX=4, NPTMAX=193)
REAL*8 Y(NUM_YMAX), DYDX(NUM_YMAX),SK(3),PH,KOH,KW,PKA
REAL*8 AMINE, OH

C COLD: KOH=68, KW=2.2D-7, KWATER=14.78

C PKA'S: GF=8.6, F=9.6 ,K=11.3

C WARM: KOH=78.3, KW=1.70D-5 KWATER=14.08

C PKA'S: GF=8.1, F=9.1 ,K=10.7

KOH=68D0*60D0*5D0
KW=2.2D-7*60D0*5D0
OH=10.D0**(PH-14.78D0)
PKA=8.6D0

AMINE=10.D0**(PH-PKA)/(1D0+10.D0**(PH-PKA))*Y(3)

C PROT=Y(3)-AMINE

C NOTE: SK(2)=K2/K'

DYDX(1) = -(KW + KOH*OH + SK(1)*AMINE)*Y(1)
DYDX(2) = SK(1)*AMINE*Y(1)

```

        DYDX(3) = -(SK(1)*AMINE+KOH*OH
*          *(SK(2)*AMINE/(1D0+SK(2)*AMINE)))
*          *Y(1)

        DYDX(4) = KW*Y(2)
C        Y(4) NOT BEING USED
C        IF (Y(2).LT.0) THEN
C          WRITE (6,*) "Y(2) NEGATIVE ",Y(1),Y(2),Y(3)
C        ENDIF
        RETURN
        END

        SUBROUTINE
RUNGE_KUTTA(SK,NUM_YVAR,NPOINTS,XSTART,XSTOP,
* YSTART,Y,PH)
        IMPLICIT REAL*8 (A-H,O-Z)
        PARAMETER (NUM_YMAX=4, NPTMAX=193)
        REAL*8 X(NPTMAX),Y(NUM_YMAX,NPTMAX),SK(3),PH
        REAL*8 YSTART(NUM_YMAX), YI(NUM_YMAX), YO(NUM_YMAX)

        X(1) = XSTART
        DO 60 I=1,NUM_YVAR
            Y(I,1) = YSTART(I)
60        CONTINUE

        STEP = (XSTOP-XSTART)/(NPOINTS-1)

        DO 63 ISTEP=1,NPOINTS-1
            DO 61 I=1,NUM_YVAR
                YI(I) = Y(I,ISTEP)
61            CONTINUE

            CALL RK4(SK,NUM_YVAR,STEP, X(ISTEP),YI,YO,PH)
            DO 62 I=1,NUM_YVAR
                Y(I,ISTEP+1) = YO(I)
62            CONTINUE
            X(ISTEP+1) = X(ISTEP) + STEP

63        CONTINUE

        RETURN

```

```

END

SUBROUTINE RK4(SK,NUM_YVAR,STEP,X,YI,YO,PH)
IMPLICIT REAL*8 (A-H,O-Z)
PARAMETER (NUM_YMAX=4, NPTMAX=193)
REAL*8 YI(NUM_YMAX),YO(NUM_YMAX),
YT(NUM_YMAX),SK(2),PH
REAL*8
A1J(NUM_YMAX),A2J(NUM_YMAX),A3J(NUM_YMAX),A4J(NUM_YMAX)
CALL DERIVS(SK,X,YI,A1J,PH)
HSTEP = STEP/2.D0
DO 100 I=1,NUM_YVAR
  YT(I) = YI(I) + HSTEP*A1J(I)
100  CONTINUE

CALL DERIVS(SK,X+HSTEP,YT,A2J,PH)
DO 200 I=1,NUM_YVAR
  YT(I) = YI(I) + HSTEP*A2J(I)
200  CONTINUE

CALL DERIVS(SK,X+HSTEP,YT,A3J,PH)
DO 300 I=1,NUM_YVAR
  YT(I) = YI(I) + STEP*A3J(I)
300  CONTINUE

CALL DERIVS(SK,X+STEP,YT,A4J,PH)
DO 400 I=1,NUM_YVAR
  YO(I) = YI(I) +
  * (STEP/6.D0)*(A1J(I)+2.D0*(A2J(I)+A3J(I))+A4J(I))
400  CONTINUE
RETURN
END

```

C3 References

1. Press, W.H., Flannery, B.P., Teukolsky, S.A. & Vetterling, W.T. *Numerical Recipes*, 1986, Cambridge University Press, Cambridge.